
Manual for A Multi-machine Small-signal Stability Programme (Version 1.0)

Prepared by

Dr. K.N. Shubhanga

Mr. Yadi Anantholla



Department of Electrical Engineering
NITK, Surathkal
Srinivasnagar, Mangalore - 575025
KARNATAKA, INDIA

Contents

List of Figures	iv
List of Tables	vi
1 Introduction	1
1.1 Power System Oscillations:	1
1.2 Classification of Power System Oscillation:	2
1.2.1 Swing Mode Oscillations:	3
1.2.2 Control Mode Oscillations:	4
1.2.3 Torsional Mode Oscillations:	4
1.3 Methods of Analysis of Small Signal Stability:	4
1.3.1 Eigenvalue Analysis:	5
1.3.2 Synchronizing and Damping Torque Analysis:	7
1.3.3 Frequency Response- and Residue- Based Analysis:	9
1.3.4 Time-Domain Solution:	9
1.4 Advantages of Eigenvalue or Modal Analysis:	10
1.4.1 Computation of Eigenvalues:	10
1.4.1.1 QR Techniques:	10
1.4.1.2 Arnoldi Method:	11
1.5 Modelling of Power System:	12
1.5.1 Linearization of DAEs:	13
1.5.1.1 Load Flow Jacobian-based Approach:	15
1.5.1.2 Current Injection-based Approach:	16
1.6 Modal Analysis of Linear Systems:	21
1.6.1 Eigenvalue Sensitivity - Participation Matrix:	24
1.7 Spring-Mass System Example:	27
2 4-machine Power System Example	41
2.1 Four Machine System Details:	41
2.2 Base Case:	41

2.2.1	Format of Data Files:	44
2.2.2	Component Selectors:	50
2.2.3	Load Modelling:	53
2.2.4	A Sample Run:	55
2.2.5	Exciters on Manual Control:	59
2.2.6	Effect of Load Model with Exciters on Manual Control:	59
3	Design of Slip-signal PSS	61
3.1	Introduction:	61
3.2	Types of Power System Stabilizers:	62
3.2.1	Slip-single Input PSS:	62
3.2.1.1	Washout Circuit:	62
3.2.1.2	Lead-Lag Compensator:	63
3.2.1.3	Torsional Filter:	63
3.2.1.4	Stabilizer Gain:	64
3.2.1.5	Stabilizer Limits:	64
3.3	Tuning of PSS:	65
3.3.1	Computation of $GEPS(s)$:	65
3.3.2	Design of Compensator $G_C(s)$:	67
3.3.3	Determination of Compensator Gain:	71
3.3.3.1	Interfacing PSS to the System Matrix:	72
3.3.3.2	Eigenvalues with Slip-input PSS:	73
3.3.4	Time-domain Verification:	74
3.3.5	Frequency response of $\frac{T_e(s)}{V_{ref}(s)}$:	76
3.4	Placement of Power System Stabilizers:	78
4	Design of Delta-P-Omega Signal PSS	81
4.1	Introduction:	81
4.2	Design of Delta-P-Omega PSS:	84
4.2.1	Design of the Compensator $G_c(s)$:	84
4.2.2	Interfacing of PSS to the System Matrix:	86
4.2.2.1	Eigenvalues with Delta-P-Omega PSS:	89
5	Design of Power-signal PSS	91
5.1	Introduction:	91
5.2	Interfacing of Power-input PSS to the State Matrix:	92
5.3	4-machine Power System Example:	93
5.3.1	Eigenvalues with Power-input PSS:	94
5.3.2	Performance of the PSS for Power Ramping:	95

6	10-machine Power System Example	97
6.1	Ten Machine System Details:	97
A	Names of State Variables	103
B	Derivation of P-matrix and Construction of P_G, P_L and Reduced State Matrices	105
B.1	Derivation of P matrix:	105
B.2	Construction of $[P_G]$ and $[P_L]$ Matrices:	107
B.3	Derivation of Reduced-State Matrix:	108
C	Generator Modelling	111
C.1	Introduction:	111
C.2	Rotor Equations:	112
C.2.1	d-axis Equations:	112
C.2.2	q-axis Equations:	112
C.3	Stator Equations:	112
C.4	Derivation of I_{Dg} and I_{Qg} :	113
C.5	Swing Equations:	114
C.6	Modification of Differential Equations:	115
C.7	Simplification of Machine Model:	119
D	Exciter Modelling	121
D.1	Single Time Constant Static Exciter:	121
D.2	IEEE-type DC1A Exciter:	122
D.3	IEEE-type AC4A Exciter:	125
E	Turbine and Speed-governor Modelling	127
E.1	Hydro Turbine and its Speed Governor Model:	127
E.2	Reheat Type Steam Turbine and its Speed-governor Model:	130
F	Network Modelling	133
F.1	Introduction:	133
F.2	Transmission Lines:	133
F.3	Transformers:	134
G	Static Loads	135
H	Initial Condition Calculations	139
	Bibliography	143

List of Figures

1.1	Phasor representation of sinusoidally varying angle, speed and torque deviations.	8
1.2	Multi-mass multi-spring system	27
1.3	Equivalent circuit for multi-mass multi-spring system.	28
1.4	Modified multi-mass multi-spring system with damping.	34
1.5	Numerical solution for Case-1.	36
1.6	Numerical solution for Case-2.	37
1.7	Numerical solution for Case-3.	38
2.1	Four machine power system.	41
2.2	Plot of slip-right eigenvector for machines 1 and 2.	57
2.3	$Slip_COI$ plots for perturbation of V_{ref} of m/c-1.	58
2.4	Variation of the magnitude of the load bus voltages.	60
3.1	Location of PSS in a power system.	61
3.2	Block diagram of a single input PSS.	62
3.3	Phase angle of $GEPS(j\omega)$, for machine-1	68
3.4	Phase angle of compensator $G_C(j\omega)$	70
3.5	Phase angle of $GEPS(j\omega)$, $G_{PSS}(j\omega)$ and $P(j\omega)$ for machine-1.	71
3.6	Plot of amplitude of $GEPS(s)$ for machine-1.	72
3.7	Variation of rotor angles with respect to COI reference without PSS.	74
3.8	Variation of rotor angles with PSS.	75
3.9	Frequency response plot with and without PSS.	77
4.1	Block schematic to generate integral of ΔT_m	82
4.2	Delta-P-Omega PSS.	83
4.3	Plot of compensated $GEPS(j\omega)$ with all blocks.	85
4.4	Delta-P-Omega PSS modified block schematic.	86
5.1	Block schematic of power-input PSS.	92
5.2	Phase angle of the compensated GEPS with power input PSS.	93

5.3	Variation of E_{fd} for power PSS gain of 0.4.	95
5.4	variation of rotor angle and the terminal voltage for machine-1 for power ramping case.	96
6.1	10-machine 39-bus power system.	97
6.2	Plot of slip-right eigenvector for machine groups 1 and 2.	100
6.3	Plot of slip-right eigenvector for machine groups 1 and 2.	100
C.1	2.2 model of a Synchronous Machine.	111
D.1	Single time constant static excitation system.	121
D.2	IEEE-type DC1A excitation system.	122
D.3	TGR block.	122
D.4	ESS block.	123
D.5	IEEE-type AC4A excitation system.	125
D.6	TGR block.	125
E.1	Hydraulic turbine model.	127
E.2	Modified hydraulic turbine model.	127
E.3	Model of speed-governor for hydro turbines.	128
E.4	Modified model of speed-governor for hydro turbine.	128
E.5	Tandem compounded, single-reheat-type steam turbine model.	130
E.6	Model for speed-governor for steam turbines.	130
E.7	Modified model for speed-governor for steam turbines.	131
F.1	Nominal π Model of transmission lines.	133
F.2	Transformer Model	134

List of Tables

2.1	Eigenvalues for four machine system -base case.	42
2.2	Oscillatory modes - 4 machine system (Base case).	58
2.3	Swing modes with all exciters on manual control.	59
2.4	Effect of constant power type load model for P & Q load components with manual exciter control.	60
3.1	Oscillatory modes for the base case with PSS on m/c-1.	73
4.1	Oscillatory modes with Delta-P-Omega PSS.	89
5.1	Swing modes with power-input PSS for the base case.	94
A.1	System state variables.	103
A.2	Machine state variables.	103
A.3	DC1A-exciter state variables.	103
A.4	AC4A-exciter state variables.	104
A.5	Reheat steam turbine state variables.	104
A.6	Hydraulic turbine state variables.	104
C.1	Simplifications in 2.2 model.	119

Chapter 1

Introduction

Small-signal rotor angle stability analysis mainly deals with a study of electromechanical oscillations-related performance of the system about an operating point when the system is subjected to sufficiently small magnitude of disturbance that will not trigger non-linear behaviour of the system. Thus, this study is mainly concerned with the ability of the power system to maintain synchronism under small disturbances. The disturbances are considered to be sufficiently small that linearization of system equations is possible for analysis purposes. This permits linear system theory to be applied for system analysis even though the system is inherently non-linear.

A power system at a given operating condition may be large disturbance unstable, still such a system can be operated, though unsecurely. However, if the system is small-signal unstable at a given operating condition, it cannot be operated. Therefore, small-signal stability is a fundamental requirement for the satisfactory operation of power systems. Such a study mainly involves the verification of sufficiency of damping of all modes associated with a system so that power transfer is not constrained.

It is known that when a dynamic system such as power system is perturbed from its steady state condition, the system variables trace out a flow, referred to as trajectories. These trajectories may exhibit oscillatory or monotonic behaviour. For the system to be stable, these trajectories must remain bounded and converge to an acceptable operating point.

1.1 Power System Oscillations:

A study of power system oscillations is of interest in a system where more than one generator is working in parallel to deliver a common load. In small systems, there may be only tens of generators and in large systems there may be thousands of generators working in parallel. In such a situation synchronous machines produce torques that depend on the relative angular displacement of their rotors. These torques act to keep the generators in

synchronism (synchronizing torque), thus, if the angular displacement between generators increases, an electrical torque is produced that tries to reduce that angular displacement. It is as though the generators were connected by torsional spring, and just as in spring mass system where a restraining force due to spring action against moment of mass, results in oscillations, the moment of inertia of rotors and synchronizing torques cause the angular displacement of the generators to oscillate following the occurrence of a disturbance when it is operating under steady state. Under these conditions, the generators behave as rigid bodies and oscillate with respect to one another using the electrical transmission path between them to exchange energy. If a system is small-signal unstable, oscillations can grow in magnitude over the span of many seconds and, can eventually result in outages of major portions of the power system. Further, a power system is continuously subjected to random disturbances in the form of load or generation changes/changes in controller settings. Hence it never settles to a steady state at any given point of time. Therefore having adequate damping of all system oscillations is critical to system stability and therefore, to system security and reliability.

In a well designed and operated system, these oscillations of the rotor angle displacement decay and settle to a value that will not constraint power flow through the transmission network. Such a system is said to be small-signal stable. In the following circumstances, the system may be small-signal unstable [1, 2, 3]

1. Use of high gain fast-acting exciters.
2. Heavy power transfer over long transmission lines from remote generating plants
3. Power transfer over weak ties between systems which may result due to line outages.
4. Inadequate tuning of controls of equipment such as generator excitation systems, HVDC converters, static var compensators.
5. Adverse interaction of electrical and mechanical systems causing instabilities of torsional mode oscillations.

In an over stressed system, a relatively low inherent damping and a small magnitude of synchronous torque coefficient may constrain the system operation by limiting power transfer. Further, in such cases, predicting oscillation boundaries and therefore to manage them, becomes increasingly difficult.

1.2 Classification of Power System Oscillation:

The power system oscillations are mainly concerned with small excursions of the system conditions about a steady state operating point following a small disturbance. For a

convenience of analysis, the oscillations associated with a power system is classified as follows [1, 2].

1. Swing mode oscillations.
2. Control mode oscillations.
3. Torsional mode oscillations.

1.2.1 Swing Mode Oscillations:

This mode is also referred to as electromechanical oscillations. For an n generator system, there are $(n - 1)$ swing (oscillatory) modes associated with the generator rotors. A swing mode oscillation is characterised by a high association of the generator rotor in that mode, where generator(s) in two coherent groups swinging against each other with an approximate phase difference of 180° among the groups. It is shown later that in the eigenvalue analysis, a high association is denoted by participation factors and formation the of coherent groups is identified by right eigenvectors associated with rotor slip. In addition, there will be a mode referred to as a rigid body mode or zero mode, in which all generator rotor take part as a single rigid rotor. This mode is generally associated with the movement of the center of inertia which corresponds to the dynamics of the average frequency. Not all generators are involved in all modes. Typically, each mode is associated with a group of generators swinging against another group. The location of generators in the system determines the type of swing mode.

Swing mode oscillations can be further grouped into four broad categories:

1. Local machine-system oscillations.
 2. Interunit (Intra-plant) mode oscillations.
 3. Local mode oscillations.
 4. Inter-area mode oscillations.
1. **Local Machine-system oscillations:** These oscillations generally involve one or more synchronous machines at a power station swinging together against a comparatively large power system or load center at a frequency in the range of 0.7 Hz to 2 Hz. These oscillations become particularly troublesome when the plant is at high load with a high reactance transmission system. The term local is used because the oscillations are localized at one station or a small part of the power system.
 2. **Interunit (Intra-plant) mode oscillations:** These oscillations typically involve two or more synchronous machines at a power plant swing against each other, usually at a frequency of between 1.5 Hz to 3 Hz.

3. **Local mode oscillations:** These oscillations generally involve nearby power plants in which coherent groups of machines within an area swing against each other. The frequency of oscillations are in the range of 0.8 to 1.8 Hz.
4. **Inter-area mode oscillations:** These oscillations usually involve combinations of many synchronous machines on one part of a power system swinging against machines on another part of the system. Inter-area oscillations are normally of a much lower frequency than local machine system oscillations in the range of 0.1 to 0.5 Hz. These modes normally have wide spread effects and are difficult to control.

1.2.2 Control Mode Oscillations:

Control modes are associated with generating units and other controls. Poorly tuned exciters, speed governors, HVDC converters and static var compensators are the usual causes of instability of these modes.

1.2.3 Torsional Mode Oscillations:

These oscillations involve relative angular motion between the rotating elements (synchronous machine, turbine, and exciter) of a unit, with frequencies ranging from 4Hz and above. This mechanical system has very little inherent natural damping. The source of torque for inducing torsional oscillations with the excitation system comes from a combination of modulation of excitation system output power, and modulation of synchronous machine power due to changes in generator field voltage. Beside the excitation systems, there are other mechanisms that can excite torsional oscillations such as dc lines, static converters, series-capacitor-compensated lines and other devices.

A wide bandwidth excitation system may have the capability to provide enough negative damping at any of these torsional natural frequencies to destabilize one or more of these torsional modes, particularly with the application of a power system stabilizer.

Of these oscillations, local machine-system mode, local mode, intra-plant mode, control mode and torsional mode are generally categorized as local problems as it involves a small part of the system. Further, inter-area mode oscillations are categorized as global small-signal stability problems and are caused by interactions among large groups of generators and have widespread effects.

1.3 Methods of Analysis of Small Signal Stability:

1. Eigenvalue analysis [4].
2. Synchronizing and damping torque analysis [1, 5].

3. Frequency response- and residue-based analysis [6, 7].
4. Time-domain solution analysis [2, 1, 8, 10]

1.3.1 Eigenvalue Analysis:

Eigenvalues:

The eigenvalue of a matrix is given by the value of the scalar parameter λ for which there exist non-trivial solution (i.e. other than $\underline{u} = 0$) to the equation

$$A\underline{u} = \lambda\underline{u} \quad (1.1)$$

where A is an $(n \times n)$ matrix (real for a physical system such as a power system) and \underline{u} is an $(n \times 1)$ vector referred to as eigenvector.

To find the eigenvalue, (1.1) may be written in the form

$$(A - \lambda I)\underline{u} = 0 \quad (1.2)$$

where I is an identity matrix of dimension $(n \times n)$.

For a non-trivial solution,

$$\det(A - \lambda I) = 0 \quad (1.3)$$

Expansion of the determinant gives the characteristic equation. The n solutions of $\lambda = \lambda_1, \lambda_2, \dots, \lambda_n$ are referred to as the eigenvalues of the matrix A . The eigenvalues may be real or complex, and a complex eigenvalue always occur in conjugate pair. In general, $\lambda_i = \sigma_i + j\omega_i$, where σ_i is referred to as neper frequency (neper/s), and ω_i is referred to as radian frequency (rad/s).

Eigenvectors:

For any eigenvalue λ_i , the n element column vector \underline{u}_i , which satisfies (1.1) is called the *right eigenvector* of A associated with eigenvalue λ_i , Therefore we have

$$A\underline{u}_i = \lambda_i\underline{u}_i \quad i = 1, 2, \dots, n \quad (1.4)$$

The eigenvector \underline{u}_i has the form

$$\underline{u}_i = \begin{bmatrix} u_{1i} \\ u_{2i} \\ \vdots \\ u_{ni} \end{bmatrix}$$

Since (1.4) is homogeneous, $k \underline{u}_i$ (where k is a scalar) is also a solution. Thus, the eigenvectors are determined only to within a scalar multiplier.

Similarly, the n element row vector \underline{w}_j which satisfies

$$\underline{w}_j A = \lambda_j \underline{w}_j \quad j = 1, 2, \dots, n \quad (1.5)$$

is called the *left eigenvector* associated with the eigenvalue λ_j , and has the form

$$\underline{w}_j = \begin{bmatrix} w_{j1} & w_{j2} & \cdots & w_{jn} \end{bmatrix}$$

The left and right eigenvector corresponding to different eigenvalues are orthogonal. In other words, if λ_i is not equal to λ_j , we have,

$$\underline{w}_j \underline{u}_i = 0 \quad (1.6)$$

However, in case of eigenvectors corresponding to the same eigenvalue λ_i , we have,

$$\underline{w}_i \underline{u}_i = C_i \quad (1.7)$$

where C_i is a non-zero constant.

Since, as noted above, the eigenvectors are determined only to within a scalar multiplier, it is common practice to normalize these vectors so that

$$\underline{w}_i \underline{u}_i = 1 \quad (1.8)$$

Eigenvalues and Stability:

The time-dependent characteristic of a mode corresponding to an eigenvalue λ_i is given by $e^{\lambda_i t}$. Therefore, the stability of the system is determined by the eigenvalues as follows:

1. A real eigenvalue corresponds to a non-oscillatory mode. A negative real eigenvalue represents a decaying mode. The larger its magnitude, the faster the decay. A positive real eigenvalue represents aperiodic monotonic instability.
2. Complex eigenvalues occur in conjugate pairs and each pair corresponds to an oscillatory mode. The real component of the eigenvalues gives the damping, and the imaginary component gives the frequency of oscillations. A negative real part represents damped oscillations whereas a positive real part represents oscillation of increasing amplitude. Thus, for a complex pair of eigenvalues given by,

$$\lambda = \sigma \pm j\omega \quad (1.9)$$

The frequency of oscillation in Hz is given by

$$f = \frac{\omega}{2\pi} \quad (1.10)$$

The damping ratio is given by

$$\zeta = -\frac{\sigma}{\sqrt{\sigma^2 + \omega^2}} \quad (1.11)$$

The damping ratio ζ determines the rate of decay of the amplitude of the oscillation. The time constant of amplitude decay is $\frac{1}{|\sigma|}$. In other words, the amplitude decays to $\frac{1}{e}$ or 37% of the initial amplitude in $\frac{1}{|\sigma|}$ seconds or in $\left(\frac{1}{2\pi} \frac{\sqrt{1-\zeta^2}}{\zeta}\right)$ cycles of oscillations. This also corresponds to $\left(\frac{f}{|\sigma|}\right)$ cycles. For example, a damping ratio of 5% means that in 3 oscillation periods the amplitude is damped to about $e^{-|\sigma|t} = e^{-\frac{|\sigma|}{f}(\text{cycles})} = e^{-0.3146 \times 3} = 0.3892$ of its initial value. The small-signal stability analysis program determines the dynamic performance of the system by computing the eigenvalues and eigenvectors of the state matrix of the linearized power system model. In a power system, it is required that all modes, i.e., all eigenvalues are stable. Moreover, it is desired that all electromechanical oscillations are damped out as quickly as possible.

1.3.2 Synchronizing and Damping Torque Analysis:

With electric power system, the change in electrical torque of a synchronous machine following a perturbation can be resolved into two components as follows:

$$\Delta T_e = T_S \Delta \delta + T_D \Delta S_m \quad (1.12)$$

where

- $T_S \Delta \delta$ is the component of torque change in phase with the rotor angle perturbation and is referred to as the synchronizing torque component; T_S is the synchronizing torque coefficient.
- $T_D \Delta S_m$ is the component of torque in phase with the speed deviation and is referred to as the damping torque component; T_D is the damping torque coefficient.

System stability depends on the existence of both components of torque for each of the synchronous machine. This analysis assumes that the rotor angle and the speed deviations oscillate sinusoidally. Hence, the phasor notations can be used to analyse the stability performance of power systems. Figure (1.1) is drawn based on the observation that

$$\frac{d\delta}{dt} = S_m \omega_B \quad (1.13)$$

and

$$\frac{d\Delta\delta}{dt} = \Delta S_m \omega_B \quad (1.14)$$

For sinusoidal oscillations

$$j\omega\Delta\delta(j\omega) = \Delta S_m(j\omega)\omega_B$$

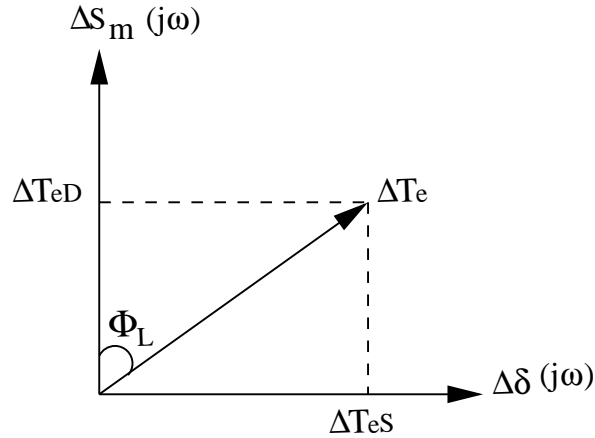


Figure 1.1: Phasor representation of sinusoidally varying angle, speed and torque deviations.

From the figure the damping torque component can be written as

$$\Delta T_{eD} = \Delta T_e \cos \phi_L \quad (1.15)$$

and the synchronizing torque component can be written as

$$\Delta T_{eS} = \Delta T_e \sin \phi_L \quad (1.16)$$

If either or both damping and synchronizing torques are negative, i.e., if $\Delta T_{eD} < 0$ and/or $\Delta T_{eS} < 0$, then the system is unstable. A negative damping torque implies that the response will be in the form of growing oscillations, and a negative synchronizing torque implies monotonic instability.

NOTE:

The phase angle ϕ_L can be related to the compensated phase angle obtained in the design of power system stabilizers -see section 3.3.2. In this analysis, the angle ϕ_L is measured taking $\Delta S_m(j\omega)$ phasor as reference and is treated as positive for lagging angle.

1.3.3 Frequency Response- and Residue- Based Analysis:

Frequency response is just another characterisation of a systems' transfer function between a given input and output. Frequency response methods allow a deeper insight into small-signal dynamics and have widespread use in the design of power system controllers. Frequency response can also be measured directly, even in a power system. It is thus an excellent method to validate mathematical models that are to be used in control design and stability analysis [6, 7].

Residues give the contribution of a mode to a transfer function. They also give the sensitivity of the corresponding eigenvalue to a positive feedback between the output of the transfer function and its input [5]. Thus, residues are useful to get an idea of which modes will be affected most by feedback. This concept has been used in [11] to determine the suitable location of power system stabilizers. An advantage of using residues in such analysis is that it takes into account the transfer function structure of the excitation system unlike participation factors. However, evaluation of residues dependent on the specific input/output combinations and may be computationally intensive for large systems.

1.3.4 Time-Domain Solution:

Conventional method solves the non-linear differential-algebraic system of equations numerically, employing numerical techniques to provide solution to each variable at rectangular intervals of time and thus, they basically provide time domain solutions. Time-domain techniques provide an exact determination of stability of non-linear systems both for small and large disturbances. However, the use of time response alone to look at small disturbance damping can be misleading. The choice of disturbance and selection of variables to be observed in time response are critical. The input, if not chosen properly, may not provide substantial excitation of the important modes. The observed response may contain many modes and the poorly damped modes may not be dominant. Number of modes depends on modeling details employed for different dynamic components. Larger systems may have a number of inter-area modes of similar frequencies, and it is quite difficult to separate them from a response in which more than one is excited. Therefore, for a large power system it is not possible to identify any desired mode and study their characteristics.

Of all these methods, eigenvalue or modal analysis is widely used for analysing the small-signal stability of power system [7, 12, 14].

1.4 Advantages of Eigenvalue or Modal Analysis:

With eigenvalue techniques, oscillations can be characterized easily, quickly and accurately. Different modes, which are mixed with each other in curves of time-domain simulation, are identified separately. Root loci plotted with variations in system parameters or operating conditions provide valuable insight into the dynamic characteristics of the system. Using eigenvectors coherent groups of generators which participate in a given swing mode can be identified. In addition, linear models can be used to design controllers that damp oscillations. Further, information regarding the most effective site of controller, tuning of existing one, installation of new controller can be decided.

From the eigenvalue-based analysis, time responses to any chosen small disturbance can be generated for comparison with field test results. In addition, frequency response characteristics of the model can be generated. This is useful for comparison with system models developed from frequency response measurements.

Eigenvalue or modal analysis describes the small-signal behavior of the system about an operating point, and does not take into account the nonlinear behavior of components such as controller's limits at large system perturbations. Further, design and analysis carried out using various indices such as participation factors, residues, etc. may lead to many alternate options. These options need to be verified for their effectiveness using system responses for small/large disturbances. In such cases, time-domain simulations are very essential. In this context, time-domain simulation, and modal analysis in the frequency domain should be used in a complement manner in analyzing small-signal stability of power systems [2, 15].

1.4.1 Computation of Eigenvalues:

Following are the important algorithms used in the literature [16, 17] to compute eigenvalues numerically.

1.4.1.1 QR Techniques:

The QR method is one of the most widely used decomposition methods for calculating eigenvalues of matrices. It uses a sequence of orthogonal similarity transformations. Similar to the LU factorization, the matrix A can also be factored into two matrices such that

$$A = QR \quad (1.17)$$

where Q is a unitary matrix, i.e., $Q^{-1} = Q^*$, and R is an upper triangular matrix, $*$ denotes complex conjugate transpose.

The following algorithm may be used for finding the eigenvalues [16]:

1. Perform QR factorization of $A_0 (= A)$. The QR factors are denoted as Q_0 and R_0 .
2. Compute $A_1 = R_0 Q_0$.
3. Perform QR factorization of A_1 . The QR factors are denoted as Q_1 and R_1 .
4. Repeat the above steps till convergence. In the k^{th} iteration, the matrix A_k converges to an upper triangular matrix with eigenvalues of A as its diagonal elements.

It is numerically stable, robust, and converges rapidly. The QR method with the support of inverse iteration scheme [6], has been used in many standard packages [12] to determine all eigenvalues to check interaction among various modes.

1.4.1.2 Arnoldi Method:

In large interconnected systems, it is either impractical or intractable to find all of the eigenvalues of the system state matrix due to restrictions on computer memory and computational speed. The Arnoldi method has been developed as an algorithm that iteratively computes k eigenvalues of an $n \times n$ matrix A , where k is typically much smaller than n . This method therefore bypasses many of the constraints imposed by large matrix manipulation required by methods such as QR decomposition. If the k eigenvalues are chosen selectively, they can yield rich information about the system under consideration, even without the full set of eigenvalues.

The basic approach of the Arnoldi method [17] is to iteratively update a low order matrix H whose eigenvalues successively approximate the selected eigenvalues of the larger A matrix, such that

$$AV = VH; \quad V^*V = I \quad (1.18)$$

where V is an $n \times k$ matrix and H is a $k \times k$ Hessenberg matrix. As the method progresses, the eigenvalues of A are approximated by the diagonal entries of H yielding

$$HV_i = V_i D_\lambda \quad (1.19)$$

where V_i is a $k \times k$ matrix whose columns are the eigenvectors of H (approximating the eigenvectors of A) and D_λ is a $k \times k$ matrix whose diagonal entries are the eigenvalues of H (approximating the eigenvalues of A).

In the original form, the Arnoldi method had poor numerical properties, the main problems being loss of orthogonality and slow convergence if several dominant eigenvalues are needed. These problems are solved by using complete re-orthogonalization and an iterative process in the modified Arnoldi method (MAM) [12].

NOTE: The following functions in MATLAB [13] are used in the programme to compute eigenvalues numerically:

- **eig**: It finds all eigenvalues and the corresponding eigenvectors. It uses Hessenberg/QZ factorization techniques.
- **eigs** : It uses modified Arnoldi method and is used to obtain the eigenvalues selectively and it can handle sparse matrices. It employs an algorithm based on ARPACK.

1.5 Modelling of Power System:

The behaviour of a power system is described by a set of n first order nonlinear ordinary differential equations of the following form

$$\dot{\underline{x}} = F(\underline{x}, \underline{u}, t) \quad (1.20)$$

where

$$\underline{x} = \begin{bmatrix} x_1 \\ x_2 \\ \vdots \\ x_n \end{bmatrix} \quad \underline{u} = \begin{bmatrix} u_1 \\ u_2 \\ \vdots \\ u_r \end{bmatrix} \quad F = \begin{bmatrix} f_1 \\ f_2 \\ \vdots \\ f_n \end{bmatrix}$$

The column vector \underline{x} is referred to as the state vector, and its entries x_i as state variables. The column vector \underline{u} is the vector of inputs to the system. These are the external signals that influence the performance of the system. Time is denoted by t , If the derivatives of the state variables are not explicit functions of time, the system is said to be *autonomous*. In this case, (1.20) simplifies to

$$\dot{\underline{x}} = F(\underline{x}, \underline{u}) \quad (1.21)$$

We are often interested in output variables which can be observed on the system. These may be expressed in terms of the state variables and the input variables in the following form:

$$\underline{y} = \underline{g}(\underline{x}, \underline{u}) \quad (1.22)$$

where

$$\underline{y} = \begin{bmatrix} y_1 \\ y_2 \\ \vdots \\ y_m \end{bmatrix} \quad \underline{g} = \begin{bmatrix} g_1 \\ g_2 \\ \vdots \\ g_m \end{bmatrix}$$

The column vector \underline{y} is the vector of outputs, and \underline{g} is a vector of nonlinear functions relating state and input variables to output variables. The set of equations (1.21) and (1.22) together constitute the differential algebraic equations (DAEs) for the system.

1.5.1 Linearization of DAEs:

Let \underline{x}_0 be the initial state vector and \underline{u}_0 be the input vector corresponding to the equilibrium point about which the small-signal performance is to be investigated. Since \underline{x}_0 and \underline{u}_0 satisfy (1.21), we have

$$\dot{\underline{x}}_0 = F(\underline{x}_0, \underline{u}_0) = 0 \quad (1.23)$$

Let us perturb the system from the above state, by letting

$$\underline{x} = \underline{x}_0 + \Delta \underline{x} \quad \underline{u} = \underline{u}_0 + \Delta \underline{u}$$

where the prefix Δ denotes a small deviation.

The new state must satisfy (1.21). Hence,

$$\begin{aligned} \dot{\underline{x}} &= \dot{\underline{x}}_0 + \Delta \dot{\underline{x}} \\ &= F[(\underline{x}_0 + \Delta \underline{x}), (\underline{u}_0 + \Delta \underline{u})] \end{aligned} \quad (1.24)$$

As the perturbations are assumed to be small, the nonlinear function $F(\underline{x}, \underline{u})$ can be expressed in terms of Taylor's series expansion. With terms involving second and higher order powers of $\Delta \underline{x}$ and $\Delta \underline{u}$ neglected, we can write

$$\begin{aligned} \dot{x}_i &= \dot{x}_{i0} + \Delta \dot{x}_i = f_i[(\underline{x}_0 + \Delta \underline{x}), (\underline{u}_0 + \Delta \underline{u})] \\ &= f_i(\underline{x}_0, \underline{u}_0) + \frac{\partial f_i}{\partial x_1} \Delta x_1 + \cdots + \frac{\partial f_i}{\partial x_n} \Delta x_n + \frac{\partial f_i}{\partial u_1} \Delta u_1 + \cdots + \frac{\partial f_i}{\partial u_r} \Delta u_r \end{aligned} \quad (1.25)$$

Since $\dot{x}_{i0} = f_i(\underline{x}_0, \underline{u}_0) = 0$, we obtain

$$\Delta \dot{x}_i = \frac{\partial f_i}{\partial x_1} \Delta x_1 + \cdots + \frac{\partial f_i}{\partial x_n} \Delta x_n + \frac{\partial f_i}{\partial u_1} \Delta u_1 + \cdots + \frac{\partial f_i}{\partial u_r} \Delta u_r$$

for $i = 1, 2, \dots, n$.

In a like manner, from (1.22), we have

$$\Delta y_j = \frac{\partial g_j}{\partial x_1} \Delta x_1 + \dots + \frac{\partial g_j}{\partial x_n} \Delta x_n + \frac{\partial g_j}{\partial u_1} \Delta u_1 + \dots + \frac{\partial g_j}{\partial u_r} \Delta u_r$$

for $j = 1, 2, \dots, m$.

Therefore, the linearized forms of (1.21) and (1.22) in matrix notation can be written as

$$\Delta \dot{\underline{x}} = A \Delta \underline{x} + B \Delta \underline{u} \quad (1.26)$$

$$\Delta \underline{y} = C \Delta \underline{x} + D \Delta \underline{u} \quad (1.27)$$

where

$$A = \begin{bmatrix} \frac{\partial f_1}{\partial x_1} & \dots & \frac{\partial f_1}{\partial x_n} \\ \dots & \dots & \dots \\ \frac{\partial f_n}{\partial x_1} & \dots & \frac{\partial f_n}{\partial x_n} \end{bmatrix} \quad B = \begin{bmatrix} \frac{\partial f_1}{\partial u_1} & \dots & \frac{\partial f_1}{\partial u_r} \\ \dots & \dots & \dots \\ \frac{\partial f_n}{\partial u_1} & \dots & \frac{\partial f_n}{\partial u_r} \end{bmatrix}$$

$$C = \begin{bmatrix} \frac{\partial g_1}{\partial x_1} & \dots & \frac{\partial g_1}{\partial x_n} \\ \dots & \dots & \dots \\ \frac{\partial g_m}{\partial x_1} & \dots & \frac{\partial g_m}{\partial x_n} \end{bmatrix} \quad D = \begin{bmatrix} \frac{\partial g_1}{\partial u_1} & \dots & \frac{\partial g_1}{\partial u_r} \\ \dots & \dots & \dots \\ \frac{\partial g_m}{\partial u_1} & \dots & \frac{\partial g_m}{\partial u_r} \end{bmatrix}$$

The above partial derivatives are evaluated at the equilibrium point about which the small perturbation is being analyzed.

$\Delta \underline{x}$ is the state vector of dimension $(n \times 1)$

$\Delta \underline{y}$ is the output vector of dimension $(m \times 1)$

$\Delta \underline{u}$ is the input vector of dimension $(r \times 1)$

A is the state or plant matrix of size $(n \times n)$

B is the control or input matrix of size $(n \times r)$

C is the output matrix of size $(m \times n)$

D is the (feed forward) matrix which defines the proportion of input which appears directly in the output of size $(m \times r)$.

In general, to determine the small-signal stability behaviour of a non-linear dynamic system it is sufficient to obtain the eigenvalues of A matrix indicated above. However, for power system applications, determination of A matrix may be more involved because of intricate relationship between the state variables and the algebraic variables. In practice, the following are the two important methods for obtaining the state matrix:

1. Numerical approach.
2. Analytical approach.

Numerical approach:

In this approach, the state matrix is obtained using numerical differentiation. Here, starting from a valid equilibrium condition \underline{x}_0 , a second state vector is created \underline{x}_i , in which the i^{th} component of \underline{x}_0 is perturbed by a very small amount and the $\dot{\underline{x}}_i$ is computed using the F . This provides an intermediate state matrix in which only i^{th} column is non zero. This process is repeated until all columns of the state matrix are obtained by sequentially perturbing all entries of \underline{x}_0 . After constructing the state matrix, eigenvalues can be obtained in an usual manner [18]. In SIMULINK toolbox [19], a function namely, `linmod` is available for numerical linearization of systems.

Analytical approach:

In this approach, analytical expressions are obtained for all partial derivatives of variables. These expression are assembled in such a way that all elements are written only in terms of state variables. In the literature, the following two basic approaches are employed:

1. Load flow Jacobian-based approach [8].
2. Current injection-based approach [1, 2].

1.5.1.1 Load Flow Jacobian-based Approach:

The nonlinear model is of the form

$$\dot{\underline{x}} = f(\underline{x}, \underline{y}, \underline{u}) \quad (1.28)$$

$$0 = \mathbf{g}(\underline{x}, \underline{y}) \quad (1.29)$$

where the vector \underline{y} indicates both machine currents \underline{I}_{d-q} and $\bar{\underline{V}}$ vectors. Expression (1.29) consists of the stator algebraic equations and the network equations in the power-balance form. To show explicitly the traditional load flow equations and the other algebraic equations, \underline{y} is partitioned as

$$\begin{aligned} \underline{y} &= [\underline{I}_{d-q}^t \theta_1 V_1 \cdots V_m | \theta_2 \cdots \theta_n V_{m+1} \cdots V_n]^T \\ \underline{y} &= [\underline{y}_a^t | \underline{y}_b^t] \end{aligned} \quad (1.30)$$

Here, the vector \underline{y}_b corresponds to the load flow variables, and the vector \underline{y}_a corresponds to the other algebraic variables. Linearizing (1.28) and (1.29) around an operating point gives,

$$\begin{bmatrix} \frac{d\Delta \underline{x}}{dt} \\ 0 \end{bmatrix} = \begin{bmatrix} A & B \\ C & J_{AE} \end{bmatrix} \begin{bmatrix} \Delta \underline{x} \\ \Delta \underline{y} \end{bmatrix} + E [\Delta \underline{u}] \quad (1.31)$$

where

$$\Delta \underline{y} = \begin{bmatrix} \Delta \underline{y}_a \\ \Delta \underline{y}_b \end{bmatrix}$$

$$J_{AE} = \begin{bmatrix} D_{11} & D_{12} \\ D_{21} & J_{LF} \end{bmatrix} \quad (1.32)$$

Eliminating $\Delta \underline{y}_a$, $\Delta \underline{y}_b$, we get $\Delta \dot{\underline{x}} = A_{sys} \Delta \underline{x}$ where $A_{sys} = (A - BJ_{AE}^{-1}C)$ and J_{LF} is the load flow Jacobian. The model represented by (1.31) is useful in both small-signal stability analysis and voltage stability, since J_{LF} is explicitly shown as part of the system differential-algebraic Jacobian.

1.5.1.2 Current Injection-based Approach:

Generator Equations:

For i^{th} generator, the differential equations are written as

$$\Delta \dot{\underline{x}}_g = [A_g] \Delta \underline{x}_g + [B_g^p] \Delta V_g^p + [E_g] \Delta \underline{u}_c \quad (1.33)$$

where $\Delta \underline{u}_c$ is the vector of small perturbation in the reference input variables of the generator controllers given by $\Delta \underline{u}_c = [(\Delta V_{ref} + \Delta V_s), \Delta \omega_B]^T$. With $\Delta \omega_B$ is assumed to be zero, we have $\Delta \underline{u}_c = [\Delta V_{ref} + \Delta V_s]$ and ΔV_g^p are the small deviations in the generator terminal voltage expressed in polar coordinates given by

$$\Delta V_g^p = \begin{bmatrix} V_{g0} \Delta \theta_g \\ \Delta V_g \end{bmatrix}$$

Using currents as the output variables of the generator, we have in Kron's reference frame

$$\Delta I_g = \begin{bmatrix} \Delta I_{Dg} \\ \Delta I_{Qg} \end{bmatrix} = [C_g] \Delta \underline{x}_g + [D_g^p] \Delta V_g^p \quad (1.34)$$

The derivations for I_{Dg} and I_{Qg} are given in Appendix- C.4.

In this analysis, a synchronous machine is represented by 2.2 model -see Figure C.1. In addition, three IEEE-type exciters [2, 22]- single-time constant exciter, DC1A exciter and AC4A exciter, and two IEEE specified turbines [23]- hydro turbine and reheat-type

steam turbine, are considered. This results in the state variable vector given by

$$\Delta \underline{x}_g = \begin{bmatrix} \Delta \delta & \Delta S_m & \Delta \psi_f & \Delta \psi_h & \Delta \psi_g & \Delta \psi_k & \Delta E_{fd} & \Delta v_R \\ \Delta x_B & \Delta x_F & \Delta x_1 & \Delta x_2 & \Delta x_3 & \Delta y_1 & \Delta P_{GV} & \Delta z \end{bmatrix}^T$$

The association of different state variables with different components are depicted in Appendix -A. The nonzero elements of matrix $[A_g]$, $[B_g^p]$, $[C_g]$, $[D_g^p]$, and $[E_g]$ are given in Appendix -C,-D and -E.

Transformation of Matrices from Polar to Rectangular forms:

It is given that

$$\Delta V_g^p = \begin{bmatrix} V_{g0} \Delta \theta_g \\ \Delta V_g \end{bmatrix}$$

In rectangular coordinates we have,

$$\Delta V_g^r = \begin{bmatrix} \Delta V_{Qg} \\ \Delta V_{Dg} \end{bmatrix}$$

The two expressions are related by

$$\Delta V_g^p = \frac{1}{V_{g0}} \begin{bmatrix} -V_{Dg0} & V_{Qg0} \\ V_{Qg0} & V_{Dg0} \end{bmatrix} \begin{bmatrix} \Delta V_{Qg} \\ \Delta V_{Dg} \end{bmatrix} = [P] \Delta V_g^r$$

The derivation of $[P]$ matrix is given in Appendix -B.1.

It can be seen that

$$[P]^{-1} = [P]$$

The matrices $[B_g^r]$ is obtained as

$$[B_g^r] = [B_g^p] [P]$$

where $[B_g^p] = [B_g^p(2,1) \ B_g^p(2,2)]$ and $[B_g^r] = [B_g^r(2,1) \ B_g^r(2,2)]$

Similarly, $[D_g^r]$ can be obtained as

$$[D_g^r] = [D_g^p] [P]$$

The superscript r indicates the representation of matrices in rectangular coordinates.

Network Equations:

The linearized network equations can be expressed either using admittance matrix (in DQ variables) or using Jacobian matrix (obtained from power balance equations). Using the former, we have

$$[Y_{DQ}]_{(2n_b \times 2n_b)} \Delta V_{QD(2n_b \times 1)} = \Delta I_{DQ(2n_b \times 1)} \quad (1.35)$$

where each element of $[Y_{DQ}]$ is a 2x2 matrix. For example,

$$Y_{DQ}(i, j) = \begin{bmatrix} B_{ij} & G_{ij} \\ G_{ij} & -B_{ij} \end{bmatrix}$$

ΔV_{QDi} and ΔI_{DQi} are vectors with elements

$$\Delta V_{QDi} = \begin{bmatrix} \Delta V_{Qi} \\ \Delta V_{Di} \end{bmatrix} \text{ and } \Delta I_{DQi} = \begin{bmatrix} \Delta I_{Di} \\ \Delta I_{Qi} \end{bmatrix}$$

Note that the voltages are expressed with ΔV_{Qi} preceding ΔV_{Di} . On the other hand, the currents are expressed with ΔI_{Di} preceding ΔI_{Qi} . This is deliberately done so that the matrix $[Y_{DQ}]$ is a real symmetric matrix (if phase shifting transformers are not considered). Also note that the admittance matrix representation is independent of the operating point.

Derivation of System Equations:

Let the number of generators in the system be n_g , the number of loads be m_l . Let the number of buses in the network be n_b . Rewriting (1.35) we have,

$$[Y_{DQ}] \Delta V_{QD} = [P_G] \Delta I_G - [P_L] \Delta I_L \quad (1.36)$$

where $[P_G]$ is a $(2n_b \times 2n_g)$ and $[P_L]$ is a $(2n_b \times 2m_l)$ matrix with elements

$$P_G(i, j) = \begin{bmatrix} 1 & 0 \\ 0 & 1 \end{bmatrix}$$

if generator j is connected to bus i .

Otherwise,

$$P_G(i, j) = \begin{bmatrix} 0 & 0 \\ 0 & 0 \end{bmatrix}$$

Similarly, $[P_L]$ can be defined. $P_L(i, j)$ is a unit matrix of dimension 2×2 if load j is connected to bus i , otherwise, $P_L(i, j)$ is a null matrix. Notice that the signs associated

with I_L is negative as the load currents are assumed to flow away from the bus (load convention).

NOTE:

The structure of $[P_G]$ and $[P_L]$ matrices for a 4 machine, 10-bus power system is presented in Appendix -B.2.

The load current ΔI_{Lj} at the j^{th} load bus can be expressed as

$$\Delta I_{Lj} = [Y_L]_j \Delta V_{Lj} \quad (1.37)$$

where

$$\begin{aligned} \Delta I_{Lj} &= [\Delta I_{DLj} \quad \Delta I_{QLj}]^T \\ \Delta V_{Lj} &= [\Delta V_{QLj} \quad \Delta V_{DLj}]^T \end{aligned}$$

and

$$[Y_L]_j = \begin{bmatrix} -B_{DQ} & G_{DD} \\ G_{QQ} & B_{QD} \end{bmatrix}$$

The elements of $[Y_L]_j$ are given in Appendix -G, and $[Y_L]$ is a block diagonal matrix. In general we have,

$$\Delta V_L = [P_L]^T \Delta V_{QD}$$

Using the above equation in (1.37) we get,

$$\Delta I_L = [Y_L] [P_L]^T \Delta V_{QD} \quad (1.38)$$

The generator current vector, ΔI_G is collection of the quantities $\Delta I_{g1}, \Delta I_{g2}, \Delta I_{g3} \dots \Delta I_{gn_g}$ and using (1.34), ΔI_G can be expressed as

$$\Delta I_G = [C_G] \Delta \underline{X}_G - [Y_G] \Delta \underline{V}_G \quad (1.39)$$

where

$$\Delta \underline{X}_G^T = [\Delta x_{g1}^T \quad \Delta x_{g2}^T \quad \dots \Delta x_{gn_g}^T]$$

$$\Delta \underline{V}_G^T = [\Delta V_{g1}^{Tr} \quad \Delta V_{g2}^{Tr} \quad \dots \Delta V_{gn_g}^{Tr}]$$

$$\Delta I_G^T = \begin{bmatrix} \Delta I_{g1}^T & \Delta I_{g2}^T & \dots & \Delta I_{gn_g}^T \end{bmatrix}$$

$[C_G]$ and $[Y_G]$ matrices are given by,

$$[C_G] = \text{Diag} [C_{g1} \ C_{g2} \ \dots C_{gn_g}]$$

$$[Y_G] = \text{Diag} \begin{bmatrix} -D_{g1}^r & -D_{g2}^r & \dots & -D_{gn_g}^r \end{bmatrix}$$

We know that

$$\Delta \underline{V}_G = [P_G]^T \Delta V_{QD} \quad (1.40)$$

Using the above equation, (1.39) can be rewritten as

$$\Delta I_G = [C_G] \Delta \underline{X}_G - [Y_G] [P_G]^T \Delta V_{QD} \quad (1.41)$$

Substituting (1.38) and (1.41) in (1.36) we get

$$[Y_{DQ}] \Delta V_{QD} = [P_G] [C_G] \Delta \underline{X}_G - [P_G] [Y_G] [P_G]^T \Delta V_{QD} - [P_L] [Y_L] [P_L]^T \Delta V_{QD}$$

Rearranging the terms associated with ΔV_{QD} we get

$$\begin{bmatrix} Y'_{DQ} \end{bmatrix} \Delta V_{QD} = [P_G] [C_G] \Delta \underline{X}_G \quad (1.42)$$

where

$$\begin{bmatrix} Y'_{DQ} \end{bmatrix} = [Y_{DQ}] + [P_G] [Y_G] [P_G]^T + [P_L] [Y_L] [P_L]^T$$

Solving for ΔV_{QD} from (1.42) and using it in (1.40) we get $\Delta \underline{V}_G$ as,

$$\Delta \underline{V}_G = [P_G]^T \begin{bmatrix} Y'_{DQ} \end{bmatrix}^{-1} [P_G] [C_G] \Delta \underline{X}_G \quad (1.43)$$

From (1.33), the collection of all the generator equations is expressed by

$$\Delta \dot{\underline{X}}_G = [A_G] \Delta \underline{X}_G + [B_G] \Delta V_G + [E_G] \Delta \underline{U}_c \quad (1.44)$$

where

$$\begin{aligned} [A_G] &= \text{Diag} [A_{g1} \ A_{g2} \ \cdots \ A_{gn_g}] \\ [B_G] &= \text{Diag} [B_{g1}^r \ B_{g2}^r \ \cdots \ B_{gn_g}^r] \\ [E_G] &= \text{Diag} [E_{g1} \ E_{g2} \ \cdots \ E_{gn_g}] \\ \Delta \underline{U}_c^T &= [\Delta \underline{u}_{c1}^T, \Delta \underline{u}_{c2}^T \cdots \Delta \underline{u}_{cn_g}^T] \end{aligned}$$

Substituting (1.43) in (1.44) gives,

$$\Delta \dot{X}_G = [A_T] \Delta X_G + [E_G] \Delta \underline{U}_c \quad (1.45)$$

where

$$[A_T] = [A_G] + [B_G] [P_G]^T [Y'_{DQ}]^{-1} [P_G] [C_G] \quad (1.46)$$

Since analytical approach provides better insight into linearization of system of equations and it is more accurate compared to numerical approach (which may suffer from the problem of inaccurate estimates depending upon the amount of perturbation chosen), in this report, the current injection-based analytical method is employed and the system matrix $[A_T]$ given in (1.46) is used to perform the eigenvalue analysis.

1.6 Modal Analysis of Linear Systems:

For an n^{th} order LTI system, the zero-input-response, i.e., the natural response can be described in state space form as [4].

$$\dot{\underline{x}} = A \underline{x} \quad (1.47)$$

with initial value of states, $\underline{x}(0)$ and the state matrix A is of dimension $(n \times n)$.

Consider the transformation given by,

$$\underline{x} = U \underline{y} \quad (1.48)$$

where U is assumed to be a matrix of right eigenvectors of A , pertaining to distinct eigenvalues, $[\lambda_1, \lambda_2, \cdots, \lambda_n]$ of A .

From (1.47) we have

$$\begin{aligned} U \dot{\underline{y}} &= A U \underline{y} \\ \dot{\underline{y}} &= U^{-1} A U \underline{y} \end{aligned} \quad (1.49)$$

The operation, $U^{-1} A U$ represents the similarity transformation such that

$$W A U = D_\lambda \quad (1.50)$$

where $W = U^{-1}$, is a matrix of left eigenvector of A .

$$U = \begin{bmatrix} \vdots & \vdots & \cdots & \vdots \\ \underline{u}_1 & \underline{u}_2 & \cdots & \underline{u}_n \\ \vdots & \vdots & \cdots & \vdots \end{bmatrix} \quad \text{with } A \underline{u}_i = \lambda_i \underline{u}_i \quad i = 1, 2, 3, \dots, n$$

$$W = \begin{bmatrix} \cdots & \underline{w}_1 & \cdots \\ \cdots & \underline{w}_2 & \cdots \\ \vdots & \vdots & \vdots \\ \cdots & \underline{w}_n & \cdots \end{bmatrix} \quad \text{with } \underline{w}_j A = \lambda_j \underline{w}_j \quad j = 1, 2, 3, \dots, n$$

and

$$D_\lambda = \begin{bmatrix} \lambda_1 & & & \\ & \lambda_2 & & \\ & & \ddots & \\ & & & \lambda_n \end{bmatrix}$$

NOTE:

1. \underline{u}_i is a column vector and \underline{w}_j is a row vector.
2. \underline{u}_i and \underline{w}_j are orthonormal vector, i.e.,

$$\begin{aligned} \underline{w}_j \underline{u}_i &= 1 \quad \text{for } i = j \\ &= 0 \quad \text{for } i \neq j \end{aligned} \quad (1.51)$$

Using (1.50) in (1.49) we have,

$$\dot{\underline{y}} = D_\lambda \underline{y} \quad (1.52)$$

From (1.48), the initial value of \underline{y} is given by

$$\underline{y}(0) = U^{-1} \underline{x}(0) = W \underline{x}(0) \quad (1.53)$$

The solution of (1.52) is obtained as

$$\underline{y}(t) = \begin{bmatrix} y_1(t) \\ y_2(t) \\ \vdots \\ y_n(t) \end{bmatrix} = \begin{bmatrix} e^{\lambda_1 t} & & & \\ & e^{\lambda_2 t} & & \\ & & \ddots & \\ & & & e^{\lambda_n t} \end{bmatrix} \begin{bmatrix} y_1(0) \\ y_2(0) \\ \vdots \\ y_n(0) \end{bmatrix}$$

From (1.48) and (1.53) we have,

$$\begin{bmatrix} x_1(t) \\ x_2(t) \\ \vdots \\ x_n(t) \end{bmatrix} = \begin{bmatrix} \underline{u}_1 & \underline{u}_2 & \cdots & \underline{u}_n \end{bmatrix} \begin{bmatrix} e^{\lambda_1 t} \underline{w}_1 \underline{x}(0) \\ e^{\lambda_2 t} \underline{w}_2 \underline{x}(0) \\ \vdots \\ e^{\lambda_n t} \underline{w}_n \underline{x}(0) \end{bmatrix}$$

or

$$\begin{bmatrix} x_1(t) \\ x_2(t) \\ \vdots \\ x_n(t) \end{bmatrix} = \begin{bmatrix} \vdots \\ \underline{u}_1 \\ \vdots \end{bmatrix} e^{\lambda_1 t} \underline{w}_1 \underline{x}(0) + \begin{bmatrix} \vdots \\ \underline{u}_2 \\ \vdots \end{bmatrix} e^{\lambda_2 t} \underline{w}_2 \underline{x}(0) + \cdots + \begin{bmatrix} \vdots \\ \underline{u}_n \\ \vdots \end{bmatrix} e^{\lambda_n t} \underline{w}_n \underline{x}(0)$$

$$\text{or} \quad \underline{x}(t) = \sum_{i=1}^n (\underline{w}_i \underline{x}(0)) e^{\lambda_i t} \underline{u}_i \quad (1.54)$$

NOTE:

1. $(\underline{w}_i \underline{x}(0))$ is a scalar and it gives the contribution of the initial condition $\underline{x}(0)$ to the i^{th} mode. In other words, \underline{u}_i determines to what extent the i^{th} mode gets excited (in a state) for a given initial condition vector $\underline{x}(0)$. Thus, a left eigenvector carries mode controllability information.
2. \underline{u}_i describes the activity of each state variable in i^{th} mode. In other words, it shows how i^{th} mode of oscillation is distributed among the system states. Thus, it is said to describe the *mode shape* of each state variable in i^{th} mode. The magnitude, $|u_{ki}|$ gives the relative magnitude of activity and the angle, $\angle u_{ki}$ represents relative phase displacement of k^{th} state in constituting the i^{th} mode. The angle information will be useful to group machines which swing together in a mode. A right eigenvector carries information regarding on which state variables the mode is more observable.

If $\underline{x}(0) = \underline{u}_j$ then from (1.54), we have

$$\underline{x}(t) = \sum_{i=1}^n (\underline{w}_i \ \underline{u}_j) e^{\lambda_i t} \underline{u}_i$$

Using (1.51), a non zero value results only for $i = j$, hence we get,

$$\underline{x}(t) = (\underline{w}_j \ \underline{u}_j) e^{\lambda_j t} \underline{u}_j \quad (1.55)$$

The above equation implies that only j^{th} mode is excited.

Further, (1.55) is re-written as

$$\underline{x}(t) = \sum_{k=1}^n (w_{jk} \ u_{kj}) e^{\lambda_j t} \underline{u}_j \quad (1.56)$$

where w_{jk} (u_{kj}) represents the k^{th} entry of the j^{th} left(right) eigenvectors, \underline{w}_j (\underline{u}_j) of A , which are normalized so that (1.51) is valid.

1.6.1 Eigenvalue Sensitivity - Participation Matrix:

In the analysis of large power systems. it is desirable to know the level of impact that a set of state variables has on a given mode so that methods can be devised to control those modes. In this regard, eigenvalue sensitivity analysis- participation factor, provides a tool to identify the nature of modes. In the following lines, a derivation has been presented to obtain the participation matrix [5].

Assuming that the eigenvalues are distinct, we have

$$A\underline{u}_j = \lambda_j \underline{u}_j \quad (1.57)$$

Now consider,

$$\left(\frac{\partial A}{\partial a_{rs}} \right) \underline{u}_j + A \left(\frac{\partial \underline{u}_j}{\partial a_{rs}} \right) = \left(\frac{\partial \lambda_j}{\partial a_{rs}} \right) \underline{u}_j + \lambda_j \left(\frac{\partial \underline{u}_j}{\partial a_{rs}} \right)$$

where a_{rs} is an element in the A matrix in the r^{th} row and s^{th} column position.

Simplifying the above expression, we get,

$$\left(\frac{\partial A}{\partial a_{rs}} \right) \underline{u}_j + A \left(\frac{\partial \underline{u}_j}{\partial a_{rs}} \right) - \lambda_j \left(\frac{\partial \underline{u}_j}{\partial a_{rs}} \right) = \left(\frac{\partial \lambda_j}{\partial a_{rs}} \right) \underline{u}_j$$

$$\left(\frac{\partial A}{\partial a_{rs}}\right) \underline{u}_j + (A - \lambda_j I) \left(\frac{\partial \underline{u}_j}{\partial a_{rs}}\right) = \left(\frac{\partial \lambda_j}{\partial a_{rs}}\right) \underline{u}_j \quad (1.58)$$

Pre-multiply the above equation by the left eigenvector \underline{w}_j , we get,

$$\underline{w}_j \left(\frac{\partial A}{\partial a_{rs}}\right) \underline{u}_j + \underline{w}_j (A - \lambda_j I) \left(\frac{\partial \underline{u}_j}{\partial a_{rs}}\right) = \underline{w}_j \left(\frac{\partial \lambda_j}{\partial a_{rs}}\right) \underline{u}_j \quad (1.59)$$

Since we know that $\underline{w}_j (A - \lambda_j I) = 0$ (from the definition of the left eigenvectors) we have,

$$\underline{w}_j \left(\frac{\partial \lambda_j}{\partial a_{rs}}\right) \underline{u}_j = \underline{w}_j \left(\frac{\partial A}{\partial a_{rs}}\right) \underline{u}_j$$

Since $\frac{\partial A}{\partial a_{rs}}$ is a scalar, we can write

$$\frac{\partial \lambda_j}{\partial a_{rs}} = \frac{\underline{w}_j \left(\frac{\partial A}{\partial a_{rs}}\right) \underline{u}_j}{\underline{w}_j \underline{u}_j}$$

Note that in $\frac{\partial A}{\partial a_{rs}}$ all elements are zero except $(r, s)^{th}$ element which is 1. Therefore,

$$\frac{\partial \lambda_j}{\partial a_{rs}} = \frac{w_{jr} u_{sj}}{\underline{w}_j \underline{u}_j} \quad (1.60)$$

where $w_{jr} = \underline{w}_j(r)$ and $u_{sj} = \underline{u}_j(s)$, r^{th} element and s^{th} element in the vectors \underline{w}_j and \underline{u}_j respectively.

Participation Matrix is obtained when $r = s = k$ in (1.60), (i.e., when eigenvalue sensitivity is obtained corresponding to the diagonal element, a_{kk} of A). With this substitution for r and s , we get,

$$P_{jk} = \frac{\partial \lambda_j}{\partial a_{kk}} = \frac{w_{jk} u_{kj}}{\underline{w}_j \underline{u}_j} \quad (1.61)$$

NOTE:

1. In the above expression for the participation factor, a division by a scalar $\underline{w}_j \underline{u}_j$ normalizes the eigenvectors.
2. In MATLAB, if `eig` function is used, then the eigenvectors are inherently normalized. If `eigs` is used, the normalization should be carried out using the above expression.

Using (1.61) in (1.56) we get

$$\underline{x}(t) = \sum_{k=1}^n P_{jk} e^{\lambda_j t} \underline{u}_j$$

Note that the value of P_{jk} is decided based on the value of u_{kj} for a given w_{jk} . From this it can be said that u_{kj} measures the activity of k^{th} state variable in j^{th} mode, w_{jk} weighs the contribution of this activity to the mode. Thus, P_{jk} can be used as a relative measure to indicate the net participation of the k^{th} state variable in building the time response of the j^{th} mode [20, 21].

REMARKS:

1. The components obtained in (1.60) are referred to as dimensional “generalised participation”. As a special case when we set $r = s = k$, the components constitute a P matrix. The entries, P_{jk} with $j, k = 1, 2, \dots, n$, of the P matrix are termed as the participation factors (PF) of the system.
2. w_{jk} and u_{kj} when taken separately, are unit dependent. However, P_{jk} s’ are dimensionless, i.e., independent of the units used for the state variable. This provides a straight forward measure of relative participation of states in a mode.
3. The sum of the values of all the entries of j^{th} row or column of P is always equal to 1.0, i.e.,

$$\sum_{k=1}^n P_{jk} = 1.0 \quad \text{and} \quad \sum_{j=1}^n P_{jk} = 1.0 \quad (1.62)$$

4. Even if P_{jk} is a complex number, the condition given by (1.62) is satisfied. However, the relative participation is measured by computing the absolute value of P_{jk} .
5. The participation factor, P_{jk} represents the sensitivity of the j^{th} eigenvalue to the variations in k^{th} diagonal element, (a_{kk}) of A matrix. For example, a positive real participation factor denotes that an introduction of a damping coefficient usually shifts λ to the left.
6. A large P_{jk} indicates that j^{th} eigenvalue is very sensitive to a local feedback around the k^{th} state variable.
7. The participation factor (or residue)-based analysis is valid only if the eigenvalues are distinct. If eigenvalues are nearly identical, the mode shapes given by the right-eigenvectors are physically meaningless and participation factors do not give the

correct sensitivity information. It is observed in [5] that a situation of eigenvalues with degree of multiplicity greater than 1 rarely arises in power systems. Even in such cases, frequency response or linear response calculated using these eigenvalues/eigenvectors is correct.

The complete eigenvalue analysis of dynamic system is demonstrated below through a linear spring-mass system.

1.7 Spring-Mass System Example:

Let us consider a multi-mass, multi-spring system as shown in Figure (1.2). There are 2 small masses connected by a very stiff spring which in turn are connected to a relatively larger mass via a much less stiff spring.

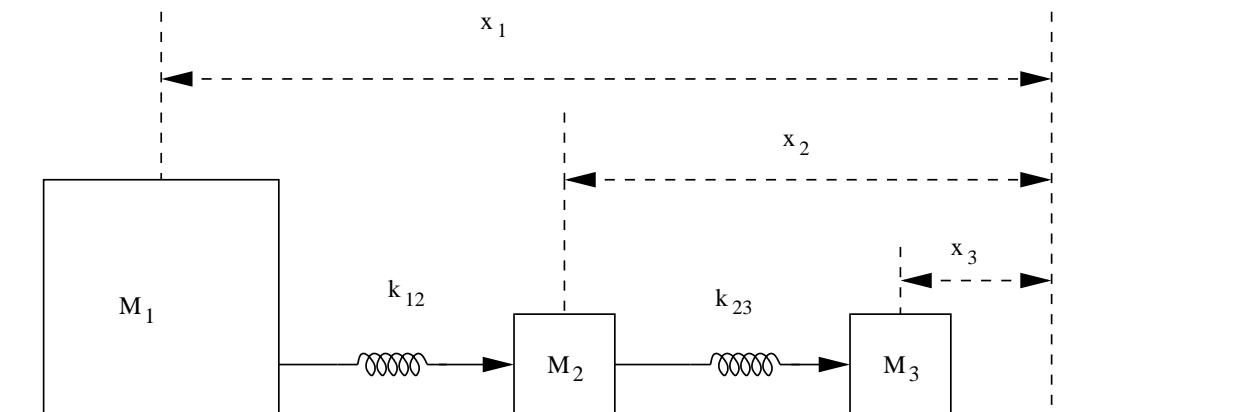


Figure 1.2: Multi-mass multi-spring system

An equivalent circuit for the system is shown in Figure 1.3. Choosing the state variable vector as $\underline{x} = [x_1, x_2, x_3, v_1, v_2, v_3]^T$, we can write the dynamic equation in state-space as

$$\frac{dx_1}{dt} = v_1 \quad (1.63)$$

$$\frac{dx_2}{dt} = v_2 \quad (1.64)$$

$$\frac{dx_3}{dt} = v_3 \quad (1.65)$$

$$\frac{dv_1}{dt} = -\frac{k_{12}}{M_1} (x_1 - x_2) \quad (1.66)$$

$$\frac{dv_2}{dt} = \frac{k_{12}}{M_2} x_1 - \left(\frac{k_{12}}{M_2} + \frac{k_{23}}{M_2} \right) x_2 + \frac{k_{23}}{M_2} x_3 \quad (1.67)$$

$$\frac{dv_3}{dt} = \frac{k_{23}}{M_3} (x_2 - x_3) \quad (1.68)$$

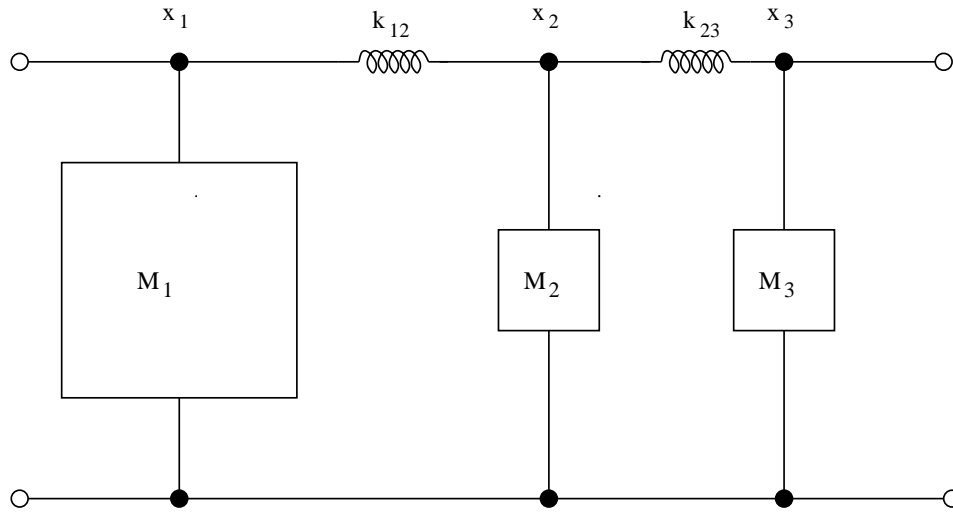


Figure 1.3: Equivalent circuit for multi-mass multi-spring system.

Writing the above equations in matrix form, we get,

$$\begin{bmatrix} \dot{x}_1 \\ \dot{x}_2 \\ \dot{x}_3 \\ \dot{v}_1 \\ \dot{v}_2 \\ \dot{v}_3 \end{bmatrix} = \begin{bmatrix} 0 & 0 & 0 & 1 & 0 & 0 \\ 0 & 0 & 0 & 0 & 1 & 0 \\ 0 & 0 & 0 & 0 & 0 & 1 \\ -\frac{k_{12}}{M_1} & \frac{k_{12}}{M_1} & 0 & 0 & 0 & 0 \\ \frac{k_{12}}{M_2} & -\left(\frac{k_{12}}{M_2} + \frac{k_{23}}{M_2}\right) & \frac{k_{23}}{M_2} & 0 & 0 & 0 \\ 0 & \frac{k_{23}}{M_3} & -\frac{k_{23}}{M_3} & 0 & 0 & 0 \end{bmatrix} \begin{bmatrix} x_1 \\ x_2 \\ x_3 \\ v_1 \\ v_2 \\ v_3 \end{bmatrix}$$

or

$$\begin{bmatrix} \dot{x}_1 \\ \dot{x}_2 \\ \dot{x}_3 \\ \dot{v}_1 \\ \dot{v}_2 \\ \dot{v}_3 \end{bmatrix} = \begin{bmatrix} \begin{bmatrix} 0 \end{bmatrix}_{3 \times 3} & \begin{bmatrix} I \end{bmatrix}_{3 \times 3} \\ \begin{bmatrix} A_k \end{bmatrix}_{3 \times 3} & \begin{bmatrix} 0 \end{bmatrix}_{3 \times 3} \end{bmatrix} \begin{bmatrix} x_1 \\ x_2 \\ x_3 \\ v_1 \\ v_2 \\ v_3 \end{bmatrix} = A \underline{x}$$

where

$$[A_k] = \begin{bmatrix} -\frac{k_{12}}{M_1} & \frac{k_{12}}{M_1} & 0 \\ \frac{k_{12}}{M_2} & -\left(\frac{k_{12}}{M_2} + \frac{k_{23}}{M_2}\right) & \frac{k_{23}}{M_2} \\ 0 & \frac{k_{23}}{M_3} & -\frac{k_{23}}{M_3} \end{bmatrix}$$

Choose the parameters as follows:

$$\begin{aligned} k_{12} &= 2 \text{ N/m}; \quad k_{23} = 20 \text{ N/m}; \\ M_1 &= 10 \text{ kg}; \quad M_2 = 1 \text{ kg}; \quad M_3 = 1 \text{ kg} \end{aligned}$$

We can observe that $k_{23} \gg k_{12}$. This means is that masses M_2 and M_3 more rigidly coupled than the group M_2 and M_3 with M_1 . Also observe that $M_1 \gg M_2$ and M_3 . From the knowledge of a simple spring-mass system it can be predicted that low frequency oscillations are mainly due to mass M_1 and high frequency oscillation is predominantly associated with M_2 and M_3 . Substituting the numerical values of the parameters, we get $[A_k]$ as

$$[A_k] = \begin{bmatrix} -0.2 & 0.2 & 0 \\ 2 & -22 & 20 \\ 0 & 20 & -20 \end{bmatrix}$$

To determine the eigenvalues of the original system, let us first obtain the eigenvalues γ of $[A_k]$. To this effect compute,

$$\det [\gamma I - A_k] = \det \begin{bmatrix} \gamma + 0.2 & -0.2 & 0 \\ -2 & \gamma + 22 & -20 \\ 0 & -20 & \gamma + 20 \end{bmatrix}$$

The characteristic equation is, $\gamma^3 + 42.2\gamma^2 + 48\gamma = 0$. The roots of the polynomial are given by,

$$\gamma_1 = 0, \quad \gamma_2 = -1.1699, \quad \gamma_3 = -41.0301$$

The eigenvalues of A can be obtained as follows:

Let λ be an eigenvalue of A and \underline{u} be the corresponding eigenvector. From the definition, we have

$$A \underline{u} = \lambda \underline{u}$$

or

$$\begin{bmatrix} 0 & I \\ [A_k] & 0 \end{bmatrix} \begin{bmatrix} \underline{u}_1 \\ \underline{u}_2 \end{bmatrix} = \lambda \begin{bmatrix} \underline{u}_1 \\ \underline{u}_2 \end{bmatrix} \quad (1.69)$$

Simplifying (1.69), we get

$$\underline{u}_2 = \lambda \underline{u}_1 \quad (1.70)$$

$$[A_k] \underline{u}_1 = \lambda \underline{u}_2 \quad (1.71)$$

Using (1.70) in (1.71), we obtain

$$[A_k] \underline{u}_1 = \lambda^2 \underline{u}_1$$

Again from the definition, we can write that

$$\lambda^2 = \gamma$$

and the eigenvalues of A is given by

$$\lambda = \pm\sqrt{\gamma}$$

Thus,

$$\lambda_i \text{ with } i=1,2,3,4,5 = 0, 0, \pm j1.0816, \pm j6.4055$$

NOTE:

1. Two zero eigenvalues represent non-uniqueness of state variables. One zero eigenvalue is due to the displacement variable x , and the other is due to the velocity variable v .
2. A zero eigenvalue implies that if states x_1, x_2 and x_3 are changed by a given amount, it still unalters the relative displacement between the masses. Similar inferences can be made about the states v_1, v_2 and v_3 .
3. A zero eigenvalue due to v also demonstrates the absence of damping factor i.e., a force component which is a linear function of velocity.

To eliminate one-zero eigenvalue due to the variable x , the state variables are redefined as $\underline{x}_n = [p, q, v_1, v_2, v_3]^T$, where,

$$(x_2 - x_1) = p \text{ and } (x_3 - x_1) = q$$

Using this new state-vector, the state-space equations from (1.63) to (1.68) are rewritten

as:

$$\frac{dp}{dt} = v_2 - v_1 \quad (1.72)$$

$$\frac{dq}{dt} = v_3 - v_1 \quad (1.73)$$

$$\frac{dv_1}{dt} = \frac{k_{12}}{M_1} p \quad (1.74)$$

$$\frac{dv_2}{dt} = -\frac{k_{12}}{M_2} p + \frac{k_{23}}{M_2} (q - p) \quad (1.75)$$

$$\frac{dv_3}{dt} = -\frac{k_{23}}{M_3} (q - p) \quad (1.76)$$

Writing the above equation in matrix form, we have,

$$\begin{bmatrix} \dot{p} \\ \dot{q} \\ \dot{v}_1 \\ \dot{v}_2 \\ \dot{v}_3 \end{bmatrix} = \begin{bmatrix} 0 & 0 & -1 & 1 & 0 \\ 0 & 0 & -1 & 0 & 1 \\ \frac{k_{12}}{M_1} & 0 & 0 & 0 & 0 \\ \left(-\frac{k_{12}}{M_2} - \frac{k_{23}}{M_2}\right) & \frac{k_{23}}{M_2} & 0 & 0 & 0 \\ \frac{k_{23}}{M_3} & -\frac{k_{23}}{M_3} & 0 & 0 & 0 \end{bmatrix} \begin{bmatrix} p \\ q \\ v_1 \\ v_2 \\ v_3 \end{bmatrix} = A_m \underline{x}_n$$

Using the numerical values of the parameters, we obtain,

$$A_m = \begin{bmatrix} 0 & 0 & -1 & 1 & 0 \\ 0 & 0 & -1 & 0 & 1 \\ 0.2 & 0 & 0 & 0 & 0 \\ -22 & 20 & 0 & 0 & 0 \\ 20 & -20 & 0 & 0 & 0 \end{bmatrix}$$

The eigenvalues of A_m are

$$\begin{aligned} \lambda_1 &= +j6.4055, \quad \lambda_2 = -j6.4055, \\ \lambda_3 &= +j1.0816, \quad \lambda_4 = -j1.0816, \\ \lambda_5 &= 0 \end{aligned}$$

The matrix of left-eigenvectors is given by,

$$U = \begin{bmatrix} \lambda_1 & \lambda_2 & \lambda_3 & \lambda_4 & \lambda_5 \\ 0.1123\angle-90^\circ & 0.1123\angle90^\circ & 0.5096\angle0^\circ & 0.5096\angle0^\circ & 0 \\ 0.1057\angle90^\circ & 0.1057\angle-90^\circ & 0.5358\angle0^\circ & 0.5358\angle0^\circ & 0 \\ 0.0035\angle-180^\circ & 0.0035\angle180^\circ & 0.0942\angle-90^\circ & 0.0942\angle90^\circ & 0.5774\angle0^\circ \\ 0.7160\angle0^\circ & 0.7160\angle0^\circ & 0.4569\angle90^\circ & 0.4569\angle-90^\circ & 0.5774\angle0^\circ \\ 0.6809\angle-180^\circ & 0.6809\angle180^\circ & 0.4853\angle90^\circ & 0.4853\angle-90^\circ & 0.5774\angle0^\circ \end{bmatrix} \begin{matrix} p \\ q \\ v_1 \\ v_2 \\ v_3 \end{matrix}$$

The matrix of right-eigenvectors is given by,

$$W = \begin{bmatrix} p & q & v_1 & v_2 & v_3 \\ 2.3486\angle90^\circ & 2.2336\angle-90^\circ & 0.0180\angle-180^\circ & 0.3666\angle0^\circ & 0.3487\angle180^\circ \\ 2.3486\angle-90^\circ & 2.2336\angle90^\circ & 0.0180\angle180^\circ & 0.3666\angle0^\circ & 0.3487\angle-180^\circ \\ 0.4635\angle0^\circ & 0.4923\angle0^\circ & 0.8837\angle90^\circ & 0.4285\angle-90^\circ & 0.4552\angle-90^\circ \\ 0.4635\angle0^\circ & 0.4923\angle0^\circ & 0.8837\angle-90^\circ & 0.4285\angle90^\circ & 0.4552\angle90^\circ \\ 0 & 0 & 1.4434\angle0^\circ & 0.1443\angle0^\circ & 0.1443\angle0^\circ \end{bmatrix} \begin{matrix} \lambda_1 \\ \lambda_2 \\ \lambda_3 \\ \lambda_4 \\ \lambda_5 \end{matrix}$$

The participation matrix is given by,

$$P = \begin{bmatrix} \lambda_1 & \lambda_2 & \lambda_3 & \lambda_4 & \lambda_5 \\ 0.2638 & 0.2638 & 0.2362 & 0.2362 & 0 \\ 0.2362 & 0.2362 & 0.2638 & 0.2638 & 0 \\ 0.0001 & 0.0001 & 0.0833 & 0.0833 & 0.8333 \\ 0.2625 & 0.2625 & 0.1958 & 0.1958 & 0.0833 \\ 0.2374 & 0.2374 & 0.2209 & 0.2209 & 0.0833 \end{bmatrix} \begin{matrix} p \\ q \\ v_1 \\ v_2 \\ v_3 \end{matrix}$$

NOTE:

- The eigenvalues for the above matrix A_m are determine using the MATLAB command $[U, D] = \text{eig}(A_m)$ where U is the matrix of right-eigenvectors and D is the diagonal matrix having the eigenvalues as the diagonal elements.
- The matrix of left-eigenvectors is determine using the command $W = \text{inv}(U)$
- the participation factor matrix P is determine using the command $P=U.*\text{conj}(W')$

Observations:

1. All the participation factors are real and positive.
2. For the low frequency oscillation of 1.0816 rad/s (λ_3 and λ_4), the participation factors corresponding to the velocities (v_1, v_2 and v_3) are relatively close to each

other, and from the right-eigenvector matrix we can see that (v_2, v_3) are in phase, and 180° out-of phase with v_1 . From this, we can conclude that M_1 , M_2 and M_3 participate almost equally in this mode and masses M_2 and M_3 together swing against M_1 .

3. For the high frequency oscillations of 6.4055 rad/s (λ_1 and λ_2), the participation factors corresponding to the velocities (v_2 and v_3) are relatively higher than that for the velocity v_1 , and from the right-eigenvector matrix we can see that v_2 and v_3 are 180° out-of phase with respect to each other. From this, we can conclude that the mass M_1 has very low participation in this mode. This mode is predominantly seen in velocities v_2 and v_3 , and the mass M_2 swinging against the mass M_3 .
4. The zero-mode (λ_5) is not seen in p and q since, $U(1, 5) = 0$ and $U(2, 5) = 0$. Further, since $U(3, 5) = U(4, 5) = U(5, 5)$, it is clear that the zero-mode (the rigid-body mode) is seen almost equally in state variables, v_1 , v_2 and v_3 , and the mode exists due to the redundancy of the velocity state variables.
5. The positive participation factor denotes that a damping coefficient usually shifts λ to the left.
6. For a 3- mass system there are only 2 oscillatory modes: 6.4055 rad/s and 1.0816 rad/s. These represent swing modes in a power system as these modes are mainly constituted by velocity associated with (rotor) masses.

Analysis with Damping Coefficient:

Figure (1.2) is modified as follows to include the effect of damping coefficient. Assuming $B_2 = B_3 = 0$, and considering only B_1 , the differential equations for the reduced system are written as follows:

$$\frac{dp}{dt} = v_2 - v_1 \quad (1.77)$$

$$\frac{dq}{dt} = v_3 - v_1 \quad (1.78)$$

$$\frac{dv_1}{dt} = \frac{k_{12}}{M_1}p - \frac{B_1}{M_1}v_1 \quad (1.79)$$

$$\frac{dv_2}{dt} = -\frac{k_{12}}{M_2}p + \frac{k_{23}}{M_2}(q - p) \quad (1.80)$$

$$\frac{dv_3}{dt} = -\frac{k_{23}}{M_3}(q - p) \quad (1.81)$$

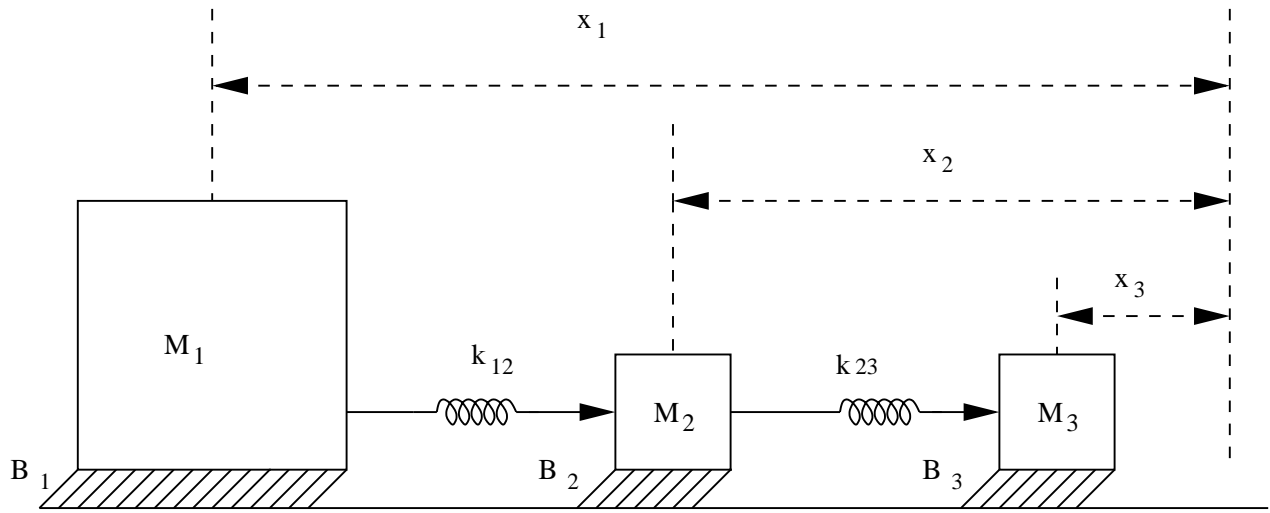


Figure 1.4: Modified multi-mass multi-spring system with damping.

The above equations are written in the matrix form as,

$$\begin{bmatrix} \dot{p} \\ \dot{q} \\ v_1 \\ v_2 \\ v_3 \end{bmatrix} = \begin{bmatrix} 0 & 0 & -1 & 1 & 0 \\ 0 & 0 & -1 & 0 & 1 \\ \frac{k_{12}}{M_1} & 0 & -\frac{B_1}{M_1} & 0 & 0 \\ \left(-\frac{k_{12}}{M_2} - \frac{k_{23}}{M_2}\right) & \frac{k_{23}}{M_2} & 0 & 0 & 0 \\ \frac{k_{23}}{M_3} & -\frac{k_{23}}{M_3} & 0 & 0 & 0 \end{bmatrix} \begin{bmatrix} p \\ q \\ v_1 \\ v_2 \\ v_3 \end{bmatrix} = A_n \underline{x}_n$$

For the chosen parameters with $B_1 = 1 \text{ N/m/s}$, we have,

$$A_n = \begin{bmatrix} 0 & 0 & -1 & 1 & 0 \\ 0 & 0 & -1 & 0 & 1 \\ 0.2 & 0 & -0.1 & 0 & 0 \\ -22 & 20 & 0 & 0 & 0 \\ 20 & -20 & 0 & 0 & 0 \end{bmatrix}$$

The eigenvalues of A_n are

$$\lambda_1 = -0.0000 + j6.4055, \quad \lambda_2 = -0.0000 - j6.4055,$$

$$\lambda_3 = -0.0083 + j1.0809, \quad \lambda_4 = -0.0083 - j1.0809,$$

$$\lambda_5 = -0.08340$$

(λ_1 and λ_2 have negligible damping)

NOTE:

From the definition of participation factor, it can be verified that due to the intro-

duction of a diagonal term, $A_n(3, 3) = -0.1$ which is brought about by a non-zero viscous damping B_1 , the eigenvalue with damping can be approximately estimated as

$$\begin{aligned}\lambda_{3 \text{ new}} &= \lambda_{3 \text{ old}} + P(3, 3) \times -0.01 \\ &= j1.0816 + 0.0833 \times -0.1 \\ &= -0.00833 + j1.0816 \text{ (there is a small change in frequency)}\end{aligned}$$

Similar observation can be made with respect to $\lambda_{4 \text{ new}}$

Construction of Time-domain Response:

We know from (1.54) that having determined the eigenvalues and eigenvectors (right and left), we can estimate the time-domain zero-input response as:

$$\underline{x}_n(t) = \sum_{i=1}^n (\underline{w}_i \underline{x}(0)) e^{\lambda_i t} \underline{u}_i$$

or

$$\begin{aligned}\underline{x}_n(t) &= \underline{w}_1 \underline{x}(0) e^{\lambda_1 t} \underline{u}_1 + \underline{w}_2 \underline{x}(0) e^{\lambda_2 t} \underline{u}_2 + \underline{w}_3 \underline{x}(0) e^{\lambda_3 t} \underline{u}_3 + \\ &\quad + \underline{w}_4 \underline{x}(0) e^{\lambda_4 t} \underline{u}_4 + \underline{w}_5 \underline{x}(0) e^{\lambda_5 t} \underline{u}_5\end{aligned}\quad (1.82)$$

where $\underline{x}_n = [p, q, v_1, v_2, v_3]^T$.

In the following lines, the time-domain response is constructed for 3 different initial values of states without accounting any damping.

Case-1 $\underline{x}_n(0) = [-1, -1, 0, 0, 0]^T$

From (1.82), the time-domain response is obtained as:

$$\underline{x}_n(t) = -j0.1150 e^{\lambda_1 t} \underline{u}_1 + j0.1150 e^{\lambda_2 t} \underline{u}_2 - 0.9558 e^{\lambda_3 t} \underline{u}_3 - 0.9558 e^{\lambda_4 t} \underline{u}_4 - (0) e^{\lambda_5 t} \underline{u}_5$$

Further simplification leads us to the following result:

$$p(t) = -0.0258 \cos(6.4055t) - 0.9742 \cos(1.0816t) \quad (1.83)$$

$$q(t) = +0.0242 \cos(6.4055t) - 1.0242 \cos(1.0816t) \quad (1.84)$$

$$v_1(t) = -0.0008 \sin(6.4055t) - 0.1800 \sin(1.0816t) \quad (1.85)$$

$$v_2(t) = +0.1646 \sin(6.4055t) + 0.8734 \sin(1.0816t) \quad (1.86)$$

$$v_3(t) = -0.1566 \sin(6.4055t) + 0.9276 \sin(1.0816t) \quad (1.87)$$

The above response is verified by numerical solution of system of equation from (1.72) to (1.76). The plots obtained are as shown in Figure 1.5.

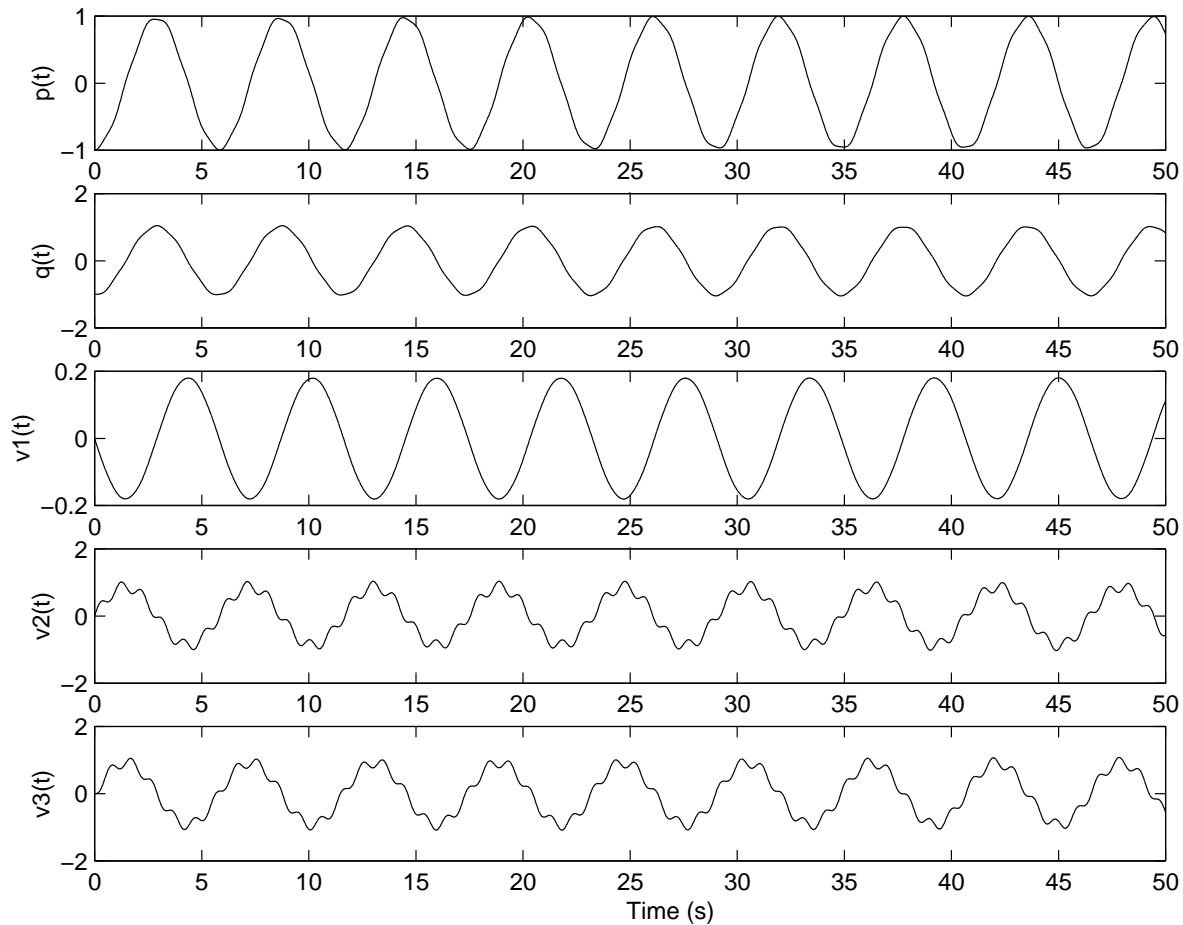


Figure 1.5: Numerical solution for Case-1.

Note that for this $\underline{x}_n(0)$, where $v_i(0) = 0$ for $i=1, 2$ and 3 , the zero-mode is not excited and the lower frequency mode is excited to a larger extent than the higher frequency mode in all the state variables.

Case-2 $\underline{x}_n(0) = [1, 0, 0, 0, 0]^T$

From (1.82), the time-domain response is obtained as:

$$\underline{x}_n(t) = j2.3486 e^{\lambda_1 t} \underline{u}_1 - j2.3486 e^{\lambda_2 t} \underline{u}_2 + 0.4635 e^{\lambda_3 t} \underline{u}_3 + 0.4635 e^{\lambda_4 t} \underline{u}_4 - (0) e^{\lambda_5 t} \underline{u}_5$$

Further simplification leads us to the following result:

$$p(t) = +0.5274 \cos(6.4055t) + 0.4724 \cos(1.0816t) \quad (1.88)$$

$$q(t) = -0.4964 \cos(6.4055t) + 0.4966 \cos(1.0816t) \quad (1.89)$$

$$v_1(t) = +0.0164 \sin(6.4055t) + 0.0872 \sin(1.0816t) \quad (1.90)$$

$$v_2(t) = -3.3632 \sin(6.4055t) - 0.4234 \sin(1.0816t) \quad (1.91)$$

$$v_3(t) = +3.1984 \sin(6.4055t) - 0.4498 \sin(1.0816t) \quad (1.92)$$

The above response is verified by numerical solution of system of equation from (1.72) to (1.76). The plots obtained are as shown in Figure 1.6.

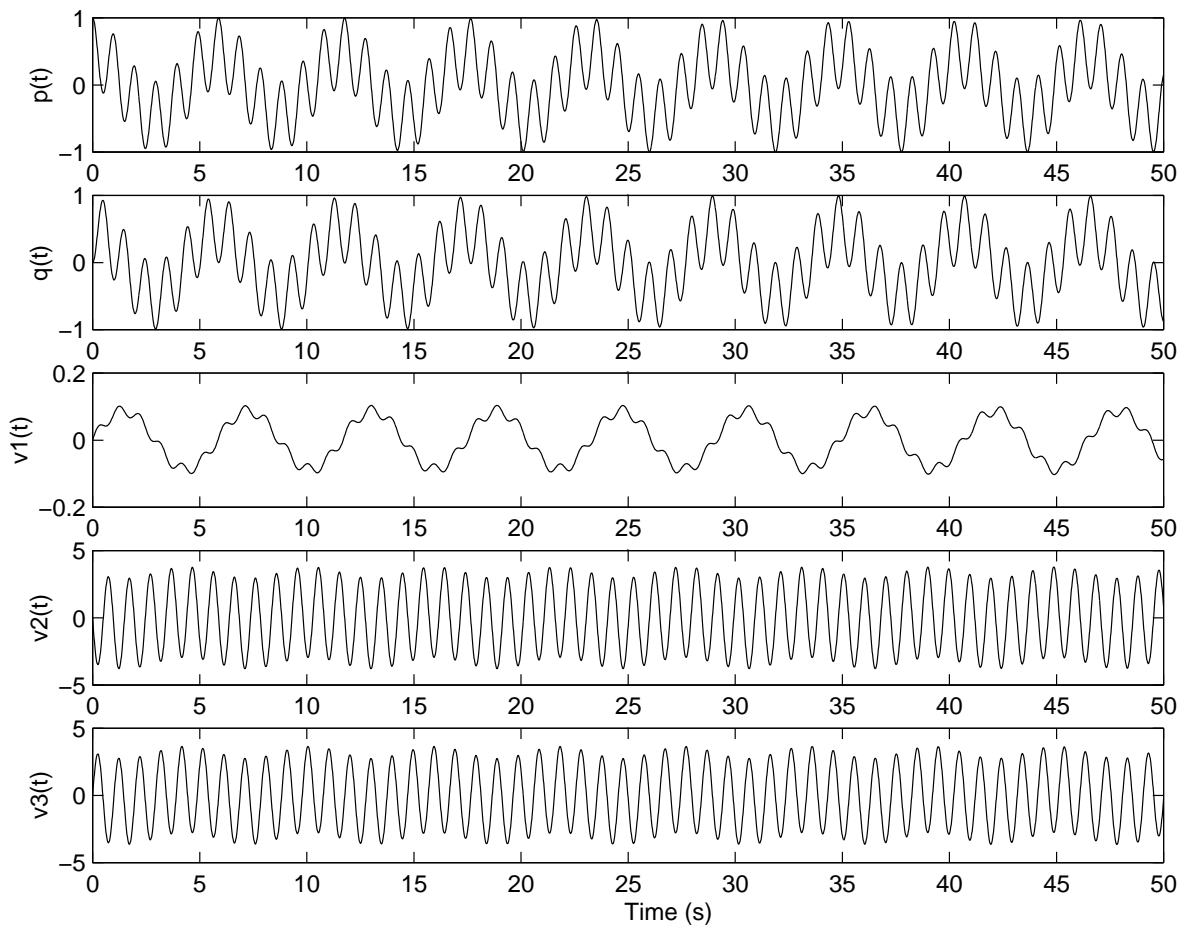


Figure 1.6: Numerical solution for Case-2.

Note that for this $\underline{x}_n(0)$, where only $p(0) \neq 0$, the higher frequency mode is excited to a larger extent in $v_2(t)$ and $v_3(t)$.

Case-3 $\underline{x}_n(0) = [0, 0, 1, 0, 0]^T$

From (1.82), the time-domain response is obtained as:

$$\underline{x}_n(t) = -0.0180 e^{\lambda_1 t} \underline{u}_1 - 0.0180 e^{\lambda_2 t} \underline{u}_2 + j0.8837 e^{\lambda_3 t} \underline{u}_3 - j0.8837 e^{\lambda_4 t} \underline{u}_4 + 1.4434 e^{\lambda_5 t} \underline{u}_5$$

Further simplification leads us to the following result:

$$p(t) = -0.0040 \sin(6.4055t) - 0.9006 \sin(1.0816t) \quad (1.93)$$

$$q(t) = +0.0038 \sin(6.4055t) - 0.9468 \sin(1.0816t) \quad (1.94)$$

$$v_1(t) = +0.0001 \cos(6.4055t) + 0.1664 \cos(1.0816t) + 0.8335 \quad (1.95)$$

$$v_2(t) = -0.0256 \cos(6.4055t) - 0.8074 \cos(1.0816t) + 0.8335 \quad (1.96)$$

$$v_3(t) = +0.0244 \cos(6.4055t) - 0.8576 \cos(1.0816t) + 0.8335 \quad (1.97)$$

The above response is verified by numerical solution of system of equation from (1.72) to (1.76). The plots obtained are as shown in Figure 1.7.

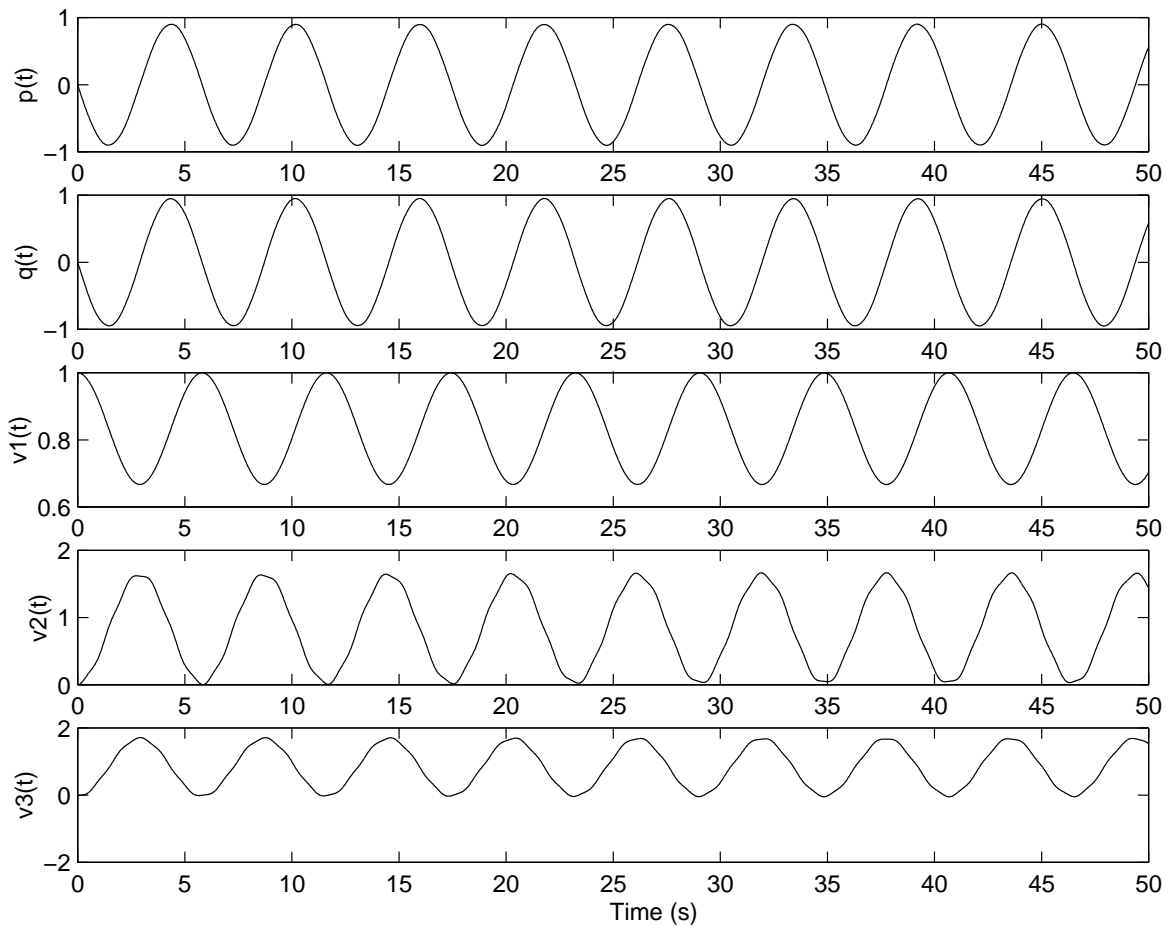


Figure 1.7: Numerical solution for Case-3.

Note that for this $\underline{x}_n(0)$, where only $v_1(0) \neq 0$, the mode-zero is excited and only the low frequency mode is predominantly seen in all the state variables.

Observations:

1. If $p(0) = q(0)$ with $v_i(0) = 0$ for $i = 1, 2$ and 3 , the modal frequency 1.0816 rad/s is excited to a larger extent than that of the modal frequency 6.4055 rad/s. This is to some extent true as an equal amount of initial displacement is given to masses M_2 and M_3 .
2. As long as $v_i(0) = 0$ for $i = 1, 2$ and 3 , mode-zero (rigid-body mode) is not excited.
3. In all cases the modal frequency 6.4055 rad/s is not predominantly seen in the state variable v_1 as is evident from the participation factor-vector pertaining to v_1 .
4. Mode-zero is absent in state variables p and q as is clear from the right eigenvector corresponding to mode-zero. Further, any specification of $p(0)$ and/or $q(0)$ alone cannot excite mode-zero.

NOTE:

The above case studies have been illustrated in `spring_mass.m` file. Having selected a case in the MATLAB file, the numerical solution of the differential equations (1.72) to (1.76) can be obtained by running a SIMULINK file `spring_mass_sim.mdl`.

Chapter 2

4-machine Power System Example

2.1 Four Machine System Details:

A well known 4 machine, 10-bus power system has been used to demonstrate the modal analysis of a power system. The single line diagram of the system is shown in Figure 2.1. The system details are adopted from [1].

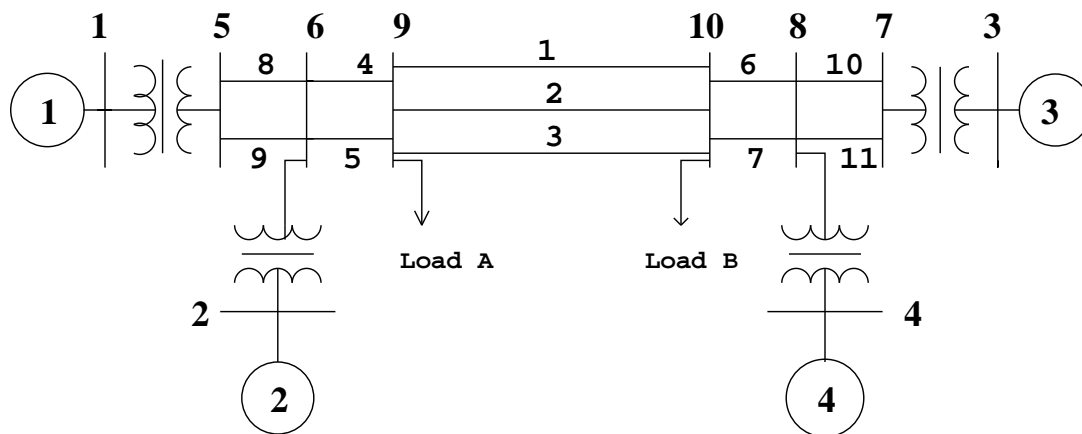


Figure 2.1: Four machine power system.

In all case studies presented 2.2 model has been used for all machines. The programme permits the selection of simplified models (even classical model) for generator. See Appendix (C.7) for details.

2.2 Base Case:

In this case, generators are provided with a single-time constant static exciter with no PSS, and turbines are not considered. Further, constant impedance type load model has been employed for both real and reactive components of loads. The eigenvalues obtained

are shown in Table 2.1. Here, reduced state matrix has been used. In this case the number of valid state variables is 27 (including 1-zero eigenvalue).

Mode No.	Eigenvalue	Damp. factor	Freq.(Hz)
1	-42.9191	1.0000	0
2	-42.7135	1.0000	0
3,4	$-16.0251 \pm j 16.9998$	0.6859	2.7056
5	-38.6952	1.0000	0
6	-37.6193	1.0000	0
7	-33.9306	1.0000	0
8	-33.6063	1.0000	0
9,10	$-16.3995 \pm j 12.2283$	0.8017	1.9462
11	-27.4529	1.0000	0
12	-25.3330	1.0000	0
13,14	$-1.1037 \pm j 7.4473$	0.1466	1.1853
15,16	$-1.0488 \pm j 6.7981$	0.1525	1.0820
17,18	$-0.0372 \pm j 4.4583$	0.0083	0.7096
19	-17.5410	1.0000	0
20,21	$-15.6187 \pm j 0.9081$	0.9983	0.1445
22	-13.6191	1.0000	0
23	-0.0000	1.0000	0
24	-4.5000	1.0000	0
25	-4.8931	1.0000	0
26	-5.0199	1.0000	0
27	-4.6860	1.0000	0

Table 2.1: Eigenvalues for four machine system -base case.

The above results are obtained by executing the following steps:

1. Perform the power flow studies by running: `fdlf_loadflow.m` file. It requires the following `.m` and data files:
 - (a) `B_bus_form.m`, `fdlf_jacob_form.m`, `powerflow.m` and `lfl_result.m`.
 - (b) `busno.dat` : System details- number of lines, buses, transformers, etc
 - (c) `nt.dat` : Transmission line and transformer data
 - (d) `pvpq.dat` : Generation data and load data.
 - (e) `shunt.dat` : Shunt data

On successful run, it generates two output files: `lfl.dat` and `report.dat`. The converged loadflow results are available in `lfl.dat`.

2. To perform the small-signal analysis execute the main file: `small_sig.m`. This file in turn calls the following `.m` files:

- (a) `initcond.m` : It calculates the initial conditions. The other `.m` files used by this file are:
- exciter-related files: `static_exciter.m`, `DC1A_exciter.m` and `AC4A_exciter.m`.
 - turbine-related files: `hydro_turbine.m` and `Reheat_turbine.m`.
 - PSS-related files: `pss_slip_signal.m`, `pss_delpw_signal.m` and `pss_power_signal.m`.
 - load model related file: `load_zip_model.m`.
- (b) `yform.m`: It constructs the Y_{DQ} and Y_{BUS} matrices and prepares data for running time-domain simulation programme.
- (c) `pmat.m` : It prepares P_G and P_L matrices.
- (d) `exciter_settings.m` : Linearizes the equations pertaining to static, DC1A and AC4A exciters.
- (e) `primemover_settings.m` : Linearizes the equations pertaining to hydro and reheat steam -type turbines with their associated speed-governors.
- (f) `genmat.m` : Constructs generator related A_g , B_g^r , C_g and E_g matrices.
- (g) `statld.m` : It constructs Y_L matrix for the static loads.
3. Run `trace_mode.m` to evaluate eigenvalues and identify the nature of a mode. It in turn calls `r_eig_plot.m` for obtaining the compass plot of right-eigenvectors pertaining to slip in an interactive fashion.
4. Run `pss_selection.m` to identify the candidate generators for PSS placement. It in turn calls `pss_design.m` for determining the GEPS plot, and the compensated GEPS plot for a chosen PSS.
5. Run `freq_response.m` to draw frequency response of the transfer function $\frac{\Delta T_e(j\omega)}{\Delta V_{ref}(j\omega)}$.
6. Run `transtability.mdl` to perform time-domain simulation in SIMULINK.

NOTE: Programmes given in items (3), (4), (5) and (6) can be executed in any order having executed `small_sig.m` file.

The main `small_sig.m` file requires the following data files:

- (i) `lf1.dat` : Converged loadflow results.
- (ii) `nt.dat` : Transmission line and transformer data.
- (iii) `ld.dat` : Load data.

- (iv) `shunt.dat` : Shunt data.
- (v) `gen.dat` : Generator data.
- (vi) `busno.dat` : System details- number of lines, buses, transformers, etc.
- (vii) `exc_static.dat` : Single-time constant static exciter data .
- (viii) `exc_AC4A.dat` : IEEE AC4A type AC exciter data.
- (ix) `exc_DC1A.dat` : IEEE DC1A type DC commutator exciter data.
- (x) `turb_hydro.dat` : Simplified hydro-turbine data.
- (xi) `turb_rhst.dat` : Reheat-type steam turbine data.
- (xii) `slip_pss.dat` : Slip-signal-based PSS data.
- (xiii) `power_pss.dat` : Power-signal-based PSS data.
- (xiv) `delPw_pss.dat` : Delta-P-Omega type PSS data.

2.2.1 Format of Data Files:

In the following lines the format of each of the data file has been given using 4 machine power system data:

System details:

File name: `busno.dat`

```
-----
3          ---> Slack bus number.
0.001      ---> Loadflow convergence tolerance.
10         ---> Number of buses in the system.
11         ---> Number of lines.
4          ---> Number of transformers.
3          ---> Number of PV buses = (Number of generators - 1).
0          ---> Q-bit (please set this bit to zero only).
2          ---> Number of load buses (including loads at PV and slack buses).
2          ---> Number of shunts.
1.03       ---> Slack bus voltage magnitude.
60         ---> Nominal frequency in Hz.
-----
```

Network data:

File name: nt.dat

From	To	R	X	B (total)/Tap ratio	Remarks
9	10	0.022	0.220	0.330	---Line 1
9	10	0.022	0.220	0.330	---Line 2
9	10	0.022	0.220	0.330	---Line 3
9	6	0.002	0.020	0.030	---Line 4
9	6	0.002	0.020	0.030	---Line 5
10	8	0.002	0.020	0.030	---Line 6
10	8	0.002	0.020	0.030	---Line 7
5	6	0.005	0.050	0.075	---Line 8
5	6	0.005	0.050	0.075	---Line 9
7	8	0.005	0.050	0.075	---Line 10
7	8	0.005	0.050	0.075	---Line 11
1	5	0.001	0.012	1.000	---> Transformer data starts here.
2	6	0.001	0.012	1.000	
3	7	0.001	0.012	1.000	
4	8	0.001	0.012	1.000	

Generation and load data:

File name: pvpq.dat

Bus No.	Vg/PL0	Pg0/QL0	Remarks
1	1.03	7.00	---> Generator buses other than the slack bus are specified as PV buses
2	1.01	7.00	
4	1.01	7.00	
9	11.59	2.12	---> Load data starts here (including loads at PV and slack buses)
10	15.75	2.88	

Shunt admittances:

File name: shunt.dat

Bus No.	G	B
9	0.0	3.0
10	0.0	4.0

Converged load flow results:

File name: lfl.dat

Bus No.	Vb0	theta0	Pg0	Qg0	PL0	QL0
1	1.030000	8.215523	7.000000	1.338523	0.00	0.00
2	1.010000	-1.503809	7.000000	1.591791	0.00	0.00
3	1.030000	0.000000	7.217178	1.446427	0.00	0.00
4	1.010000	-10.204916	7.000000	1.807834	0.00	0.00
5	1.010800	3.661654	0.000000	0.000000	0.00	0.00
6	0.987533	-6.243121	0.000000	0.000000	0.00	0.00
7	1.009533	-4.697706	0.000000	0.000000	0.00	0.00
8	0.984958	-14.944164	0.000000	0.000000	0.00	0.00
9	0.976120	-14.419101	0.000000	0.000000	11.59	2.12
10	0.971659	-23.291847	0.000000	0.000000	15.75	2.88

Load data:

File name: ld.dat

Load Bus No.	PL0	QL0
9	11.59	2.12
10	15.75	2.88

Generator data (2.2 model):

File name: gen.dat

Gen.No.	xd	xdd	xddd	Td0d	Td0dd	xq	xqd	xqdd	Tq0d	Tq0dd	H	D
1	0.2	0.033	0.0264	8.0	0.05	0.190	0.061	0.03	0.4	0.04	54	0
2	0.2	0.033	0.0264	8.0	0.05	0.190	0.061	0.03	0.4	0.04	54	0
3	0.2	0.033	0.0264	8.0	0.05	0.190	0.061	0.03	0.4	0.04	63	0
4	0.2	0.033	0.0264	8.0	0.05	0.190	0.061	0.03	0.4	0.04	63	0

NOTE: Armature resistance, R_a is neglected. Generators are identified by their bus numbers to which they are connected.

Single-time constant static exciter:

File name: exc_static.dat

Gen.no.	KA	TA	EFDMIN	EFDMAX
1	200	0.02	-6.0	6.0
2	200	0.02	-6.0	6.0
3	200	0.02	-6.0	6.0
4	200	0.02	-6.0	6.0

IEEE AC4A-type exciter:

File name: exc_AC4A.dat

Gen.no.	Tr	KA	TA	TC	TB	VIMAX	VIMIN	VRMIN	VRMAX	KC
1	0.02	200	0.02	1.0	10	10	-10	-4.53	5.64	0
2	0.02	200	0.02	1.0	10	10	-10	-4.53	5.64	0
3	0.02	200	0.02	1.0	10	10	-10	-4.53	5.64	0
4	0.02	200	0.02	1.0	10	10	-10	-4.53	5.64	0

IEEE DC1A-type exciter:

File name: exc_DC1A.dat

Gen. no.	Tr	KA	TA	TC	TB	VRMAX	VRMIN	KE	TE	E1	SE1
1	0.02	20	0.06	1	1	6.0	-6.0	-0.0485	0.250	3.5461	0.08
2	0.02	20	0.06	1	1	6.0	-6.0	-0.0633	0.405	0.9183	0.66
3	0.02	20	0.06	1	1	6.0	-6.0	-0.0198	0.500	2.3423	0.13
4	0.02	20	0.06	1	1	6.0	-6.0	-0.0525	0.500	2.8681	0.08

E2 SE2 KF TF											

4.7281 0.260 0.040 1.0											
1.2244 0.880 0.057 0.5											
3.1230 0.340 0.080 1.0											
3.8241 0.314 0.080 1.0											

Speed-governor for hydro-turbine:

File name: turb_hydro.dat

Gen. no.	TW	TG	SIGMA	T2	PMAX_fac	PMIN_fac
1	1	0.2	0.05	0	1.1	0.1
2	1	0.2	0.05	0	1.1	0.1
3	1	0.2	0.05	0	1.1	0.1
4	1	0.2	0.05	0	1.1	0.1

Speed-governor for steam turbine- reheat type:

File name: turb_rhst.dat

Gen.no.	T1	T2	T3	SIGMA	PMAX_fac	PMIN_fac	TCH	TRH	TCO	FHP	FIP	FLP
1	0.2	0.0	0.1	0.05	1.1	0.1	0.3	10	0.4	0.3	0.3	0.4
2	0.2	0.0	0.1	0.05	1.1	0.1	0.3	10	0.4	0.3	0.3	0.4
3	0.2	0.0	0.1	0.05	1.1	0.1	0.3	10	0.4	0.3	0.3	0.4
4	0.2	0.0	0.1	0.05	1.1	0.1	0.3	10	0.4	0.3	0.3	0.4

NOTE: The data files turb_hydro.dat, and turb_rhst.dat should not contain any entries for generators whose $P_{g0} = 0$.

Slip-signal PSS:

File name: slip_pss.dat

Gen.no.	KS	TR	TW	T1	T2	VSMAX	VSMIN	a0	a1	TRF
1	15	0.02	10	0.07577	0.03715	0.1	-0.1	570	35	1

TRF = 0 enables torsional filter, 1 disables it.

NOTE: In pss_slip_signal.m, a variable Tmd_slip_nt and Tmd_slip_t provides an option to enable/disable input measurement delay given by TR depending on the value of TRF.

Power-signal PSS:

File name: power_pss.dat

Gen.No.	TW	TR	KS	VSMAX	VSMIN
1	10	0.05	0.03	0.1	-0.1
2	10	0.05	0.07	0.1	-0.1
3	10	0.05	0.07	0.1	-0.1
4	10	0.05	0.03	0.1	-0.1

Delta-P-Omega PSS:

File name: delPw_pss.dat

Gen.No.	Tw1	Tw2	Tw3	Tw4	T6	T7	H	KS3	T8	T9
2	10	10	10	10	0.01	10	54	1	0	0.1
1	10	10	10	10	0.01	10	54	1	0	0.1
3	10	10	10	10	0.01	10	63	1	0	0.1
4	10	10	10	10	0.01	10	63	1	0	0.1

T1	T2	T3	T4	KS1	VSMAX	VSMIN
0.06322	0.04452	0.06322	0.04452	10	0.1	-0.1
0.06322	0.04452	0.06322	0.04452	15	0.1	-0.1
0.06322	0.04452	0.06322	0.04452	10	0.1	-0.1
0.06322	0.04452	0.06322	0.04452	10	0.1	-0.1

2.2.2 Component Selectors:

To perform stability studies with a variety of exciters, power system stabilizers and turbines, the following kinds of selectors are used:

1. Main Selectors.
2. Individual Selectors.

These selectors permit us to choose a specific type of exciter/PSS/turbine for a given generator. For example, if one wants to select any one type of exciter for a given generator out of 3 different IEEE-type exciters (for which data files have been prepared), it can be carried out by using Individual Selectors without altering the data files. Whereas, the Main Selectors can be used to disable an exciter on a generator without modifying the Individual Selectors.

The Main Selectors are as follows:

Variable name	Component	Enable	Disable
AVR	Exciters	0	1
TURB	Turbines	0	1
PSS	Power System Stabilizers	0	1

NOTE:

These selectors have been provided in file `initcond.m`. The vector size of these variables is equal to the number of buses in a system.

The Individual Selectors are as follows:

1. Individual Selectors for exciters:

```
ng_static    ---> Single-time constant static type exciter.
ng_AC4A      ---> IEEE AC4A-type exciter.
ng_DC1A      ---> IEEE DC1A-type exciter.
```

Indicate the generator number on which a specific type of exciter is present, otherwise null. For example, if all generators are with single-time constant static type exciters, then the selectors are initialized as follows:

```
ng_static=[1,2,3,4]
ng_AC4A=[]
ng_DC1A=[]
```

The Main Selector, `AVR` is enabled for all exciters as: `AVR = zeros(1,nb)`, where `nb` denotes the number of buses in the system.

NOTE:

- (a) Since all the variables used in `.m` and `transtability.mdl` files are to be initialized, it is necessary to prepare the data file for IEEE AC4A and IEEE DC1A -type exciters, atleast for one machine. One may use typical data for the same. However, the respective exciter output is not used in the programme.
- (b) If it is required to enter a large set of generator numbers to initialize the Individual Selectors, one can list the generator numbers in a file `ng_****.dat` and use the `load ng_****.dat` command. This has to be done after commenting out the corresponding initialization command as `%ng_**** = [...]` in file `initcond.m`.
- (c) If classical model is used for a machine, then it is recommended to disable the exciter of that machine by using the Main Selector, `AVR`.

2. Individual Selectors for turbines:

```
ng_hydro    ---> Hydro-turbines.
ng_rht      ---> Reheat-type steam turbines.
```

The procedure to initialize these selectors is the same as that described for the exciters. For example, if no generators are with any types of turbines, then the selectors are initialized as follows:

```
ng_hydro = []
ng_rht = []
```

In addition, the Main Selector, TURB is set as `TURB=ones(1,nb)`

NOTE:

- (a) To initialize the variables pertaining to all turbines, it is necessary to prepare the data file using typical data for any one machine. However, the respective turbine output is not used in the programme.
- (b) If it is required to enter a large set of generator numbers to initialize the Individual Selectors, one can list the generator numbers in a file `ng_****.dat` and use the `load ng_****.dat` command. This has to be done after commenting out the corresponding initialization command as `%ng_**** = [...]` in file `initcond.m`.

3. Individual Selectors for power system stabilizers:

```
ng_slip_pss    ---> Slip signal-based PSS.
ng_power_pss   ---> Power signal-based PSS.
ng_delPw_pss   ---> Delta-P-Omega signal-based PSS.
```

The procedure to initialize these selectors is the same as that described for the exciters. For example, for the case in hand, no power system stabilizer on any generators is considered. This is implemented by making the following settings:

```
ng_slip_pss = []
ng_power_pss = []
ng_delPw_pss = []
```

The Main Selector, PSS is set as `PSS = ones(1,nb)`.

NOTE:

- (a) To initialize the variables pertaining to slip signal-, power signal- and delta-P-omega signal- based PSS, it is necessary to prepare the data files using typical data for any one machine. However, the respective PSS outputs are not used in the programme.
- (b) If it is required to enter a large set of generator numbers to initialize the Individual Selectors, one can list the generator numbers in a file `ng_****.dat` and use the `load ng_****.dat` command. This has to be done after commenting out the corresponding initialization command as `%ng_**** = [...]` in file `initcond.m`.
- (c) The Main Selector, PSS is normally used to disable any PSS without changing the Individual Selectors. For example, even if `ng_slip_pss=[1]`, with all other selectors initialized to `[]`, a setting given by `PSS=ones(1,nb)` disables all power system stabilizers.

2.2.3 Load Modelling:

Both real and reactive components of loads are modelled following polynomial approach. The composition of real and reactive components can be specified in file `load_zip_model.m` as follows:

1. Real component of load:

```
p1 ---> fraction for constant power.
p2 ---> fraction for constant current.
p3 ---> fraction for constant impedance.
```

For example, for the case considered, the real power component is modelled as constant impedance type, then the fractions are set as follows:

```
p1 = 0;
p2 = 0;
p3 = 1;
```

2. Reactive component of load:

```
r1 ---> fraction for constant power.
r2 ---> fraction for constant current.
r3 ---> fraction for constant impedance.
```

For example, if reactive power component is modelled as constant impedance type, then the fractions are set as follows:

```
r1 = 0;
r2 = 0;
r3 = 1;
```

The frequency-dependency of loads are not accounted, hence the following variables in file `yform.m` are to be set to zero. Please do not tamper this settings.

```
kpf = 0;
kqf = 0;
```

Determination of Nature of Oscillatory Modes:

To identify the nature of an oscillator mode the following procedure is employed:

1. Compute the normalized slip participation factors (SPF) for the chosen mode.
2. Identify an actively participating generator if the amplitude of its SPF is greater than a certain value. Thus a set of candidate generators is formed.
3. If the sum of the amplitudes of the normalized participation factors pertaining to slip of the candidate generators is very low, then the mode is declared as a *Non swing mode with very low slip participation*.
4. For the mode, if the slip participation is relatively high, then the feasibility of formation of two coherent groups of generators among the generators in the set formed in item-2, is checked. The coherency of generators is verified by using the phase angle of the right eigenvector associated with slip [24]. If all modes are purely imaginary except the zero-eigenvalue(s), the phase angle difference between the coherent group is 180° . Otherwise, this angle difference may be less than 180° .
5. If the set formed in item-2 can be divided into two groups of coherent generators, then the mode is declared as a *Swing mode*, otherwise as a *Non-swing mode*.
6. If the mode has been classified as either *Non-swing mode* or *Non-swing mode with very low slip participation*, such a mode's association with the state variables is declared using the highest magnitude of state participation factor.

Using the above procedure, the oscillatory modes are characterized. For each mode, state variables which have a normalized participation factor amplitude greater than 0.1 are listed. For swing modes, the formation of coherent groups of generators is displayed by plotting the corresponding right eigenvectors associated with slip. The programme developed provides a feature to identify the generators in an interactive fashion.

2.2.4 A Sample Run:

The above case is simulated by using the following steps:

1. Prepare the data files as indicated in the previous sections.
2. Initialize the Main and Individual Selectors in file `initcond.m`
3. Execute `small_sig.m`. The statements displayed in the MATLAB Command Window and the respective inputs are shown below:

```
wB = 376.9911
```

```
Enter 1 if you want to run transtability programme for network disturbances,
      otherwise 0: 0
```

```
Enter 1 if you want to run transtability programme for perturbation of VREF,
      otherwise 0: 1
```

```
Enter the generator number whose Vref needs to be perturbed: 1
```

4. Execute `trace_mode.m`. The statements displayed in the MATLAB Command Window and the respective inputs are shown below:

```
Enter 1 to display ALL eigenvalues (EIG), otherwise 0 (using EIGS): 1
```

SL_number	Eigenvalue	dampingfactor	frequency(Hz)
1.0000	-42.9191	1.0000	0
2.0000	-42.7135	1.0000	0
3.0000	-16.0251 +16.9998i	0.6859	2.7056
4.0000	-16.0251 -16.9998i	0.6859	2.7056
5.0000	-38.6952	1.0000	0
6.0000	-37.6193	1.0000	0
7.0000	-33.9306	1.0000	0
8.0000	-33.6063	1.0000	0
9.0000	-16.3995 +12.2283i	0.8017	1.9462
10.0000	-16.3995 -12.2283i	0.8017	1.9462
11.0000	-27.4529	1.0000	0
12.0000	-25.3330	1.0000	0
13.0000	-1.1037 + 7.4473i	0.1466	1.1853

14.0000	-1.1037 - 7.4473i	0.1466	1.1853
15.0000	-1.0488 + 6.7981i	0.1525	1.0820
16.0000	-1.0488 - 6.7981i	0.1525	1.0820
17.0000	-0.0372 + 4.4583i	0.0083	0.7096
18.0000	-0.0372 - 4.4583i	0.0083	0.7096
19.0000	-0.0000	1.0000	0
20.0000	-17.5410	1.0000	0
21.0000	-15.6187 + 0.9081i	0.9983	0.1445
22.0000	-15.6187 - 0.9081i	0.9983	0.1445
23.0000	-13.6191	1.0000	0
24.0000	-4.5000	1.0000	0
25.0000	-5.0199	1.0000	0
26.0000	-4.8931	1.0000	0
27.0000	-4.6860	1.0000	0
28.0000	-0.0000	1.0000	0

Enter the serial number of the eigenvalue for which you want to obtain the
P.factor: 13

State variable	Mag(Norm PF)	ang(Norm PF)deg.	Mag(PF)	ang(PF)deg.
Delta-2	1.0000	0.00	0.5971	-8.21
Slip-2	0.5328	2.55	0.3182	-5.66
Slip-1	0.4127	2.29	0.2464	-5.92
DampG-2	0.1003	131.86	0.0599	123.65

You have chosen a SWING-MODE

The generator(s) in group-1 is(are) ...

Group1 =

2

The generator(s) in group-2 is(are) ...

Group2 =

1

Enter 1 if you want to plot the compass plot, otherwise 0: 1

NOTE: Use mouse click on the plot to identify the generator

Press any key

Current plot held

Enter 1 if you want to repeat for another eigenvalue, otherwise 0: 0

As shown above, the slip participation factor for machines 1 and 2 are more dominant. Further, the grouping of machines prepared by the programme is shown in Figure 2.2. The figure shows that this mode is a swing mode in which machine-1 swings against machine-2, and it constitute a local mode.

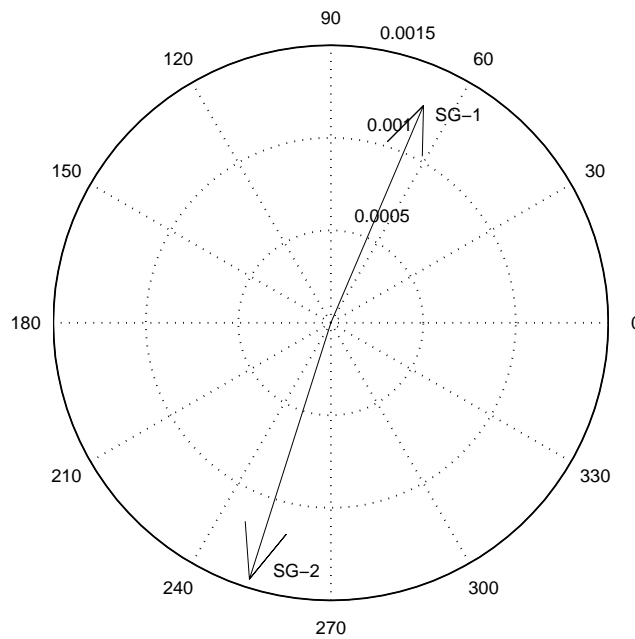


Figure 2.2: Plot of slip-right eigenvector for machines 1 and 2.

Time-domain verification:

The inference made from eigenvalue analysis is verified from a time-domain simulation by perturbing V_{ref} for generator-1. This is carried out as follows:

- By entering 1 for the option: ‘Enter 1 if you want to run transtability programme for perturbation of VREF, otherwise 0 :’ while executing `small_sig.m` (see above).
- Run `transtability.mdl` programme.
- Observe the scope labeled `Slip_COI`.

The plots are shown in Figure 2.3, where the local mode is seen clearly in the initial part of the response. The frequencies for the inter-area mode and the local mode (machines 1-2) are also verified from Figure 2.3.

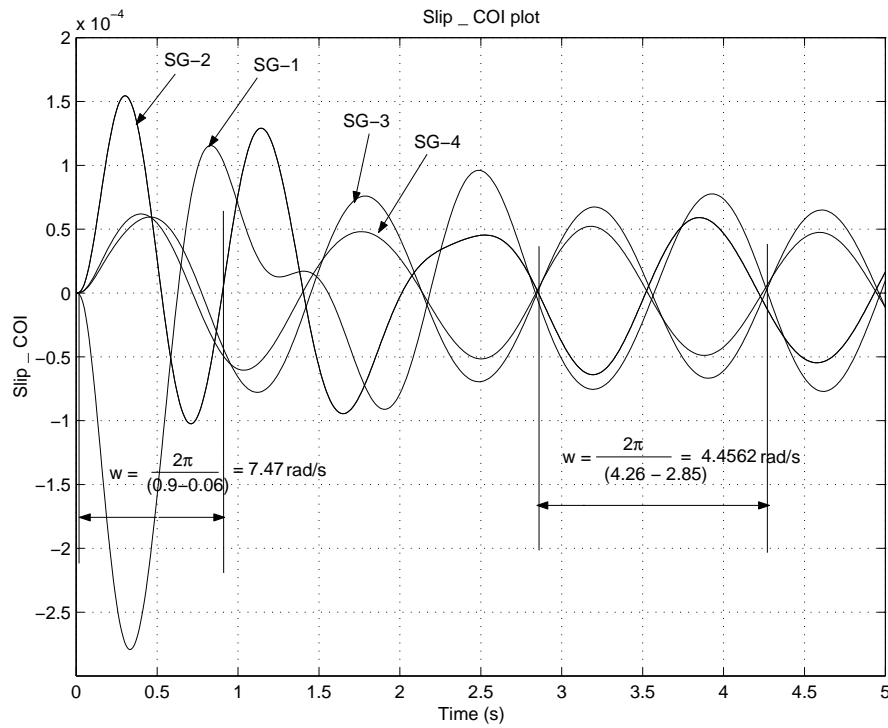


Figure 2.3: *Slip_COI* plots for perturbation of V_{ref} of m/c-1.

For clarity only oscillatory modes are listed in Table 2.2 with their nature.

SL No	Eigenvalue	Nature of Modes
1	$-16.0251 \pm j 16.9998$	Non-swing mode (exciter mode)
2	$-16.3995 \pm j 12.2283$	Non-swing mode (exciter mode)
3	$-1.1037 \pm j 7.4473$	Swing-mode (m/cs. 1 and 2)
4	$-1.0488 \pm j 6.7981$	Swing-mode (m/cs. 3 and 4)
5	$-0.0372 \pm j 4.4583$	Swing-mode (m/cs. (1,2) and (3,4))
6	$-15.6187 \pm j 0.9081$	Non-swing mode (exciter mode)

Table 2.2: Oscillatory modes - 4 machine system (Base case).

NOTE:

1. With the un-reduced state matrix, the non-zero eigenvalues are the same as that with the reduced state matrix, however, the zero eigenvalue in the reduced state matrix, is replaced by a complex conjugate pair $0.0000 \pm j0.0235$. Thus, there are 28 eigenvalues which is equal to the number of state variables in the un-reduced case. Due to errors in the load flow (mismatch in power) and other numerical errors in the computations, the two eigenvalues which should have been zero are calculated as a complex pair of small magnitude ($0.0000 \pm j0.0235$). The matrix, if reduced by following the procedure indicated in Appendix- B.3, the confusing zero eigenvalue

reduces to a *perfect* zero eigenvalue, see mode-23 in Table 2.1.

2. Another observation is that some functions like *rank* in MATLAB works unreliably with the un-reduced state matrix.

2.2.5 Exciters on Manual Control:

In this case, exciters are disabled on all machines by setting `AVR=ones(1,nb)`. For clarity, only the swing modes are listed in Table 2.3. From the table it can be inferred that the inter-area mode has a better damping than that in the base case. This demonstrates the effect of a high gain fast acting static exciter [25] in reducing the damping of the inter-area mode. However, the presence of a static exciter improves the synchronizing torque component as is reflected by an increase in the inter-area mode frequency (see Table 2.1). By comparing the results in Table 2.3 with that in Table 2.1, it can also be inferred that the exciter improves the damping of local modes.

SL No	Eigenvalues	Dampingfactor	Freq.(Hz)	Nature of the mode
1	$-0.7041 \pm j 7.2910$	0.0961	1.1604	Swing mode(2 & 1)
2	$-0.6529 \pm j 6.7193$	0.0967	1.0694	Swing mode(4 & 3)
3	$-0.1459 \pm j 4.0792$	0.0357	0.6492	Swing mode([1 2]&[3 4])

Table 2.3: Swing modes with all exciters on manual control.

2.2.6 Effect of Load Model with Exciters on Manual Control:

When both real and reactive power components of loads are model as constant power type, though the damping of swing modes are not effected with respect to constant impedance case, it makes the system small signal unstable as indicated by a negative damping factor for a pure real eigenvalue as shown in Table 2.4. This monotonic instability has been validated by plotting the magnitude of load bus voltages for a 3-phase fault at bus-1 with a fault duration of 0.01 s without line clearing - see Figure 2.4.

Modelling of P, Q components	Mode	Damping factor	Freq. (Hz)	Nature of mode
100% power $p_1 = 1, p_2 = 0, p_3 = 0$ $r_1 = 1, r_2 = 0, r_3 = 0$	$-0.7345 \pm j7.2286$	0.1011	1.1505	Swing mode(2 & 1)
	$-0.7609 \pm j6.5561$	0.1153	1.0434	Swing mode(4 & 3)
	$-0.1924 \pm j4.2506$	0.0452	0.6765	Swing mode([1 2]&[3 4])
	1.0795	-1.0000	0	Non-Oscillatory mode
	0.0046	-1.0000	0	Non-Oscillatory mode

Table 2.4: Effect of constant power type load model for P & Q load components with manual exciter control.

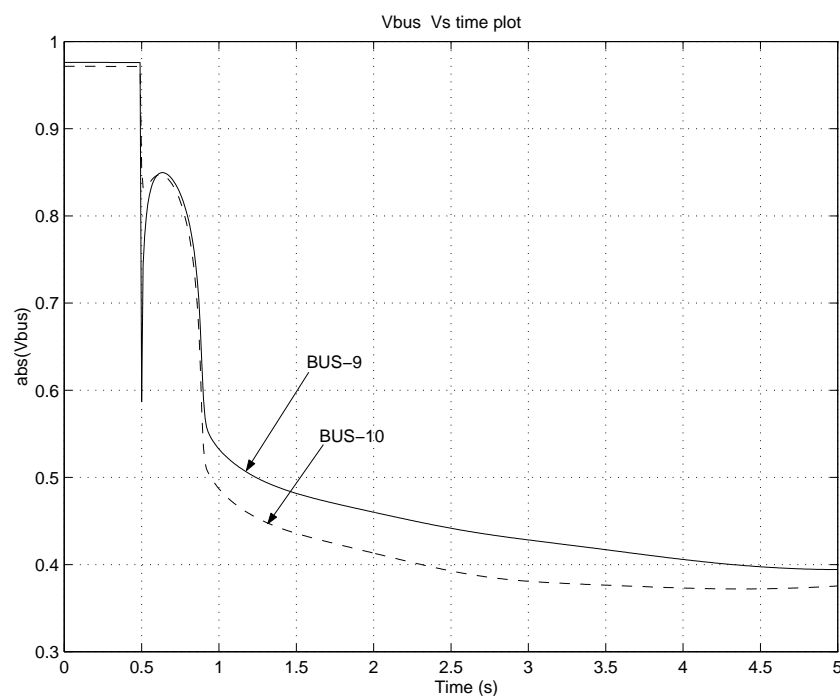


Figure 2.4: Variation of the magnitude of the load bus voltages.

Chapter 3

Design of Slip-signal PSS

3.1 Introduction:

Power system stabilizer (PSS) is a cost effective way of improving the damping of electromechanical oscillations of rotors and in turn it improves the power transfer capability of transmission lines. It provides the damping by modulating the voltage reference of exciter control so as to develop a component of electrical torque in phase with the rotor speed deviations. The location of PSS in a power system is depicted in Figure 3.1.

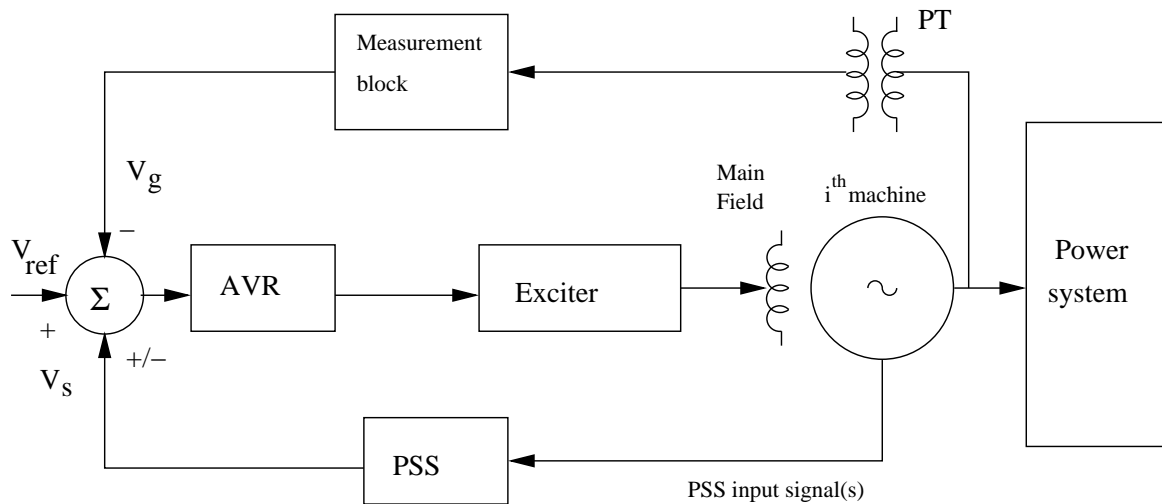


Figure 3.1: Location of PSS in a power system.

Such a way of producing damping torque is the most cost-effective method of enhancing the small-signal stability of power systems, in comparison to FACTS-based controllers [26]. The necessary power application is brought about in the normal process of torque development mechanism in the generator. Generally, PSS is installed to improve damping of local modes which is destabilized by the use of a high gain fast acting exciter. However, by judiciously placing power system stabilizers in a system, and with appropriate tuning

of PSS parameters, it is possible to even improve the damping of inter area modes. While designing a PSS to produce damping torque in a desired frequency range, care must be taken to see that the PSS does not destabilize the other oscillatory modes, for example, torsional modes [1]. Another important criterion in designing a PSS is to provide additional damping torque without affecting the synchronizing torque at critical oscillation frequencies, so that the inter-tie power transfer is not constrained.

3.2 Types of Power System Stabilizers:

As per IEEE standards 421.5 - 1992 [22], the following are the two main categories of PSS:

1. Single input power system stabilizer: It is known that in order to modify a mode of oscillation by feedback, the chosen input must excite the mode and it must be visible in the chosen output [5]. Thus, for this kind of PSS design, commonly used input signals are shaft speed, terminal bus frequency and electrical power output.
2. Dual input power system stabilizer: In this kind of PSS design, a combination of signals such as speed and electrical power output are used.

The design of speed-single input-based PSS design is presented in the following sections.

3.2.1 Slip-single Input PSS:

In the following lines, the structure of a speed-signal input PSS, is briefly discussed. Typical structure of a single input PSS -see Figure 3.2. It consists of a washout circuit, compensator, torsional filter, gain and a limiter. The function of each of the components of PSS with guidelines for the selection of parameters are given below [1].

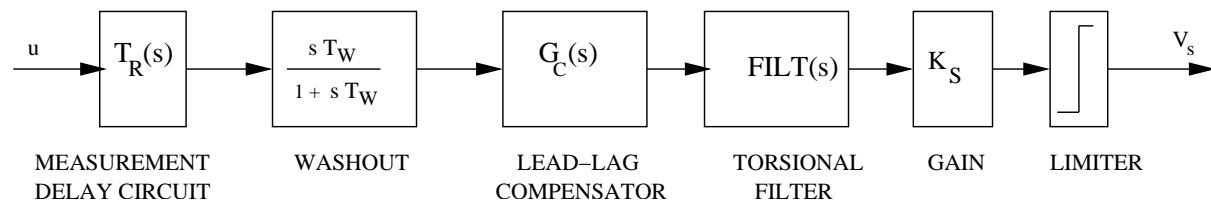


Figure 3.2: Block diagram of a single input PSS.

3.2.1.1 Washout Circuit:

Washout circuit is essentially a high-pass filter which removes dc offsets in the input signal and it eliminates the steady state bias in the output of PSS which will modify the field

voltage. From the viewpoint of the *washout function*, the value of T_W is not critical and may be anywhere in the range of 1 to 20 seconds. For local mode oscillations in the range of 0.8 to 2.0 Hz, a washout time constant of 1.5 s is satisfactory. From the viewpoint of low-frequency inter-area oscillations, a washout time constant of 10 seconds or higher is desirable, since lower-time constants result in significant phase lead at low frequencies. Unless this is compensated for elsewhere, it will reduce the synchronizing torque component at inter-area frequencies.

3.2.1.2 Lead-Lag Compensator:

To damp rotor oscillations, a PSS must produce a component of electrical torque in phase with rotor speed deviation. This requires a phase-lead circuits to be used to compensate for the lag between the PSS output point (at the exciter) and the resulting electrical torque developed. The amount of phase lag to be compensated depends on the generator parameters, the type of exciters used and the system conditions. Though the degree of phase compensation should be designed so that the PSS contributes to damping over a wide range of frequencies covering both inter-area and local modes of oscillation, a phase characteristic acceptable for different system conditions is selected. Generally, slight under-compensation is preferable to overcompensation so that the PSS does not contribute to the negative synchronizing torque component. General transfer function of $G_C(s)$ is given by

$$G_C(s) = \frac{(1 + sT_1) (1 + sT_3)}{(1 + sT_2) (1 + sT_4)}$$

If the degree of phase compensation required is small, a single first-order phase-compensation block may be used.

3.2.1.3 Torsional Filter:

The torsional filter in the PSS is essentially a band reject or a low pass filter to attenuate the first torsional mode frequency. The transfer function of the filter can be expressed as [1]

$$FILT(s) = \frac{\omega_n^2}{s^2 + 2\zeta\omega_n s + \omega_n^2} = \frac{a_0}{s^2 + a_1 s + a_0} \quad (3.1)$$

Torsional filter is necessitated by the adverse interaction of a slip-signal-based PSS with the torsional oscillations. This can be lead to shaft damage, particularly at light generator loads when the inherent mechanical damping is small. Even if shaft damage does not occur, stabilizer output can go into saturation (due to torsional frequency components) making it ineffective. The criteria for designing the torsional filter are:

1. The maximum possible change in damping of any torsional mode is less than some fraction of the inherent torsional damping.
2. The phase lag of the filter in the frequency range of the filter 1 to 3 Hz is minimized.

3.2.1.4 Stabilizer Gain:

The amount of damping associated with the rotor oscillations depends on the stabilizer gain K_S . The damping increases with an increase in stabilizer gain up to a certain value beyond which further increase in gain results in a decrease in the damping. To set the gain of the PSS, the following criterion are generally employed:

1. Based on the gain for instability: The optimal PSS gain is chosen for the particular tuning condition as the gain that results in the maximum damping of the critical (least damped) mode. The optimal gain (K_S) is related to the value of the gain K_S^* that results in instability. For example, for speed input stabilizers, $K_S = \frac{K_S^*}{3}$ may be used [27]. In [14], $K_S = \frac{K_S^*}{2}$ has been used. These studies are carried out using root locus method.
2. Damping factor of the critical mode: Here, the gain is selected such that damping factor for the mode is above some typical value say 0.05 [5].
3. High frequency gain: The high frequency gain of PSS is given by $K_S \frac{T_1 T_3}{T_2 T_4}$. This should not be too high as it would lead to noise amplification decreasing the effectiveness of a PSS.

3.2.1.5 Stabilizer Limits:

In order to restrict the level of generator terminal voltage fluctuations during transient conditions and to prevent the PSS acting to counter the action of AVR, limits are imposed on the PSS output.

The positive output limits of the stabilizer is set at a relatively large value in the range of 0.1 to 0.2 pu. This allows a high level of contribution from the PSS during large swings. With such a high value of stabilizer output limit, it is essential to have a means of limiting the generator terminal voltage to its maximum allowable value, typically in the 1.12 to 1.15 pu range [2].

The negative limit of PSS output is of importance during the back swing of the rotor (after initial acceleration is over). Negative side limit are raised to prevent the PSS from reducing the generators terminal voltage excessively following a fault. The AVR action is required to maintain the voltage (and thus prevent loss of synchronism) after the angular separation has increased. Typically, -0.02 to -0.05 pu is used for the negative limit. This allows sufficient control range while providing satisfactory transient response [28].

3.3 Tuning of PSS:

The major objective of providing PSS is to increase the power transfer in the network, which would otherwise be limited by oscillatory instability. Further the PSS must also function properly when the system is subjected to large disturbances. In the literature, two basic tuning techniques have been successfully utilized with power system stabilizer applications:

- Phase compensation method: This method consists of adjusting the stabilizer to compensate for the phase lag through the generator, excitation system, and power system such that the stabilizer path provides torque changes which are in phase with speed changes. This is the most straightforward approach, easily understood and implemented in the field [27].
- Root locus method: Synthesis by root locus involves shifting the eigenvalues associated with the power system modes of oscillation by adjusting the stabilizer pole and zero locations in the s -plane [29]. This approach gives additional insight to performance by working directly with the closed-loop characteristics of the system, as opposed to the open-loop nature of the phase compensation technique, but is more complicated to apply, particularly in the field.

The steps involved in designing a PSS are as follows:

1. Computation of $GEPS(s)$.
2. Design of compensator using phase compensation technique.
3. Determination of compensator gain.

3.3.1 Computation of $GEPS(s)$:

As stated earlier, a PSS acts through generator, exciter system, and power system (GEPS). Therefore, a PSS must compensate the phase lag through the GEPS. To obtain the phase information of GEPS, the frequency response of the transfer function between the exciter reference input (i.e., PSS output) and the generator electrical torque should be observed. In computing this response, the generator speed and rotor angle should remain constant, otherwise, when the excitation of a generator is modulated, the resulting change in electrical torque causes variations in rotor speed and angle and that in turn affect the electrical torque. As we are interested only in the phase characteristics between exciter reference input and electrical torque, the feedback effect through rotor angle variation should be eliminated by holding the speed constant. This is achieved by removing the

columns and rows corresponding to rotor speed and angle from the state matrix [5]. The procedure involved has been explained in the following lines.

The generator-exciter-power system (*GEPS*) frequency response, which involves the determination of the frequency response of a system function between T_e and V_s points, is obtained as follows:

For i^{th} machine, the expression for T_e (see C.37) is linearized as

$$\Delta T_e = C_T \Delta \underline{X}_G + B_T \Delta \underline{V}_G \quad (3.2)$$

where

- C_T is constituted by appropriately choosing the elements from $A_g(2, :)$ after multiplying it by $(-2H)$.
- B_T is constituted by using the elements from $B_g^r(2, :)$ after multiplying it by $(-2H)$.
- $\Delta \underline{X}_G$ is the vector of state variables $-(16n_g \times 1)$
- $\Delta \underline{V}_G$ is the vector of QD components of generator terminal voltages $-(2n_g \times 1)$.

C_T and B_T are filled with zeros to match the dimension of $\Delta \underline{X}_G$ and $\Delta \underline{V}_G$, respectively. From (1.43) we can relate $\Delta \underline{V}_G$ to state vector as

$$\Delta \underline{V}_G = \left([P_G]^T [Y'_{DQ}]^{-1} [P_G] [C_G] \right) \Delta \underline{X}_G \quad (3.3)$$

Using (3.3) in (3.2) we have

$$\begin{aligned} \Delta T_e &= C_T \Delta \underline{X}_G + B_T \left([P_G]^T [Y'_{DQ}]^{-1} [P_G] [C_G] \right) \Delta \underline{X}_G \\ &= \left[C_T + B_T \left([P_G]^T [Y'_{DQ}]^{-1} [P_G] [C_G] \right) \right] \Delta \underline{X}_G \end{aligned} \quad (3.4)$$

$$= D_T \Delta \underline{X}_G \quad (3.5)$$

Since $GEPS(j\omega)$ is obtained for $\Delta\delta = 0$ and $\Delta S_m = 0$, the respective elements are removed from D_T . This reduces the size of D_T to $[1 \times (16 - 2)n_g]$. Accordingly, $\Delta \underline{X}_G$ is reduced to $\Delta \underline{X}_T [(16 - 2)n_g \times 1]$

Hence,

$$\Delta T_e = D'_T \Delta \underline{X}_T \quad (3.6)$$

From (1.45), we can write that,

$$\Delta \dot{\underline{X}}_G = [A_T] \Delta \underline{X}_G + [E_G] [\Delta V_{ref} + \Delta V_s] \quad (3.7)$$

where $[E_G] = E_G(:, i)$ for i^{th} generator.

To meet the requirement of $\Delta\delta = 0$ and $\Delta S_m = 0$, the necessary changes are made in $[A_T]$ and $[E_G]$ to give.

$$\Delta \dot{\underline{X}}_T = [A'_T] \Delta \underline{X}_T + [E'_G] \Delta V_s$$

Note that in the above equation only change in V_s is considered, with $\Delta V_{ref} = 0$.

Rearranging the terms in s -domain, we get

$$\Delta \underline{X}_T(s) = [sI - A'_T]^{-1} [E'_G] \Delta V_s(s) \quad (3.8)$$

Using (3.8) in (3.6) we have,

$$\Delta T_e(s) = D'_T [sI - A'_T]^{-1} [E'_G] \Delta V_s(s)$$

$$GEPS(s) = \frac{\Delta T_e(s)}{\Delta V_s(s)} = D'_T [sI - A'_T]^{-1} [E'_G]$$

The frequency response is obtained by letting $s = j\omega$ and spanning ω in the desired range, i.e.,

$$GEPS(j\omega) = \frac{\Delta T_e(j\omega)}{\Delta V_s(j\omega)} = D'_T [j\omega I - A'_T]^{-1} [E'_G] \quad (3.9)$$

NOTE:

1. The above derivation assumes that PSS is not present on any machine.
2. The GEPS computation is independent of the turbine-governor models.

3.3.2 Design of Compensator $G_C(s)$:

Using (3.9), $GEPS(j\omega)$ for machine-1 is obtained (for the base case) and its phase response is shown in Figure 3.3.

If a PSS is to provide pure damping torque at all frequencies, ideally, the phase characteristics of PSS must balance the phase characteristics of GEPS at all frequencies. However, this is not practical, and the objective of designing a PSS is to see that it

- maximizes the damping of local modes as well as inter-area mode oscillations including other critical modes such as exciter/control modes without reducing the synchronizing torque component at those frequencies.

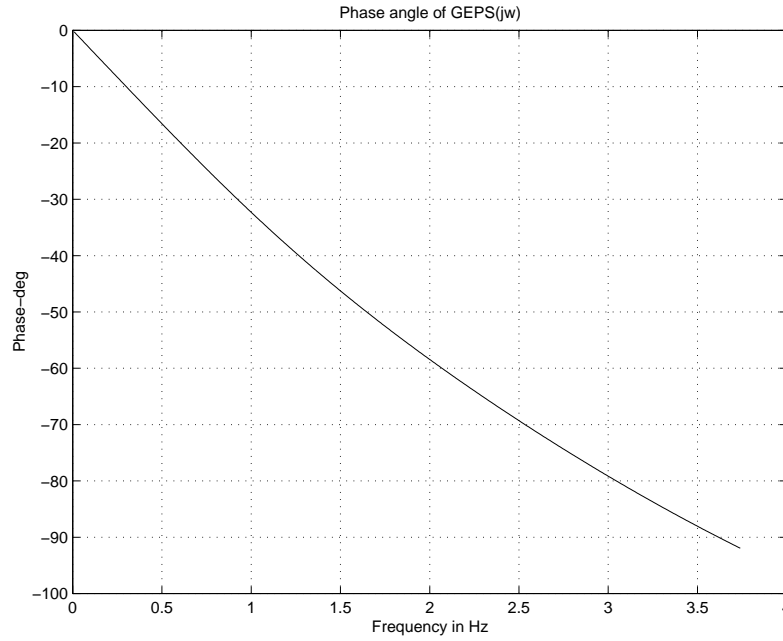


Figure 3.3: Phase angle of $GEPS(j\omega)$, for machine-1

- enhances the stability performance of a system for large disturbances.
- provides such a setting of parameters which is acceptable and does not require frequent retuning as system conditions change.
- provides better performance during major system upsets which cause large frequency excursions.
- provides such a setting of parameters which gives the required degree of tolerance to allow for uncertainties in machine and system modelling.

To meet these requirements the following criteria are chosen to design the phase compensation for PSS.

1. The compensated phase angle, $\phi_L = -\angle GEPS(j\omega)PSS(j\omega)$, should pass through 90° at frequency around 3.5 Hz.
2. The compensated phase angle at local mode frequency should be below 45° , preferably 20° .
3. The gain of the compensator at high frequencies should be minimized.

The first criterion is important to avoid destabilization of intra-plant modes with higher frequencies. It is also preferable to have the compensated phase angle to be lagging at inter-area modes so that PSS provides some synchronizing torque at these frequencies. The third criterion is required to minimize the noise amplification through PSS.

NOTE:

1. The compensated phase angle, ϕ_L can also be read from Figure 1.1 and is assumed to be positive for lagging angle. If $\phi_L=0$, it shows that the torque change produced is purely damping (at a given frequency). A negative ϕ_L denotes that the developed torque ΔT_e has a negative synchronizing torque component.
2. An improvement in the damping torque component is reflected in an increase in the damping factor of the mode.
3. An improvement in the synchronizing torque component is reflected in an increase in the frequency of the mode. This observation is identical to that in SMIB system where the natural frequency of oscillation ω of the rotor is given by $\sqrt{\frac{T_s \omega_B}{2H}}$ for classical modal of generator and with negligible damping.

For simplicity, the compensator transfer function is assumed to be of the form given by,

$$G_c(s) = \frac{(1 + sT_1) K_S}{(1 + sT_2)} \quad (3.10)$$

Determination T_1 and T_2 [30]

The phase angle lead ϕ_m to be provided by the compensator is related to T_1 and T_2 as

$$\sin \phi_m = \frac{1 - \alpha}{1 + \alpha} \quad (3.11)$$

where

$$\alpha = \frac{T_2}{T_1} \quad \text{with } 0 < \alpha < 1, \quad (3.12)$$

Further, the center frequency at which it offers a phase lead ϕ_m is given by

$$\omega_m = \frac{1}{\sqrt{\alpha} T_1} \quad (3.13)$$

Choosing $\phi_m = 20^\circ$ and $f_m = 3$ Hz, (with $\omega_m = 2\pi f_m$), and using (3.11), (3.12) and (3.13) we get $T_1 = 0.07577$ s and $T_2 = 0.03715$ s with $\frac{T_1}{T_2} = 2.0396$. The phase angle of the compensator is shown in Figure 3.4.

NOTE: Typically $\frac{T_1}{T_2}$ must be less than 10.

In Figure 3.5, the phase response of the PSS which is the combined phase response of $G_C(s)$ and a washout circuit with $T_W = 10$ s is depicted. The compensated phase response is also plotted in the figure. From the figure, it can be seen that the phase angle ϕ_L is around 60° at 3 Hz, below 2 Hz the angle ϕ_L is less than 40° and at inter-area mode of 0.7 Hz the angle is around 12.6° .

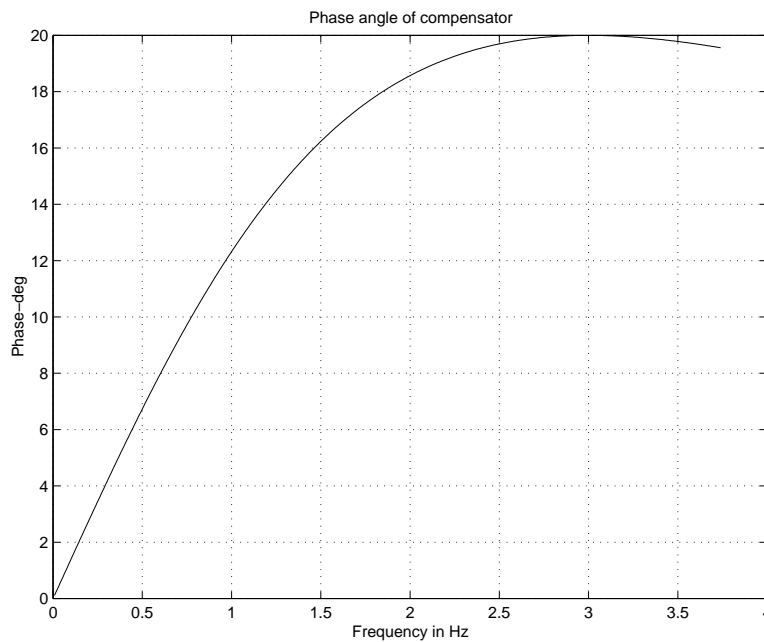


Figure 3.4: Phase angle of compensator $G_C(j\omega)$.

The above results/plots have been obtained by using the following steps:

1. Execute `small_sig.m` with appropriate options.
2. Run `pss_design.m` programme.

A list of statements printed out by the programme is given below.

```
Enter the generator number for which you want to obtain the angle of GEPS(s):  1
Enter 1  :To design single input PSS - Slip signal
      2  :To design double input PSS
      3  :To design single input PSS -Power signal
Enter your choice : 1
Enter the center frequency f_m for the PSS (in Hz) :  3
Enter the amount of phase lead required (in Degrees):  20
Enter the PSS gain Ks:  15
```

The ratio of T1 to T2 = 2.0396 is less than 10

```
Enter 1 : Only compensator
      2 : Washout only
      3 : Washout and measuring ckt.
      4 : Washout, measuring ckt. and torsional filter
Enter your choice : 2
Enter the value of Tw (in s) for the wash-out circuit [1 - 20]s :  10
```

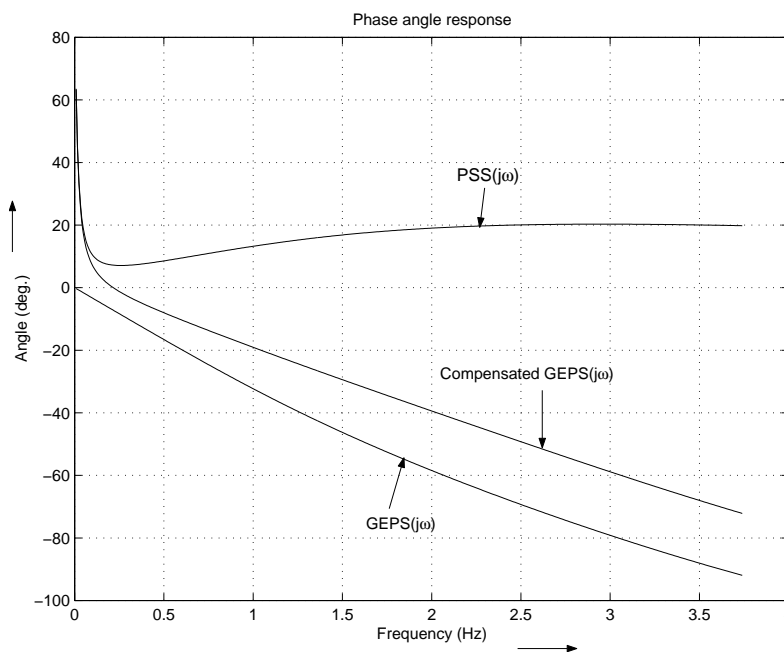


Figure 3.5: Phase angle of $GEPS(j\omega)$, $G_{PSS}(j\omega)$ and $P(j\omega)$ for machine-1.

Enter 0 if you are satisfied with the design, otherwise 1 to re-design the pss: 0

Update the slip_pss.dat for the machine 1

```
-----
gen.no   Ks      Tw      T1      T2
-----
1        15     10      0.07577  0.03715
-----
```

Use typical value for TR (0.02 s), $a_0 = 570$, and $a_1 = 35$

Press any key to obtain the amplitude response of $GEPS(i\omega)$

NOTE: A tentative value of K_S needs to be entered while feeding the data for the programme. This will be used for printing purpose only.

3.3.3 Determination of Compensator Gain:

The compensator gain is chosen based on the amplitude response of $GEPS(s)$, see Fig. 3.6. This plot also has been obtained by running the `pss_design.m` programme.

For speed input PSS, the highest amplitude results for heavily loaded system condition [27]. In this thesis, the gain is chosen to provide a damping factor of more than 0.05 for

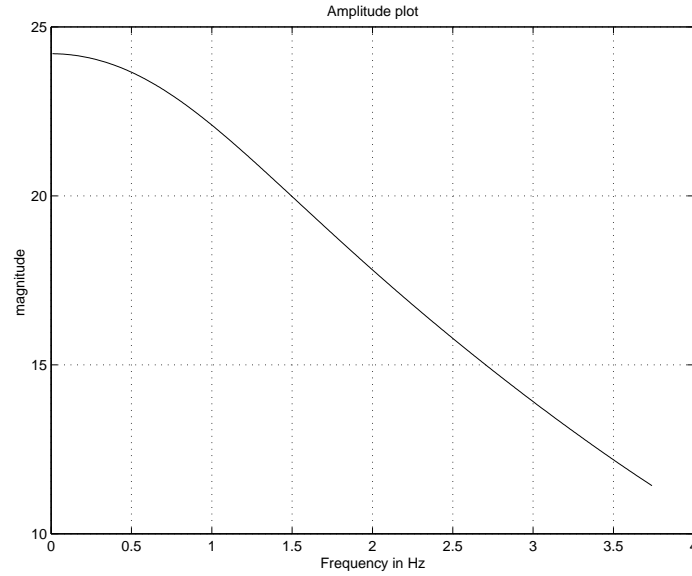


Figure 3.6: Plot of amplitude of $GEPS(s)$ for machine-1.

lightly damped modes in the base case. To see the performance of the system with PSS, the system matrix needs to be modified to account for PSS. This interfacing procedure is discussed in the following section.

3.3.3.1 Interfacing PSS to the System Matrix:

The linearized model of the slip-input PSS is given by

$$\Delta \dot{\underline{x}}_{PSS} = A_{PSS} \Delta \underline{x}_{PSS} + B_{PSS} \Delta S_m \quad (3.14)$$

$$\Delta V_s = C_{PSS} \Delta \underline{x}_{PSS} + D_{PSS} \Delta S_m \quad (3.15)$$

where ΔS_m denotes the deviation in slip for i^{th} generator.

The interfacing of the PSS to the system equations is carried out as follows:

Rewriting (1.45) considering only the change in V_s , we have,

$$\Delta \dot{\underline{X}}_G = [A_T] \Delta \underline{X}_G + [E_G] \Delta V_s \quad (3.16)$$

where $[E_G] = E_G(:, i)$ for i^{th} generator.

Writing ΔS_m in terms of $\Delta \underline{X}_G$, we have

$$\Delta S_m = e_2^T \Delta \underline{X}_G \quad (3.17)$$

where $e_2^T = [0 \cdots 1 \cdots 0 \cdots 0 \cdots 0]_{(1 \times 16n_g)}$, with 1 corresponding to slip state variable of i^{th} machine.

Now using (3.17) in (3.14) and (3.15) we get,

$$\Delta \dot{\underline{x}}_{PSS} = A_{PSS} \Delta \underline{x}_{PSS} + B_{PSS} e_2^T \Delta \underline{X}_G \quad (3.18)$$

$$\Delta V_s = C_{PSS} \Delta \underline{x}_{PSS} + D_{PSS} e_2^T \Delta \underline{X}_G \quad (3.19)$$

Using (3.19) in (3.16) and rewriting the state model accounting PSS, we obtain,

$$\Delta \dot{\underline{X}}_N = A_N \Delta \underline{X}_N$$

where $\Delta \underline{X}_N = [\Delta \underline{X}_G \ \Delta \underline{x}_{PSS}]^T$

$$A_N = \begin{bmatrix} [A_T] + [E_G] D_{PSS} e_2^T & [E_G] C_{PSS} \\ B_{PSS} e_2^T & A_{PSS} \end{bmatrix}$$

3.3.3.2 Eigenvalues with Slip-input PSS:

For the PSS designed in the previous section for machine-1, all oscillator modes are listed in Table 3.1, for $K_S = 15$. Note that in this implementation FILT(s) and TR(s) are not considered.

SL No	Eigenvalues	Dampingfactor	Freq.(Hz)	Nature of the mode
1	-15.4522± j17.0633	0.6712	2.7157	Non-Swing mode
2	-15.6284± j12.5252	0.7803	1.9934	Non-Swing mode
3	-2.5472± j8.4109	0.2899	1.3386	Swing mode(2 & 1)
4	-1.0555± j6.8044	0.1533	1.0830	Swing mode(4 & 3)
5	-0.2653± j4.5064	0.0588	0.7172	Swing mode([1 2]&[3 4])
6	-14.5481± j1.9838	0.9908	0.3157	Non-Swing mode

Table 3.1: Oscillatory modes for the base case with PSS on m/c-1.

The results are obtained by using the following steps:

1. Prepare the data file `slip_pss.dat` as shown below (see section 2.2.1):

File name: `slip_pss.dat`

```
-----
Gen.no. KS   TR   TW    T1      T2      VSMAX  VSMIN   a0     a1     TRF
-----
1         15  0.02  10  0.07577  0.03715  0.1    -0.1   570    35     1
-----
```

TRF = 0 enables torsional filter, 1 disables it.

FILT(s) is not used by setting $\text{TRF} = 1$, and $\text{TR}(s)$ is disabled by setting the variable `Tmd_slip_nt` to 1 in file `pss_slip_signal.m`. Even when TRF is 1, default value of `a0` and `a1` must be used in the data file.

2. Set `ng_slip_pss = [1]` and enable PSS by setting `PSS=zeros(1,nb)` in file `initcond.m`.
3. Run `small_sig.m` and then execute `trace_mode.m` programme.

From the tabulated results, it can be seen that the damping factor for the inter-area mode (mode-17, 18) has increased from 0.0083 (see Table 2.1) to 0.0588. We can also observe that, the local mode-13, 14 is also well damped from its previous value of 0.1466. However, the presence of PSS on machine-1 has not influenced the damping of mode-15, 16 significantly as generator-1 has the lowest participation in that mode. Also note that the PSS has contributed to the synchronizing torque component, as is demonstrated by an increase in frequency of the inter-area mode and mode-13, 14.

NOTE: From the root locus plot it was observed that one of the local modes becomes unstable when $K_S = 235$. The root locus plot is obtained by a repeated run of `small_sig.m` and `trace_mode.m` programmes.

3.3.4 Time-domain Verification:

Rotor angle plots of all machines with and without PSS are shown in the Figures (3.7 and 3.8). Fault duration is set to 0.1 s, for a fault at bus 9 with no line clearing.

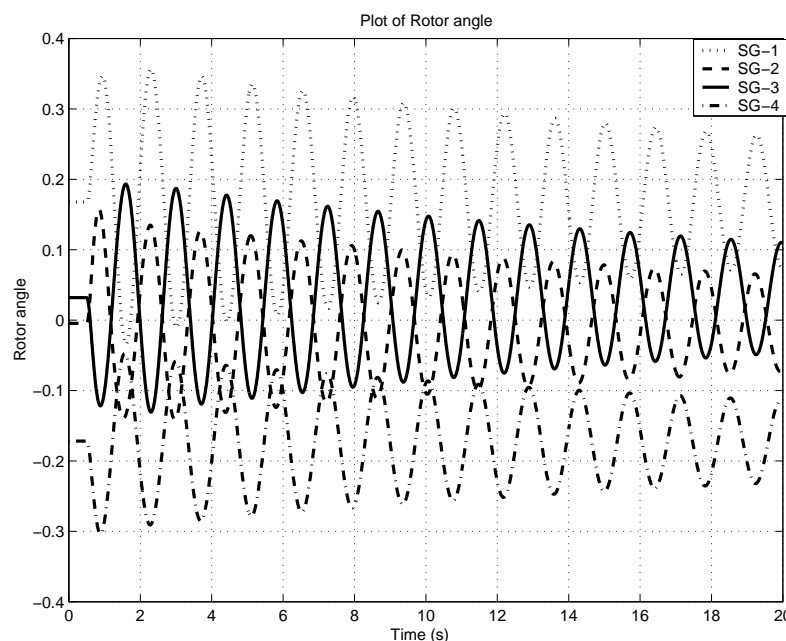


Figure 3.7: Variation of rotor angles with respect to COI reference without PSS.

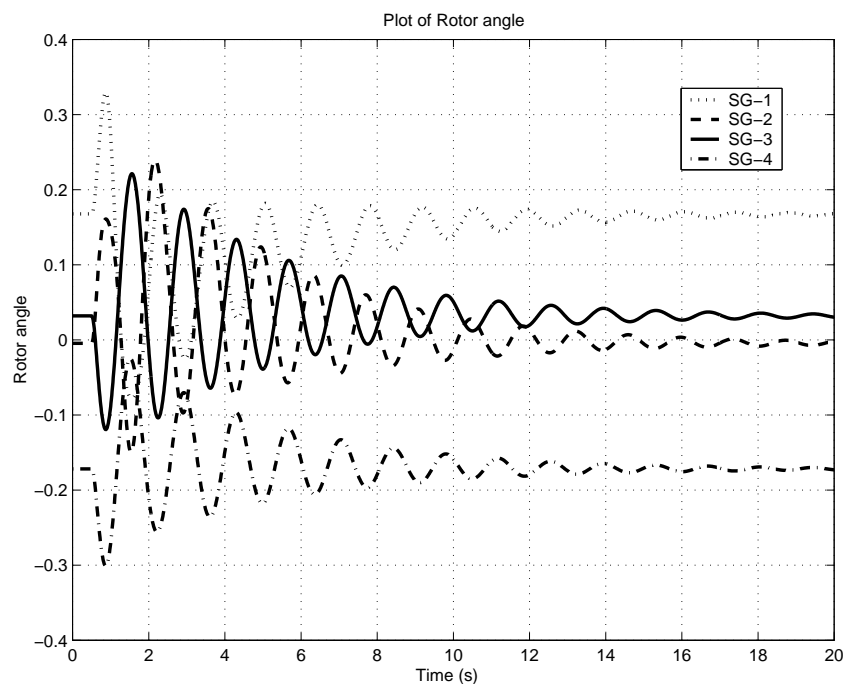


Figure 3.8: Variation of rotor angles with PSS.

The plots are obtained by employing the following steps:

1. The steps are identical to that indicated in the previous section 3.3.3.2.
2. While running `small_sig.m`, the following option is chosen:

wB =

376.9911

Enter 1 if you want to run transtability programme for network disturbances, otherwise 0: 1

If NO action to be taken, PRESS ENTER for any/every prompt.

Fault initiation time (s), Tfault= 0.5

Fault Duration,(s) Tclear= 0.1

Faulted Bus: 9

Line(s) to be tripped, [,]=

3. Run `transtability.mdl` programme.

3.3.5 Frequency response of $\frac{T_e(s)}{V_{ref}(s)}$:

Frequency response of a system function between T_e and V_{ref} -point of the exciter, is obtained as follows:

For i^{th} machine, the expression for T_e (see C.37) is linearized as

$$\Delta T_e = C_T \Delta \underline{X}_G + B_T \Delta \underline{V}_G \quad (3.20)$$

where

- C_T is constituted by appropriately choosing the elements from $A_g(2, :)$ after multiplying it by $(-2H)$.
- B_T is constituted by using the elements from $B_g^r(2, :)$ after multiplying it by $(-2H)$.
- $\Delta \underline{X}_G$ is the vector of state variables $-(16n_g \times 1)$
- $\Delta \underline{V}_G$ is the vector of QD components of generator terminal voltages $-(2n_g \times 1)$.

C_T and B_T are filled with zeros to match the dimension of $\Delta \underline{X}_G$ and $\Delta \underline{V}_G$, respectively. From (1.43) we can relate $\Delta \underline{V}_G$ to the state vector as

$$\Delta \underline{V}_G = \left([P_G]^T [Y'_{DQ}]^{-1} [P_G] [C_G] \right) \Delta \underline{X}_G \quad (3.21)$$

Using (3.21) in (3.20) we have,

$$\begin{aligned} \Delta T_e &= C_T \Delta \underline{X}_G + B_T \left([P_G]^T [Y'_{DQ}]^{-1} [P_G] [C_G] \right) \Delta \underline{X}_G \\ &= \left[C_T + B_T \left([P_G]^T [Y'_{DQ}]^{-1} [P_G] [C_G] \right) \right] \Delta \underline{X}_G \end{aligned} \quad (3.22)$$

$$= D_T \Delta \underline{X}_G \quad (3.23)$$

From (1.45), we can write that,

$$\Delta \dot{\underline{X}}_G = [A_T] \Delta \underline{X}_G + [E_G] [\Delta V_{ref} + \Delta V_s] \quad (3.24)$$

where $[E_G] = E_G(:, i)$ for i^{th} generator.

Considering only the change in V_{ref} , we have

$$\Delta \dot{\underline{X}}_G = [A_T] \Delta \underline{X}_G + [E_G] \Delta V_{ref}$$

Rearranging the terms in s -domain, we get

$$\Delta \underline{X}_G(s) = [sI - A_T]^{-1} [E_G] \Delta V_{ref}(s) \quad (3.25)$$

Using (3.25) in (3.23) we have,

$$\Delta T_e(s) = D_T [sI - A_T]^{-1} [E_G] \Delta V_{ref}(s)$$

$$F(s) = \frac{\Delta T_e(s)}{\Delta V_{ref}(s)} = D_T [sI - A_T]^{-1} [E_G]$$

The frequency response is obtained by letting $s = j\omega$ and spanning ω in the desired range, i.e.,

$$F(j\omega) = \frac{\Delta T_e(j\omega)}{\Delta V_{ref}(j\omega)} = D_T [j\omega I - A_T]^{-1} [E_G]$$

The frequency response of $\frac{\Delta T_e(j\omega)}{\Delta V_{ref}(j\omega)}$ for machine-1 is shown in Figure 3.9.

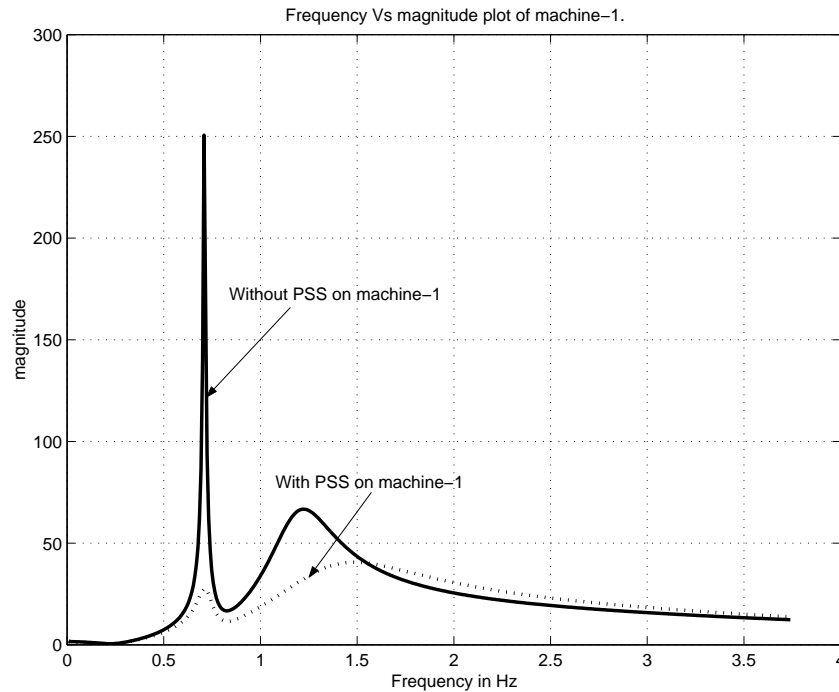


Figure 3.9: Frequency response plot with and without PSS.

From the figure it can be seen that, without PSS, the frequency response of $\frac{\Delta T_e(j\omega)}{\Delta V_{ref}(j\omega)}$ shows a prominent peak at inter-area mode (0.7003 Hz). However, with PSS (for $K_S=15$) the sharp peak is well attenuated demonstrating the effectiveness of PSS in improving the damping for inter-area mode (see Table 3.1). The figure also depicts the damping of local mode-13, 14 (1.3386 Hz) with the PSS.

NOTE:

1. The plot is obtained by executing `freq_response.m` after running `small_sig.m` programme with and without PSS.
2. In the implementation, $[j\omega I - A_T]$ is realized as follows:
Using $W A U = D_\lambda$ and $W = U^{-1}$ we have,

$$\begin{aligned}
 (j\omega I - W^{-1} D_\lambda U^{-1}) &= (j\omega I - U D_\lambda W) \\
 &= (j\omega U W - U D_\lambda W) \\
 &= U (j\omega I - D_\lambda) W
 \end{aligned}$$

The above expression is used to overcome the numerical problem faced while computing $[j\omega I - A_T]^{-1}$

3.4 Placement of Power System Stabilizers:

Placement of PSS in power system is an important issue in modal analysis. Power system stabilizers placed at the generators should be able to stabilize all of the electromechanical modes. The selection of PSS location is generally carried out using participation factor, residues and frequency response analysis [5, 27, 7].

Of these, participation factor based approach provides an initial screening of locations [7]. In this work, the following procedure is employed to decide the location of PSS.

1. List all swing modes whose damping factor is less than 0.05.
2. List participation factor for slip-signal for each of the selected swing mode.
3. Location of PSS is decided for the machine whose slip participation is the highest in that mode.

The above procedure is implemented in `pss_selection.m`. The steps to be followed are:

1. Run `small_sig.m` file with appropriate choice.
2. Execute `pss_selection.m` programme. The output of the programmes is listed below:

Enter 1 to use EIG function, otherwise 0 to use EIGS function: 1

```

-----
SL_number          Eigenvalue          dampingfactor          frequency(Hz)

```

ans =

1.0000	-42.9191	1.0000	0
2.0000	-42.7135	1.0000	0
3.0000	-16.0251 +16.9998i	0.6859	2.7056
4.0000	-16.0251 -16.9998i	0.6859	2.7056
5.0000	-38.6952	1.0000	0
----- A partial List-----			
27.0000	-4.6860	1.0000	0
28.0000	-0.0000	1.0000	0

swing modes for which dampingfactor is less than 0.05

SL_number	Eigenvalue	dampingfactor	frequency(Hz)
-----------	------------	---------------	---------------

ans =

18.0000	-0.0372 - 4.4583i	0.0083	0.7096
---------	-------------------	--------	--------

PSS is Disabled.....

State variable Mag(slip-PF-nr) angle(slip-PF-nr) in deg.

Slip-1	1.0000	0.00
Slip-3	0.9641	-6.28
Slip-2	0.6263	-4.41
Slip-4	0.6185	-1.98

Please press a key to obtain the angle of GEPS(s) for the selected machine

Here it calls pss_design.m programme.

NOTE:

1. The programme pss_selection.m also calls pss_design.m file if any of the swing mode has a damping factor less than 0.05.
2. While listing swing modes whose damping factor is less than 0.05, the presence of PSS (if enabled in the previous run) is also considered. Thus, in this method effort

is made to stabilize/improving the damping of swing modes sequentially, until all modes are stabilized.

3. As power system stabilizers are added to a system, the sensitivity of modes to power system stabilizers at other generators is altered. For example, a generator having no appreciable participation in any mode in the original unstabilized system may have a significant participation in the resulting unstable/poorly damped modes with PSS.
4. It is known that power system stabilizers do not add damping torques to a generator shaft directly, but indirectly through the generators' electrical torques. The electrical torque is altered by modulating the generator voltage. If the generator voltage is kept constant by the automatic voltage regulator of another close by generator a power system stabilizer will be less effective. Therefore, participation/residue based design should be used with care.

Various methods of PSS tuning in multimachine environment is discussed in [31].

Chapter 4

Design of Delta-P-Omega Signal PSS

4.1 Introduction:

In this chapter, a dual input PSS where speed and electrical power deviations are used as input, is analyzed. This PSS is referred to as Delta-P-Omega PSS. The objective of this PSS is to derive an equivalent speed signal $\Delta\omega_{eq}$ so that it does not contain torsional modes. The principle of this type of stabilizer is illustrated below [2, 32]:

Neglecting \overline{D} , from (C.35) we have

$$\Delta S_m = \frac{1}{2H} \int \Delta T_m dt - \frac{1}{2H} \int \Delta T_e dt \quad (4.1)$$

Note that torsional components are inherently attenuated in ΔT_e signal. Now the problem is to measure the integral of ΔT_m free of torsional modes. In many applications, the ΔT_m component is neglected. This is satisfactory, except when changing load on the unit and other system conditions when the mechanical power changes. Under such conditions, a spurious stabilizer output is produced if ΔT_e alone is used as the stabilizing signal. This in turn results in transient oscillations in voltage and reactive power. A way to measure integral of ΔT_m is presented below:

Rewriting (4.1), we have,

$$\frac{1}{2H} \int \Delta T_m dt = \Delta S_m + \frac{1}{2H} \int \Delta T_e dt \quad (4.2)$$

The delta-P-omega stabilizer makes use of the above relationship to simulate a signal proportional to the integral of mechanical power change by adding signals proportional to shaft-speed change and integral of electrical power change. This signal will contain torsional oscillations unless a filter is used. Because mechanical power changes are relatively slow even for fast-valve movements, the derived integral of the mechanical power signal can be conditioned with a simple low-pass filter to remove torsional frequencies. These

functions are realized in Figure 4.1. In the figure TF_F represents a filter. The output of the filter provides $(\frac{1}{2H} \int \Delta T_m dt)$ signal which is free from torsional oscillation.

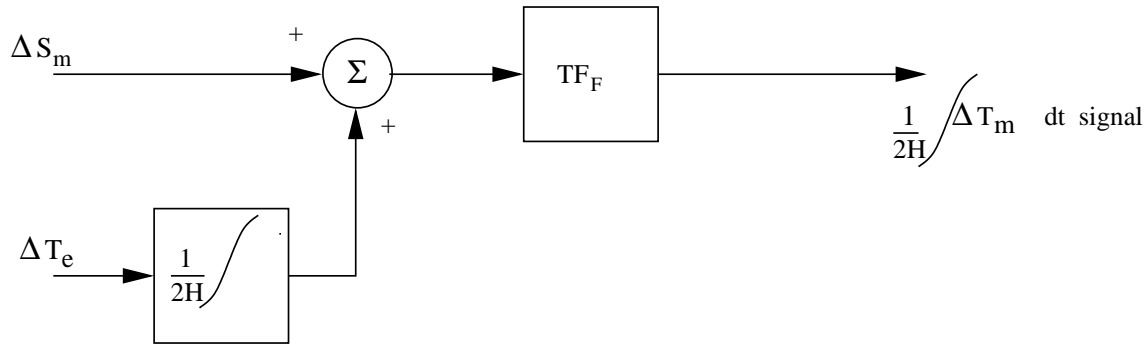


Figure 4.1: Block schematic to generate integral of ΔT_m .

Using this signal, the slip signal is synthesized which is completely free of torsional frequency components. This obtained by realizing (4.1) having simulated $(\frac{1}{2H} \int \Delta T_m dt)$ signal. This permits the selection of a higher stabilizer gain that results in better damping of system oscillations, without causing the destabilization of exciter/swing modes unlike that is observed in a slip-signal-based PSS with torsional filter, $FILT(s)$ [2]. The block schematic of a Delta-P-Omega type PSS is shown in Figure 4.2. In the figure, note that an integrator is approximated by a first order transfer function by suitably choosing the time constant T_7 . This is done to avoid offset problem in a pure integrator circuit.

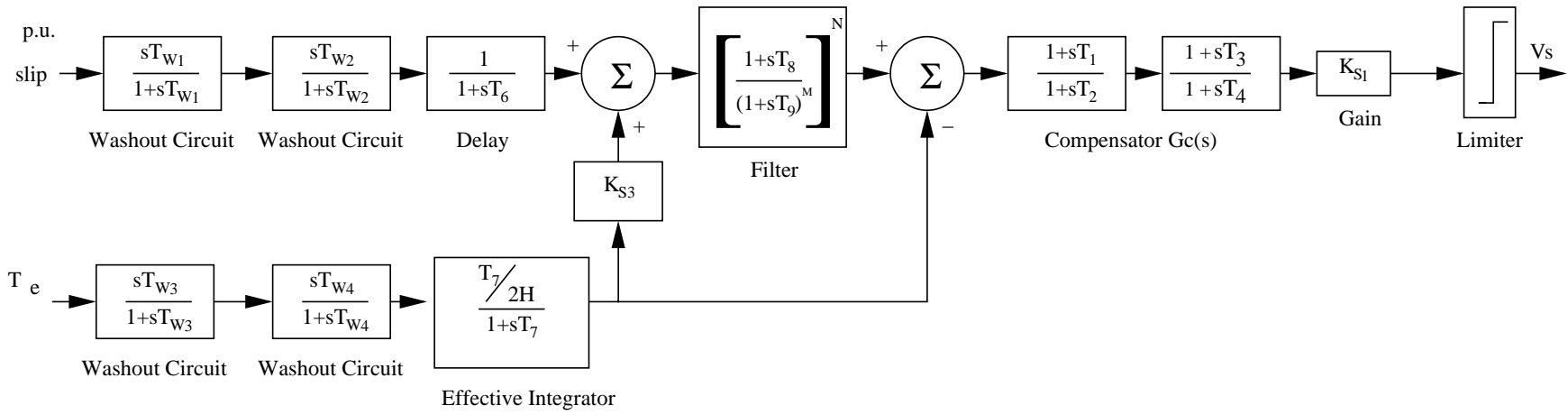


Figure 4.2: Delta-P-Omega PSS.

It has the following advantages over speed or frequency based systems:

- it inherently attenuates torsional modes to the extent that torsional filtering in the main stabilizing path is not required.
- the shaft location for speed sensing is not critical.
- without the torsional filter, increased stabilizer loop gain is available.

It is superior to systems using only electrical power, as the fastest load changes can be accommodated with minimal terminal voltage disturbance without taking the stabilizer out of service. Design of an electrical power input PSS is discussed in the next chapter.

4.2 Design of Delta-P-Omega PSS:

Following steps employed to design and analyze the PSS:

1. Design of the compensator.
2. Interfacing of PSS to the system matrix.

4.2.1 Design of the Compensator $G_c(s)$:

The main requirement is to determine the values of T_1 , T_2 , T_3 and T_4 in the compensator transfer function given by:

$$G_C(s) = G_{C1}(s) G_{C2}(s) = \frac{(1 + sT_1)}{(1 + sT_2)} \frac{(1 + sT_3)}{(1 + sT_4)}$$

To obtain the values of T_1 , T_2 , T_3 and T_4 , the compensators $G_{C1}(s)$ and $G_{C2}(s)$ are designed separately to achieve the desired overall compensated phase lag with the GEPS(s). $G_{C1}(s)$ and $G_{C2}(s)$ are designed following the steps indicated in section 3.3.2, choosing appropriate value for f_m and ϕ_m . For the 4 machine example, considering the base case, we have, $f_m = 3$ Hz, and $\phi_m = 10^\circ$ for both $G_{C1}(s)$ and $G_{C2}(s)$. This results in $T_1 = T_3 = 0.06322$ s and $T_2 = T_4 = 0.04452$ s.

The compensated phase lag considering the entire structure of PSS is shown in Figure 4.3. To get this, ΔT_e is approximately expressed in terms of ΔS_m as

$$\Delta T_e(s) = -s \ 2H \Delta S_m(s)$$

neglecting the mechanical power deviation, ΔT_m .

The above plots are obtained by executing `pss_design.m` programme. The list of statements printed out by the programme is shown below:

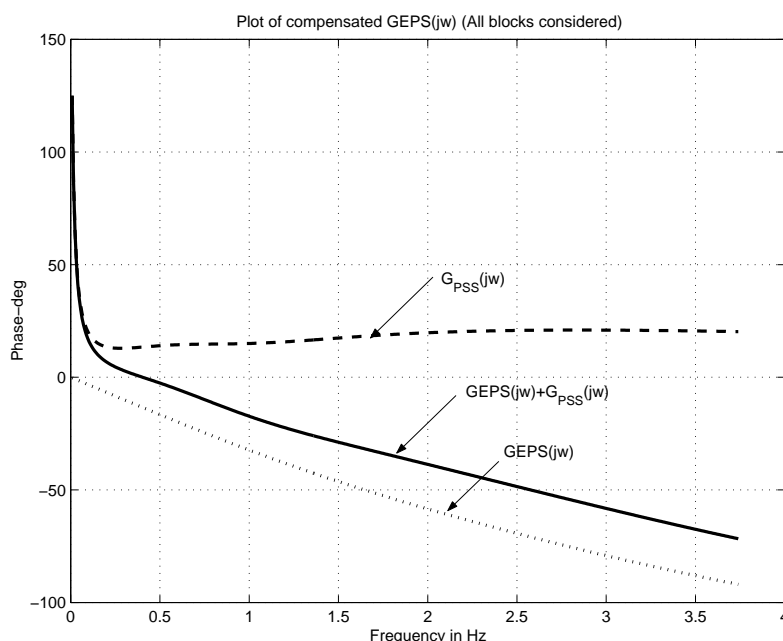


Figure 4.3: Plot of compensated $GEPS(j\omega)$ with all blocks.

Enter the generator number for which you want to obtain the angle of $GEPS(s)$: 1

Enter 1 :To design single input PSS - Slip signal

2 :To design double input PSS

3 :To design single input PSS -Power signal

Enter your choice : 2

Now you are designing compensator $G_{c1}(s)$

Enter the center frequency f_m for G_{c1} (in Hz) : 3

Enter the amount of phase lead required (in Degrees): 10

Enter the PSS gain K_s : 15

The ratio of T_1 to $T_2 = 1.4203$ is less than 10

Enter y : if compensator $G_{c2}(s)$ is same as the compensator $G_{c1}(s)$

n : if compensator $G_{c2}(s)$ is different from the compensator $G_{c1}(s)$

Enter your choice (as a character input y or n): 'y'

Enter 1 : Compensators $G_{c1}(s)*G_{c2}(s)$ only

2 : Compensators with Washout only

3 : All Blocks

Enter your choice : 3

Enter the value of Tw_1 (in s) for the wash-out circuit-1 [1 - 20]s : 10

Enter the value of Tw_2 (in s) for the wash-out circuit-2 [1 - 20]s : 10

Enter the value of Tw_3 (in s) for the wash-out circuit-3 [1 - 20]s : 10

Enter the value of Tw4 (in s) for the wash-out circuit-4 [1 - 20]s : 10
Enter the value of T6 (in s) for the slip-path delay [0.01 - 0.05]s : 0.01
Enter the value of T7 (in s) for the equivalent integrator [1 - 10]s : 10
Enter the value of T8 (in s) for the Filter circuit [0 - 0.01]s : 0
Enter the value of T9 (in s) for the Filter circuit [0.1 - 0.2]s : 0.1
Enter 0 if you are satisfied with the design, otherwise 1 to re-design the pss: 0

Update the delPW_pss.dat for the machine 1

gen.no	Ks	T1	T2	T3	T4
1	15	0.06322	0.04452	0.06322	0.04452

Press any key to obtain the amplitude response of GEPS(iw)

4.2.2 Interfacing of PSS to the System Matrix:

For the purpose of simplification, the blocks in Figure 4.2 is redrawn as in Figure 4.4.

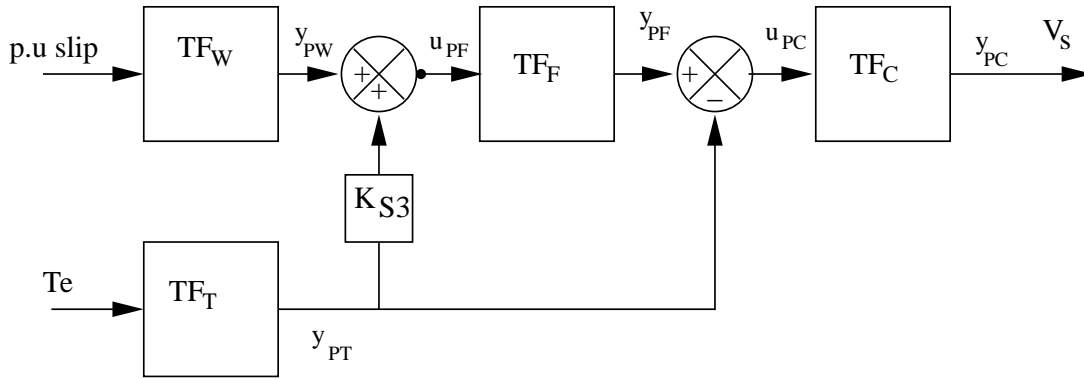


Figure 4.4: Delta-P-Omega PSS modified block schematic.

The transfer function block TF_W can be written in the state space form as:

$$\Delta \dot{\underline{x}}_{PW} = A_{PW} \Delta \underline{x}_{PW} + B_{PW} \Delta S_m \quad (4.3)$$

$$\Delta y_{PW} = C_{PW} \Delta \underline{x}_{PW} + D_{PW} \Delta S_m \quad (4.4)$$

The transfer function block TF_T can be written in the state space form as:

$$\Delta \dot{\underline{x}}_{PT} = A_{PT} \Delta \underline{x}_{PT} + B_{PT} \Delta T_e \quad (4.5)$$

$$\Delta y_{PT} = C_{PT} \Delta \underline{x}_{PT} + D_{PT} \Delta T_e \quad (4.6)$$

The transfer function block TF_F can be written in the state space form as:

$$\Delta \dot{\underline{x}}_{PF} = A_{PF} \Delta \underline{x}_{PF} + B_{PF} \Delta u_{PF} \quad (4.7)$$

$$\Delta y_{PF} = C_{PF} \Delta \underline{x}_{PF} + D_{PF} \Delta u_{PF} \quad (4.8)$$

The transfer function block TF_C can be written in the state space form as:

$$\Delta \dot{\underline{x}}_{PC} = A_{PC} \Delta \underline{x}_{PC} + B_{PC} \Delta u_{PC} \quad (4.9)$$

$$\Delta y_{PC} = C_{PC} \Delta \underline{x}_{PC} + D_{PC} \Delta u_{PC} \quad (4.10)$$

$$\Delta u_{PF} = \Delta y_{PW} - K_{S3} \Delta y_{PT} \quad (4.11)$$

$$\Delta u_{PC} = \Delta y_{PF} - \Delta y_{PT} \quad (4.12)$$

$$\Delta V_S = \Delta y_{PC} \quad (4.13)$$

Simplifications are carried out as follows:

1. Substitute (4.4) and (4.6) in (4.11) and simplify.
2. The modified (4.11) for Δu_{PF} is substituted in (4.7) and (4.8).
3. The modified (4.8) for Δy_{PF} and (4.6) are substituted in (4.12).
4. The modified (4.12) for Δu_{PC} is substituted in (4.9) and (4.10).

After the simplifications we get,

$$\Delta \dot{\underline{x}}_{PW} = A_{PW} \Delta \underline{x}_{PW} + B_{PW} \Delta S_m \quad (4.14)$$

$$\Delta \dot{\underline{x}}_{PT} = A_{PT} \Delta \underline{x}_{PT} + B_{PT} \Delta T_e \quad (4.15)$$

$$\Delta \dot{\underline{x}}_{PF} = \left[(B_{PF} C_{PW}) \Delta \underline{x}_{PW} + (B_{PF} K_{S3} C_{PT}) \Delta \underline{x}_{PT} + A_{PF} \Delta \underline{x}_{PF} \right. \\ \left. + (B_{PF} D_{PW}) \Delta S_m + (B_{PF} K_{S3} D_{PT}) \Delta T_e \right] \quad (4.16)$$

$$\Delta \dot{\underline{x}}_{PC} = \begin{bmatrix} (B_{PC}D_{PF}C_{PW}) \Delta \underline{x}_{PW} + [B_{PC}(D_{PF}K_{S3}C_{PT} - C_{PT})] \Delta \underline{x}_{PT} + (B_{PC}C_{PF}) \Delta \underline{x}_{PF} \\ A_{PC} \Delta \underline{x}_{PC} + (B_{PC}D_{PF}D_{PW}) \Delta S_m + [B_{PC}(D_{PF}K_{S3}D_{PT} - D_{PT})] \Delta T_e \end{bmatrix} \quad (4.17)$$

$$\Delta V_S = \begin{bmatrix} (D_{PC}D_{PF}C_{PW}) \Delta \underline{x}_{PW} + [D_{PC}(D_{PF}K_{S3}C_{PT} - C_{PT})] \Delta \underline{x}_{PT} + (D_{PC}C_{PF}) \Delta \underline{x}_{PF} \\ C_{PC} \Delta \underline{x}_{PC} + (D_{PC}D_{PF}D_{PW}) \Delta S_m + [D_{PC}(D_{PF}K_{S3}D_{PT} - D_{PT})] \Delta T_e \end{bmatrix} \quad (4.18)$$

Using (3.17) and (3.23), we have,

$$\Delta S_m = e_2^T \Delta \underline{X}_G ; \quad \Delta T_e = D_T \Delta \underline{X}_G$$

The state space equation for the PSS is given by,

$$\Delta \dot{\underline{x}}_{PSS} = A_{PSS} \Delta \underline{x}_{PSS} + B'_{PSS} \Delta \underline{X}_G \quad (4.19)$$

$$\Delta V_S = C_{PSS} \Delta \underline{x}_{PSS} + D'_{PSS} \Delta \underline{X}_G \quad (4.20)$$

where,

$$\Delta \underline{x}_{PSS} = [\Delta \underline{x}_{PW} \quad \Delta \underline{x}_{PT} \quad \Delta \underline{x}_{PF} \quad \Delta \underline{x}_{PC}]^T$$

$$B'_{PSS} = B_{PSS} \begin{bmatrix} e_2^T \\ D_T \end{bmatrix} ; \quad D'_{PSS} = D_{PSS} \begin{bmatrix} e_2^T \\ D_T \end{bmatrix}$$

$$A_{PSS} = \begin{bmatrix} A_{PW} & [0] & [0] & [0] \\ [0] & A_{PT} & [0] & [0] \\ B_{PF}C_{PW} & B_{PF}K_{S3}C_{PT} & A_{PF} & [0] \\ B_{PC}D_{PF}C_{PW} & [B_{PC}(D_{PF}K_{S3}C_{PT} - C_{PT})] & B_{PC}C_{PF} & A_{PC} \end{bmatrix}$$

$$B_{PSS} = \begin{bmatrix} B_{PW} & [0] \\ [0] & B_{PT} \\ B_{PF}D_{PW} & B_{PF}K_{S3}D_{PT} \\ B_{PC}D_{PF}D_{PW} & [B_{PC}(D_{PF}K_{S3}D_{PT} - D_{PT})] \end{bmatrix}$$

$$C_{PSS} = \begin{bmatrix} D_{PC}D_{PF}C_{PW} & [D_{PC}(D_{PF}K_{S3}C_{PT} - C_{PT})] & D_{PC}C_{PF} & C_{PC} \end{bmatrix}$$

$$D_{PSS} = \begin{bmatrix} D_{PC}D_{PF}D_{PW} & [D_{PC}(D_{PF}K_{S3}D_{PT} - D_{PT})] \end{bmatrix}$$

Rewriting (1.45) considering only the change in V_s , we have,

$$\Delta \dot{\underline{X}}_G = [A_T] \Delta \underline{X}_G + [E_G] \Delta V_s \quad (4.21)$$

where $[E_G] = E_G(:, i)$ for i^{th} generator.

Using (4.20) in (4.21) and rewriting the state model accounting PSS we obtain,

$$\begin{bmatrix} \Delta \dot{\underline{X}}_G \\ \Delta \dot{\underline{x}}_{PSS} \end{bmatrix} = \begin{bmatrix} A_T + E_G D'_{PSS} & E_G C_{PSS} \\ B'_{PSS} & A_{PSS} \end{bmatrix} \begin{bmatrix} \Delta \underline{X}_G \\ \Delta \underline{x}_{PSS} \end{bmatrix}$$

4.2.2.1 Eigenvalues with Delta-P-Omega PSS:

For the base case, a few oscillatory modes with the PSS are listed in Table 4.1 for $K_S = 15$. From the tabulated results it can be observed that the damping factor for inter-area mode is 0.0606 as against 0.0588 with slip-signal PSS.

SL No	Eigenvalues	Dampingfactor	Freq.(Hz)	Nature of the mode
1	$-15.44078 \pm j 17.0756$	0.6707	2.7177	Non-Swing mode
2	$-15.64061 \pm j 12.5809$	0.7792	2.0023	Non-Swing mode
3	$-2.50222 \pm j 8.4307$	0.2845	1.3418	Swing mode(2 & 1)
4	$-1.05559 \pm j 6.8045$	0.1533	1.0830	Swing mode(4 & 3)
5	$-0.27285 \pm j 4.4942$	0.0606	0.7153	Swing mode([1 2] & [3 4])

Table 4.1: Oscillatory modes with Delta-P-Omega PSS.

The above results are obtained by using the following steps:

1. Prepare the data file `delPw_pss.dat` -see section 2.2.1.
2. Set only `ng_delPw_pss=[1]`, with the other Individual Selectors initialized to `[]`.
3. Enable the Main Selector by setting `PSS=zeros(1,nb)`.
4. Run `small_sig.m` and then execute `trace_mode.m` programme.

NOTE: From the root locus plot it was observed that one of the local modes becomes unstable when $K_S = 245$. It was also observed that when `FILT(s)` and `TR(s)` are used with slip-signal based PSS, one of the local modes becomes unstable with gain $K_S = 40$.

Chapter 5

Design of Power-signal PSS

5.1 Introduction:

In a single-input power system stabilizer, electrical power output of the machine is normally used as the input signal as it provides high degree of attenuation to torsional modes unlike slip-signal [27]. An electrical power-input based PSS can be realized by observing the following relationship between ΔS_m and ΔT_e given by

$$j\omega \Delta S_m(j\omega) = -\frac{1}{2H} \Delta T_e(j\omega) \quad (5.1)$$

Note that the above relationship is obtained from (C.35) by neglecting the deviation in the mechanical power input to the machine and mechanical damping, and for sinusoidal variation of quantities. From (5.1), it can be seen that

1. To get the same effect as a slip-input PSS, with the ΔT_e input, the output of the PSS block (V_s) is fed to the exciter V_{REF} summing junction with a negative sign (as against a positive sign that has been used with the slip-input PSS).
2. The phasor $\Delta T_e(j\omega)$ leads the $\Delta S_m(j\omega)$ phasor by 90° (having accounted the negative sign in V_s). This implies that using electrical power signal is equivalent to using slip signal with 90° phase lead. In other words, to get the phase angle of the compensated GEPS, Φ_L , it is required to simply add 90° to the angle of $GEPS(j\omega)$.

From the above observations, a power-input PSS is implemented along with a measurement delay transfer function and a washout-circuit as shown in Figure 5.1.

Note that the function of the washout-circuit is identical to that with the slip-signal based PSS -see section 3.2.1.

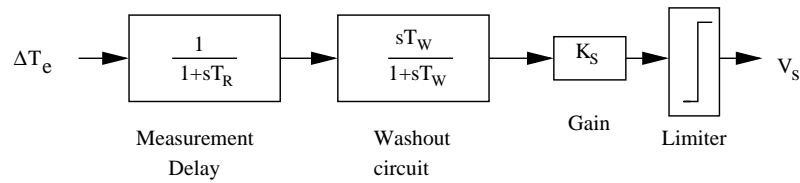


Figure 5.1: Block schematic of power-input PSS.

5.2 Interfacing of Power-input PSS to the State Matrix:

The steps employed are as follows:

1. Following the procedure indicated in section 3.3.5 and rewriting (3.23), ΔT_e for i^{th} machine is expressed in terms of the state variables as

$$\Delta T_e = D_T \Delta \underline{X}_G \quad (5.2)$$

2. The linearized model of the power-input PSS is given by

$$\Delta \dot{\underline{x}}_{PSS} = A_{PSS} \Delta \underline{x}_{PSS} + B_{PSS} \Delta T_e \quad (5.3)$$

$$\Delta V_s = C_{PSS} \Delta \underline{x}_{PSS} + D_{PSS} \Delta T_e \quad (5.4)$$

where ΔT_e denotes the deviation in electrical power output for i^{th} generator.

Using (5.2) in (5.3) and (5.4) we get,

$$\Delta \dot{\underline{x}}_{PSS} = A_{PSS} \Delta \underline{x}_{PSS} + B_{PSS} D_T \Delta \underline{X}_G \quad (5.5)$$

$$\Delta V_s = C_{PSS} \Delta \underline{x}_{PSS} + D_{PSS} D_T \Delta \underline{X}_G \quad (5.6)$$

3. Considering only the change in V_s , from (1.45) we have

$$\Delta \dot{\underline{X}}_G = [A_T] \Delta \underline{X}_G + [E_G] \Delta V_s \quad (5.7)$$

where $[E_G] = E_G(:, i)$ for i^{th} generator.

4. Using (5.6) in (5.7) and rewriting the state model accounting PSS, we obtain,

$$\Delta \dot{\underline{X}}_P = A_P \Delta \underline{X}_P$$

where $\Delta \underline{X}_P = [\Delta \underline{X}_G \ \Delta \underline{x}_{PSS}]^T$

$$A_P = \begin{bmatrix} [A_T] + [E_G] \ D_{PSS} \ D_T & [E_G] \ C_{PSS} \\ B_{PSS} \ D_T & A_{PSS} \end{bmatrix}$$

5.3 4-machine Power System Example:

A power-input PSS has been designed for machine-1 in the base case. The phase angle of the compensated $GEPS(j\omega)$ is obtained accounting the measurement delay of $T_R = 0.05$ s and the washout-circuit ($T_W = 10$ s), as shown in Figure 5.2.

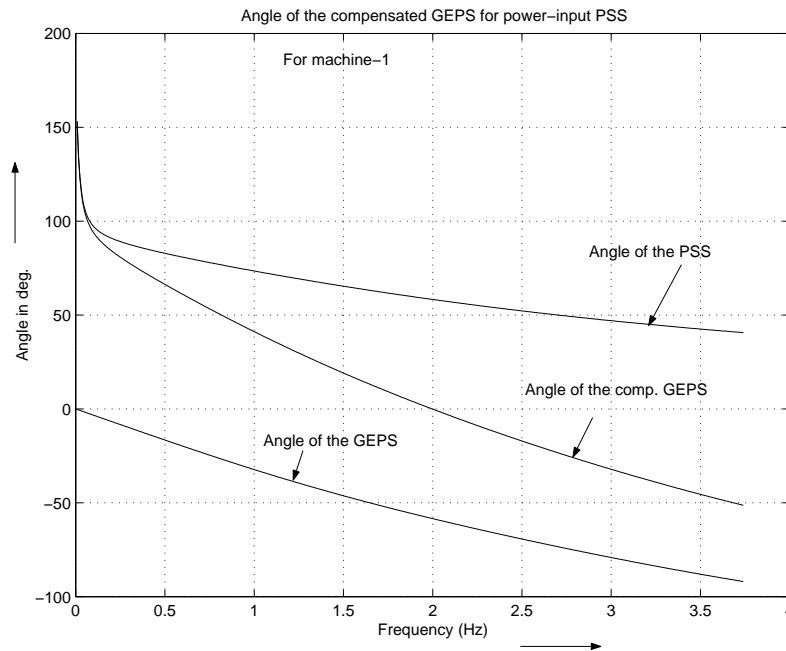


Figure 5.2: Phase angle of the compensated GEPS with power input PSS.

The above plot has been obtained by using the following steps:

1. Execute `small_sig.m` with appropriate options.
2. Run `pss_design.m` programme.

A list of statements printed out by the programme is given below.

```
Enter the generator number for which you want to obtain the angle of GEPS(s):  1
Enter 1  :To design single input PSS - Slip signal
       2  :To design double input PSS
       3  :To design single input PSS -Power signal
```

Enter your choice : 3

Enter 1 : Plain power type PSS

2 : With measurement delay and washout time constant

Enter your choice : 2

Enter the PSS gain K_s : 0.03

Enter the value of T_w (in s) for the wash-out circuit [1 - 20]s : 10

Enter the value of T_R (in s) for the measurement delay [0.01 - 0.05]s : 0.05

Enter 0 if you are satisfied with the design,

otherwise 1 to re-design the pss: 0

Update the power_pss.dat for the machine 1

```
-----
gen.no      Ks          TR          Tw
-----
1           0.03        0.05        10.0
-----
```

Press any key to obtain the amplitude response of GEPS(iw)

5.3.1 Eigenvalues with Power-input PSS:

The effect of the PSS on the swing modes is demonstrated in Table 5.1 for $K_S = 0.03$.

SL No	Eigenvalues	Damp. Factor	Freq.(Hz)	Remarks
1	$-2.0881 \pm j 5.8556$	0.3358	0.9319	Swing mode(2 & 1)
2	$-1.0596 \pm j 6.8066$	0.1538	1.0833	Swing mode(4 & 3)
3	$-0.1988 \pm j 4.2343$	0.0469	0.6739	Swing mode([1 2] & [3 4])

Table 5.1: Swing modes with power-input PSS for the base case.

The results are obtained by using the following steps:

1. Prepare the data file `power_pss.dat` as shown below (see section 2.2.1):

File name: `power_pss.dat`

```
-----
Gen.No.  TW   TR    KS  VSMAX  VSMIN
-----
1         10  0.05  0.03  0.1    -0.1
2         10  0.05  0.07  0.1    -0.1
3         10  0.05  0.07  0.1    -0.1
4         10  0.05  0.03  0.1    -0.1
-----
```

2. Set `ng_power_pss = [1]` and enable PSS by setting `PSS=zeros(1,nb)` in file `initcond.m`.
3. Run `small_sig.m` and then execute `trace_mode.m` programme.

NOTE:

1. Depending on the type of exciter and the system characteristics, the phase lead introduced by a power-input PSS may be too high at low frequencies (see Figure 5.2) leading to an increase in the damping of the swing modes at the expense of a reduction in the synchronizing torque. This is evident from a decrease in the frequency of oscillation of the modes (see also Table 2.1).
2. From the root locus plot it was observed that one of the exciter modes becomes unstable when $K_S = 0.4$. This has been verified by the time domain simulation for a perturbation of V_{ref} of machine-1 as shown in Figure 5.3.

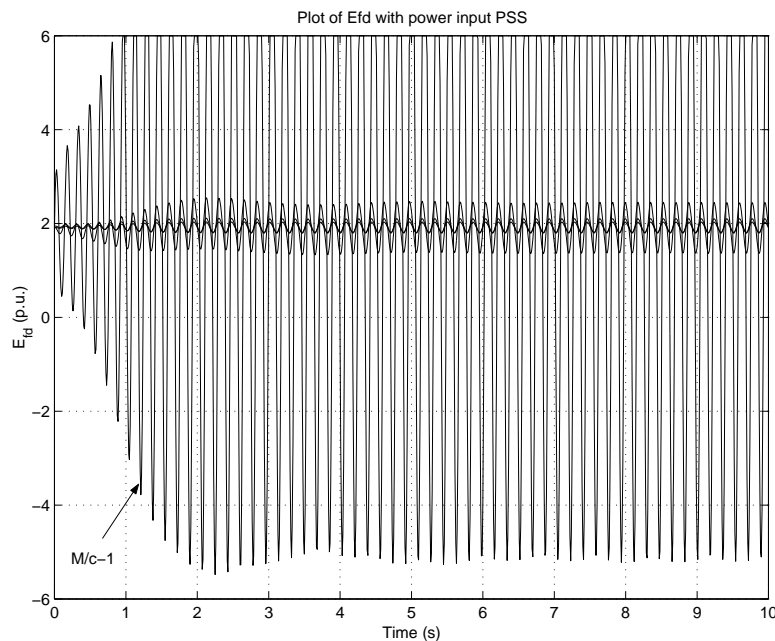


Figure 5.3: Variation of E_{fd} for power PSS gain of 0.4.

5.3.2 Performance of the PSS for Power Ramping:

A major difficulty with power-input PSS is that they respond to ramping of the generator's mechanical power or load changes. The effect is that the generator's terminal voltage may vary considerably. In some cases such a deviation in terminal voltage may even cause the machine to lose synchronism [5].

In order to check the response of power-input PSS under power ramping, the mechanical power of the machine is ramped-down to 50% of its quiescent power output, (P_{mo}), at $t = 1$ s and is ramped-up again at $t = 11$ s at a rate of P_{mo}/s . The aim here is to determine whether the machine is able to maintain synchronism and the terminal voltage remain within limits. This also provides a way to check the suitability of limits on V_s . For the case in hand, the mechanical power of machine-1 is varied as said above and the plots of its rotor angle and the terminal voltage are shown in Figure 5.4.

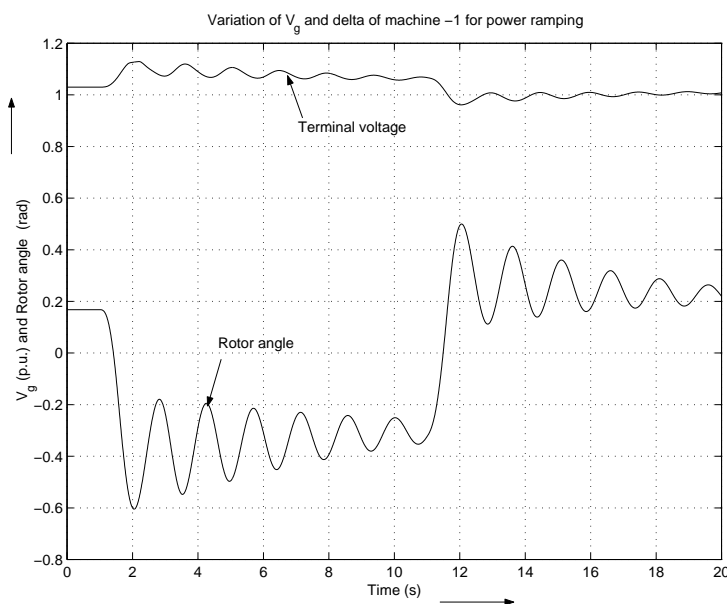


Figure 5.4: variation of rotor angle and the terminal voltage for machine-1 for power ramping case.

The results are obtained by using the following steps:

1. Prepare the data file `power_pss.dat` as shown above.
2. While running `small_sig.m`, the following option is chosen:

```
wB = 376.9911
Enter 1 if you want to run transtability programme for network
                                disturbances, otherwise 0: 0
Enter 1 if you want to run transtability programme for
                                perturbation of VREF, otherwise 0: 0
Enter 1 if you want to run transtability programme for
                                ramping of Tm, otherwise 0: 1
Enter the generator number whose Tm needs to be ramped-up/down: 1
```

3. Run time-domain simulation programme by executing `transtability.mdl` file.

Chapter 6

10-machine Power System Example

6.1 Ten Machine System Details:

A well known 10-machine, 39-bus New England power system has been used to demonstrate the modal analysis of a power system. The single line diagram of the system is shown in Figure 6.1. The system details are adopted from [1].

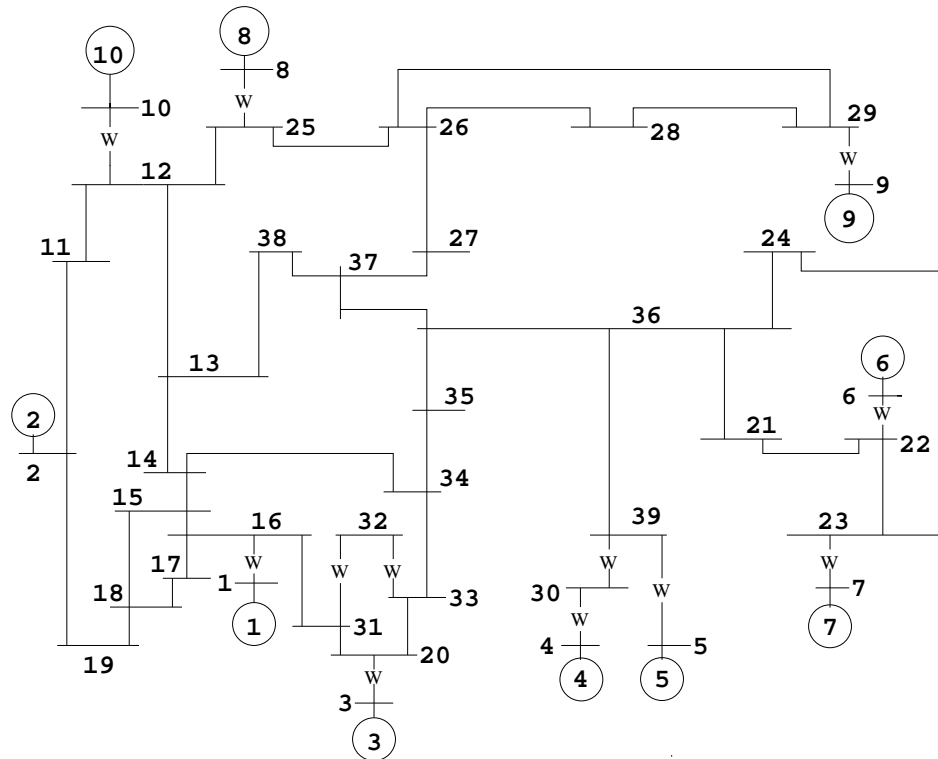


Figure 6.1: 10-machine 39-bus power system.

1.0 model has been used for the generators with all exciters on manual control. Constant impedance type loads have been employed. The modal analysis has been carried

out using the following steps:

1. Prepare the data files.
2. Initialize the Main and Individual Selectors in file `initcond.m`
3. Execute `small_sig.m` with appropriate inputs.
4. Execute `trace_mode.m`. The statements displayed in the MATLAB Command Window and the respective inputs are shown below:

Enter 1 to display ALL eigenvalues (EIG), otherwise 0 (using EIGS): 1

```
-----
SL_number      Eigenvalue      dampingfactor      frequency(Hz)
-----
```

ans =

```
-----A partial list-----
```

31.0000	-0.2541 + 8.6811i	0.0293	1.3816
32.0000	-0.2541 - 8.6811i	0.0293	1.3816
33.0000	-0.1823 + 8.3340i	0.0219	1.3264
34.0000	-0.1823 - 8.3340i	0.0219	1.3264
35.0000	-0.1865 + 8.2509i	0.0226	1.3132
36.0000	-0.1865 - 8.2509i	0.0226	1.3132
37.0000	-0.1698 + 7.1939i	0.0236	1.1449
38.0000	-0.1698 - 7.1939i	0.0236	1.1449
39.0000	-0.1624 + 6.9902i	0.0232	1.1125
40.0000	-0.1624 - 6.9902i	0.0232	1.1125
41.0000	-0.1636 + 6.3584i	0.0257	1.0120
42.0000	-0.1636 - 6.3584i	0.0257	1.0120
43.0000	-0.1609 + 6.2241i	0.0258	0.9906
44.0000	-0.1609 - 6.2241i	0.0258	0.9906
45.0000	-0.1939 + 5.9474i	0.0326	0.9466
46.0000	-0.1939 - 5.9474i	0.0326	0.9466
47.0000	-0.1560 + 3.6521i	0.0427	0.5813
48.0000	-0.1560 - 3.6521i	0.0427	0.5813
49.0000	-0.6715	1.0000	0
50.0000	-0.0000	1.0000	0
51.0000	-0.0338	1.0000	0
52.0000	-0.0898	1.0000	0
53.0000	-0.2900	1.0000	0

54.0000	-0.2663	1.0000	0
55.0000	-0.1370	1.0000	0
56.0000	-0.1575	1.0000	0
57.0000	-0.1863	1.0000	0
58.0000	-0.2285	1.0000	0
59.0000	-0.2197	1.0000	0

Enter the serial number of the eigenvalue for which you
want to obtain the P.factor: 48

State variable	Mag(Norm PF)	ang(Norm PF)deg.	Mag(PF)	ang(PF)deg.
Delta-2	1.0000	-0.00	0.4145	2.02
Slip-2	0.4996	4.92	0.2071	6.94
Slip-9	0.1604	0.23	0.0665	2.25
Slip-6	0.1278	-5.98	0.0530	-3.96
Slip-4	0.1032	-1.88	0.0428	0.13

You have chosen a SWING-MODE

The generator(s) in group-1 is(are) ...
Group1 =

4 6 7 9 5 3 1 8

The generator(s) in group-2 is(are) ...
Group2 =

2

Enter 1 if you want to plot the compass plot, otherwise 0: 1

NOTE: Use mouse click on the plot to identify the generator

Press any key

Current plot held

Current plot held

Enter 1 if you want to repeat for another eigenvalue, otherwise 0: 0

Further, the grouping of machines prepared by the programme is shown in Figures 6.2 and 6.3. Not more than 6 eigenvectors are drawn in each plot.

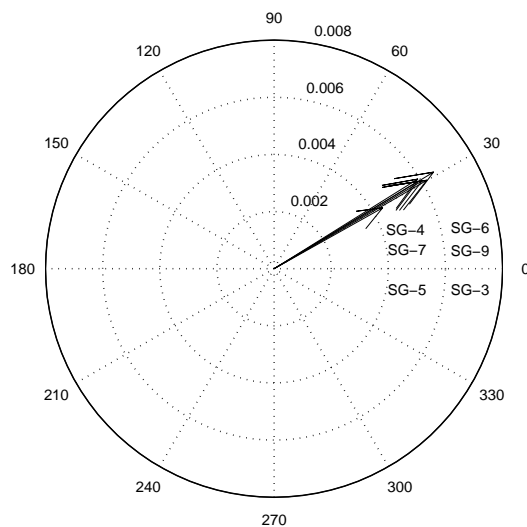


Figure 6.2: Plot of slip-right eigenvector for machine groups 1 and 2.

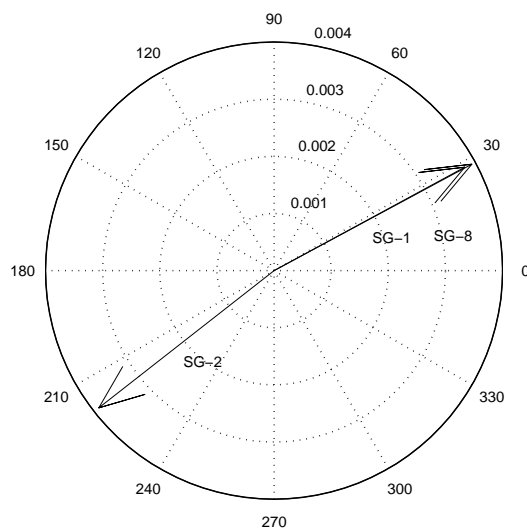


Figure 6.3: Plot of slip-right eigenvector for machine groups 1 and 2.

Note that `trace_mode.m` can also be run with the following option:

```
Enter 1 to display ALL eigenvalues (EIG), otherwise 0 (using EIGS): 0
You are scanning 10 eigenvalues around 1.000 Hz .....
Please press a key:
```

SL_number	Eigenvalue	dampingfactor	frequency(Hz)
<hr/>			
ans =			
1.0000	-0.1609 + 6.2241i	0.0258	0.9906
2.0000	-0.1636 + 6.3584i	0.0257	1.0120
3.0000	-0.1939 + 5.9474i	0.0326	0.9466
4.0000	-0.1624 + 6.9902i	0.0232	1.1125
5.0000	-0.1698 + 7.1939i	0.0236	1.1449
6.0000	-0.1865 + 8.2509i	0.0226	1.3132
7.0000	-0.1823 + 8.3340i	0.0219	1.3264
8.0000	-0.2541 + 8.6811i	0.0293	1.3816
9.0000	-0.1560 + 3.6521i	0.0427	0.5813
10.0000	-0.0000	1.0000	0

Enter the serial number of the eigenvalue for which you
want to obtain the P.factor: 9

State variable	Mag(Norm PF)	ang(Norm PF)deg.	Mag(PF)	ang(PF)deg.
<hr/>				
Delta-2	1.0000	-0.00	0.4006	-0.93
Slip-2	0.5544	-7.82	0.2221	-8.75
Slip-9	0.2207	-13.33	0.0884	-14.26
Field-9	0.1850	-15.76	0.0741	-16.69
Efd-9	0.1783	-124.43	0.0714	-125.35
Slip-6	0.1756	-7.59	0.0703	-8.52
Slip-4	0.1541	-13.09	0.0617	-14.02
Slip-5	0.1424	-15.58	0.0570	-16.50
Slip-7	0.1421	-12.34	0.0569	-13.26
Slip-3	0.1202	-14.30	0.0482	-15.23

You have chosen a SWING-MODE

The generator(s) in group-1 is(are) ...

Group1 =

4 6 7 9 5 3 1 8 10

The generator(s) in group-2 is(are) ...

Group2 =

2

Enter 1 if you want to plot the compass plot, otherwise 0: 1

NOTE: Some times, the determination of eigenvalues using `eigs` function may not converge. In such cases, one may require to alter the maximum number of iterations (currently `options.maxit` is set to 25) or tolerance values (currently `options.tol` is set to $1e^{-12}$) in `trace_mode.m`

Appendix A

Names of State Variables

The state variable strings used for the system are shown in order in the following Table.

1	Delta-	9	xB_DC_AC-
2	Slip-	10	xF_DC-
3	Field-	11	x1_st_tu-
4	DampH-	12	x2_st_tu-
5	DampG-	13	x3_st_tu-
6	DampK-	14	y1_gv-
7	Efd-	15	PG-
8	VR_DC-	16	z-

Table A.1: System state variables.

1. The state variables defined for the machine are:

Delta-	Slip-	Field-	DampH-	DampG-	DampK-
--------	-------	--------	--------	--------	--------

Table A.2: Machine state variables.

2. The state variable for the single-time constant static exciter is **Efd**.
3. The state variables for the DC1A exciter are

VR_DC-	xB_DC_AC-	xF_DC-
--------	-----------	--------

Table A.3: DC1A-exciter state variables.

4. The state variables for the AC4A exciter are

Efd-	xB_DC_AC-
------	-----------

Table A.4: AC4A-exciter state variables.

5. the state variables for the reheat-type steam turbine and the associated speed-governor, are

x1_st_tu-	x2_st_tu-	x3_st_tu-	y1_gv-	PG-
-----------	-----------	-----------	--------	-----

Table A.5: Reheat steam turbine state variables.

6. The state variables for the hydraulic turbine and the associated speed-governor, are

y1_gv-	PG-	z-
--------	-----	----

Table A.6: Hydraulic turbine state variables.

The state-vector is given by

$$\underline{x}_g = \begin{bmatrix} \delta & S_m & \psi_f & \psi_h & \psi_g & \psi_k & E_{fd} & v_R \\ x_B & x_F & x_1 & x_2 & x_3 & y_1 & P_{GV} & z \end{bmatrix}^T$$

Appendix B

Derivation of P-matrix and Construction of P_G , P_L and Reduced State Matrices

B.1 Derivation of P matrix:

The generator terminal voltage is given by,

$$V_g \angle \theta_g = V_g (\cos \theta_g + j \sin \theta_g)$$

Now consider,

$$\begin{aligned} \frac{\partial V_g \angle \theta_g}{\partial \theta_g} &= V_{g0} (-\sin \theta_g + j \cos \theta_g) \Delta \theta_g \\ &= V_{g0} \Delta \theta_g \left(e^{j(\frac{\pi}{2} + \theta_g)} \right) \end{aligned} \quad (\text{B.1})$$

Let

$$V_{g0} \Delta \theta_g e^{j(\frac{\pi}{2} + \theta_g)} = \Delta V_{Qg} + j \Delta V_{Dg} \quad (\text{B.2})$$

$$\begin{aligned} V_{g0} \Delta \theta_g &= \text{Re} \left[(\Delta V_{Qg} + j \Delta V_{Dg}) e^{-j(\frac{\pi}{2} + \theta_g)} \right] \\ V_{g0} \Delta \theta_g &= \text{Re} \left[(\Delta V_{Qg} + j \Delta V_{Dg}) \frac{(-V_{g0} \sin \theta_g - j V_{g0} \cos \theta_g)}{V_{g0}} \right] \\ V_{g0} \Delta \theta_g &= \frac{1}{V_{g0}} [-V_{Dg0} \Delta V_{Qg} + V_{Qg0} \Delta V_{Dg}] \end{aligned} \quad (\text{B.3})$$

$$(\text{B.4})$$

We know that

$$V_g^2 = V_{Qg}^2 + V_{Dg}^2$$

Now consider

$$\begin{aligned} 2V_{g0}\Delta V_g &= 2V_{Qg0}\Delta V_{Qg} + 2V_{Dg0}\Delta V_{Dg} \\ \Delta V_g &= \frac{V_{Qg0}}{V_{g0}}\Delta V_{Qg} + \frac{V_{Dg0}}{V_{g0}}\Delta V_{Dg} \end{aligned} \quad (\text{B.5})$$

From (B.3) and (B.5) we can write

$$\begin{bmatrix} V_{g0}\Delta\theta_g \\ \Delta V_g \end{bmatrix} = \frac{1}{V_{g0}} \begin{bmatrix} -V_{Dg0} & V_{Qg0} \\ V_{Qg0} & V_{Dg0} \end{bmatrix} \begin{bmatrix} \Delta V_{Qg} \\ \Delta V_{Dg} \end{bmatrix} = [P] \begin{bmatrix} \Delta V_{Qg} \\ \Delta V_{Dg} \end{bmatrix}$$

$$\Delta V_g^p = \begin{bmatrix} V_{g0}\Delta\theta_g \\ \Delta V_g \end{bmatrix} \quad \Delta V_g^r = \begin{bmatrix} \Delta V_{Qg} \\ \Delta V_{Dg} \end{bmatrix}$$

$$\Delta V_g^p = [P] \Delta V_g^r$$

where

$$[P] = \frac{1}{V_{g0}} \begin{bmatrix} -V_{Dg0} & V_{Qg0} \\ V_{Qg0} & V_{Dg0} \end{bmatrix}$$

B.2 Construction of $[P_G]$ and $[P_L]$ Matrices:

The single line diagram of a 4 machine power system is shown in Figure 2.1. The system details are adopted from [1]. In this system, machines 1, 2, 3 and 4 are connected to buses 1, 2, 3 and 4 respectively. Loads A and B are connected to buses 9 and 10 respectively. For this case, the $[P_G]$ and $[P_L]$ matrices are defined as follows.

$$P_G = \begin{matrix} & \begin{matrix} Busno \end{matrix} & \begin{matrix} Gen1 \\ \begin{bmatrix} 1 & 0 \\ 0 & 1 \end{bmatrix} \\ 0 & 0 \end{matrix} & \begin{matrix} Gen2 \\ \begin{bmatrix} 1 & 0 \\ 0 & 1 \end{bmatrix} \\ 0 & 0 \end{matrix} & \begin{matrix} Gen3 \\ \begin{bmatrix} 1 & 0 \\ 0 & 1 \end{bmatrix} \\ 0 & 0 \end{matrix} & \begin{matrix} Gen4 \\ \begin{bmatrix} 1 & 0 \\ 0 & 1 \end{bmatrix} \\ 0 & 0 \end{matrix} \end{matrix} \Bigg], \quad P_L = \begin{matrix} & \begin{matrix} LoadA \end{matrix} & \begin{matrix} LoadB \\ \begin{bmatrix} 1 & 0 \\ 0 & 1 \end{bmatrix} \\ 0 & 0 \end{matrix} & \begin{matrix} LoadB \\ \begin{bmatrix} 1 & 0 \\ 0 & 1 \end{bmatrix} \\ 0 & 0 \end{matrix} \end{matrix} \Bigg]$$

B.3 Derivation of Reduced-State Matrix:

For the 4-machine system the state equations are written in the matrix form as follows:

$$\begin{bmatrix} \Delta \dot{\delta}_1 \\ \Delta \dot{S}_{m1} \\ \vdots \\ \vdots \\ \Delta \dot{Z}_1 \\ \dots \\ \Delta \dot{\delta}_2 \\ \Delta \dot{S}_{m2} \\ \vdots \\ \vdots \\ \Delta \dot{Z}_2 \\ \dots \\ \vdots \\ \vdots \\ \vdots \\ \dots \\ \Delta \dot{\delta}_4 \\ \Delta \dot{S}_{m4} \\ \vdots \\ \vdots \\ \Delta \dot{Z}_4 \end{bmatrix} = \begin{bmatrix} 0 & \omega_B & \dots & 0 & \vdots & 0 & 0 & \dots & 0 & \vdots & 0 & 0 & \dots & 0 \\ a_{2,1} & \dots & \dots & \dots & \vdots & \dots & \dots & \dots & \dots & \vdots & \dots & \dots & \dots & a_{2,64} \\ \vdots & \vdots & \dots & \vdots & \vdots & \vdots & \vdots & \dots & \vdots & \vdots & \vdots & \vdots & \dots & \vdots \\ \vdots & \vdots & \dots & \vdots & \vdots & \vdots & \vdots & \dots & \vdots & \vdots & \vdots & \vdots & \dots & \vdots \\ a_{16,1} & \dots & \dots & \dots & \vdots & \dots & \dots & \dots & \dots & \vdots & \dots & \dots & \dots & a_{16,64} \\ \dots & \dots & \dots & \dots & \vdots & \dots & \dots & \dots & \dots & \vdots & \dots & \dots & \dots & \dots \\ 0 & 0 & \dots & 0 & \vdots & 0 & \omega_B & \dots & 0 & \vdots & 0 & 0 & \dots & 0 \\ a_{18,1} & \dots & \dots & \dots & \vdots & \dots & \dots & \dots & \dots & \vdots & \dots & \dots & \dots & a_{18,64} \\ \vdots & \vdots & \dots & \vdots & \vdots & \vdots & \vdots & \dots & \vdots & \vdots & \vdots & \vdots & \dots & \vdots \\ \vdots & \vdots & \dots & \vdots & \vdots & \vdots & \vdots & \dots & \vdots & \vdots & \vdots & \vdots & \dots & \vdots \\ a_{32,1} & \dots & \dots & \dots & \vdots & \dots & \dots & \dots & \dots & \vdots & \dots & \dots & \dots & a_{31,64} \\ \dots & \dots & \dots & \dots & \vdots & \dots & \dots & \dots & \dots & \vdots & \dots & \dots & \dots & \dots \\ \vdots & \vdots & \dots & \vdots & \vdots & \vdots & \vdots & \dots & \vdots & \vdots & \vdots & \vdots & \dots & \vdots \\ \vdots & \vdots & \dots & \vdots & \vdots & \vdots & \vdots & \dots & \vdots & \vdots & \vdots & \vdots & \dots & \vdots \\ \vdots & \vdots & \dots & \vdots & \vdots & \vdots & \vdots & \dots & \vdots & \vdots & \vdots & \vdots & \dots & \vdots \\ \dots & \dots & \dots & \dots & \vdots & \dots & \dots & \dots & \dots & \vdots & \dots & \dots & \dots & \dots \\ 0 & 0 & \dots & 0 & \vdots & 0 & 0 & \dots & 0 & \vdots & 0 & \omega_B & \dots & 0 \\ a_{50,1} & \dots & \dots & \dots & \vdots & \dots & \dots & \dots & \dots & \vdots & \dots & \dots & \dots & a_{50,64} \\ \vdots & \vdots & \dots & \vdots & \vdots & \vdots & \vdots & \dots & \vdots & \vdots & \vdots & \vdots & \dots & \vdots \\ \vdots & \vdots & \dots & \vdots & \vdots & \vdots & \vdots & \dots & \vdots & \vdots & \vdots & \vdots & \dots & \vdots \\ a_{64,1} & \dots & \dots & \dots & \vdots & \dots & \dots & \dots & \dots & \vdots & \dots & \dots & \dots & a_{64,64} \end{bmatrix} \begin{bmatrix} \Delta \delta_1 \\ \Delta S_{m1} \\ \vdots \\ \vdots \\ \Delta Z_1 \\ \dots \\ \Delta \delta_2 \\ \Delta S_{m2} \\ \vdots \\ \vdots \\ \Delta Z_2 \\ \dots \\ \vdots \\ \vdots \\ \vdots \\ \dots \\ \Delta \delta_4 \\ \Delta S_{m4} \\ \vdots \\ \vdots \\ \Delta Z_4 \end{bmatrix}$$

Original Matrix

Expressing the rotor angle of other machines wrt machine-1, we have,

$$\begin{aligned}
 \Delta\dot{\delta}_2 - \Delta\dot{\delta}_1 &= -\omega_B \Delta S_{m1} + 0 \cdots \cdots + \omega_B \Delta S_{m2} + \cdots \cdots + 0 \\
 \vdots \quad \quad \quad \vdots \quad \quad \quad \vdots \quad \quad \quad \vdots \quad \quad \quad \vdots \quad \quad \quad \vdots \\
 \vdots \quad \quad \quad \vdots \quad \quad \quad \vdots \quad \quad \quad \vdots \quad \quad \quad \vdots \quad \quad \quad \vdots \\
 \Delta\dot{\delta}_4 - \Delta\dot{\delta}_1 &= -\omega_B \Delta S_{m1} + 0 \cdots \cdots + \omega_B \Delta S_{m4} + \cdots \cdots + 0
 \end{aligned}$$

Further, the first row and column are removed from the original A-matrix. Now rewriting the state matrix we get,

$$\begin{bmatrix}
 \Delta\dot{S}_{m1} \\
 \vdots \\
 \vdots \\
 \Delta\dot{Z}_1 \\
 \cdots \\
 \Delta\dot{\delta}_2 - \Delta\dot{\delta}_1 \\
 \Delta\dot{S}_{m2} \\
 \vdots \\
 \vdots \\
 \Delta\dot{Z}_2 \\
 \cdots \\
 \vdots \\
 \vdots \\
 \vdots \\
 \cdots \\
 \Delta\dot{\delta}_4 - \Delta\dot{\delta}_1 \\
 \Delta\dot{S}_{m4} \\
 \vdots \\
 \vdots \\
 \Delta\dot{Z}_4
 \end{bmatrix}
 =
 \begin{bmatrix}
 a_{2,2} & \cdots & \cdots & \vdots & \cdots & \cdots & \cdots & \cdots & \vdots & \cdots & \cdots & \cdots & a_{2,64} \\
 \vdots & \cdots & \vdots & \vdots & \vdots & \vdots & \cdots & \vdots & \vdots & \vdots & \vdots & \vdots & \vdots \\
 \vdots & \cdots & \vdots & \vdots & \vdots & \vdots & \cdots & \vdots & \vdots & \vdots & \vdots & \vdots & \vdots \\
 a_{16,2} & \cdots & \cdots & \vdots & \cdots & \cdots & \cdots & \cdots & \vdots & \cdots & \cdots & \cdots & a_{16,64} \\
 \cdots & \cdots & \cdots & \vdots & \cdots & \cdots & \cdots & \cdots & \vdots & \cdots & \cdots & \cdots & \cdots \\
 -\omega_B & \cdots & 0 & \vdots & 0 & \omega_B & \cdots & 0 & \vdots & 0 & 0 & \cdots & 0 \\
 a_{18,2} & \cdots & \cdots & \vdots & \cdots & \cdots & \cdots & \cdots & \vdots & \cdots & \cdots & \cdots & a_{18,64} \\
 \vdots & \cdots & \vdots & \vdots & \vdots & \vdots & \cdots & \vdots & \vdots & \vdots & \vdots & \vdots & \vdots \\
 \vdots & \cdots & \vdots & \vdots & \vdots & \vdots & \cdots & \vdots & \vdots & \vdots & \vdots & \vdots & \vdots \\
 a_{32,2} & \cdots & \cdots & \vdots & \cdots & \cdots & \cdots & \cdots & \vdots & \cdots & \cdots & \cdots & a_{32,64} \\
 \cdots & \cdots & \cdots & \vdots & \cdots & \cdots & \cdots & \cdots & \vdots & \cdots & \cdots & \cdots & \cdots \\
 \vdots & \cdots & \vdots & \vdots & \vdots & \vdots & \cdots & \vdots & \vdots & \vdots & \vdots & \vdots & \vdots \\
 \vdots & \cdots & \vdots & \vdots & \vdots & \vdots & \cdots & \vdots & \vdots & \vdots & \vdots & \vdots & \vdots \\
 \vdots & \cdots & \vdots & \vdots & \vdots & \vdots & \cdots & \vdots & \vdots & \vdots & \vdots & \vdots & \vdots \\
 \cdots & \cdots & \cdots & \vdots & \cdots & \cdots & \cdots & \cdots & \vdots & \cdots & \cdots & \cdots & \cdots \\
 -\omega_B & \cdots & 0 & \vdots & 0 & 0 & \cdots & 0 & \vdots & 0 & \omega_B & \cdots & 0 \\
 a_{50,2} & \cdots & \cdots & \vdots & \cdots & \cdots & \cdots & \cdots & \vdots & \cdots & \cdots & \cdots & a_{50,64} \\
 \vdots & \cdots & \vdots & \vdots & \vdots & \vdots & \cdots & \vdots & \vdots & \vdots & \vdots & \vdots & \vdots \\
 \vdots & \cdots & \vdots & \vdots & \vdots & \vdots & \cdots & \vdots & \vdots & \vdots & \vdots & \vdots & \vdots \\
 a_{64,2} & \cdots & \cdots & \vdots & \cdots & \cdots & \cdots & \cdots & \vdots & \cdots & \cdots & \cdots & a_{64,64}
 \end{bmatrix}
 \begin{bmatrix}
 \Delta S_{m1} \\
 \vdots \\
 \vdots \\
 \Delta\dot{Z}_1 \\
 \cdots \\
 \Delta\delta_2 - \Delta\delta_1 \\
 \Delta S_{m2} \\
 \vdots \\
 \vdots \\
 \Delta Z_2 \\
 \cdots \\
 \vdots \\
 \vdots \\
 \vdots \\
 \cdots \\
 \Delta\delta_4 - \Delta\delta_1 \\
 \Delta S_{m4} \\
 \vdots \\
 \vdots \\
 \Delta Z_4
 \end{bmatrix}$$

Reduced Matrix

NOTE:

1. For the original A matrix, there will be 2-zero eigenvalues if mechanical damping on all machines is set to zero. This represents redundancy of state variables associated with rotor angle and rotor speed.
2. For the reduced A matrix, there will be 1-zero eigenvalue with zero mechanical damping on all machines. For an m -machine system, $\delta_1, \delta_2, \dots, \delta_m$ are the rotor angles. The rotor variables $(\delta_2 - \delta_1), (\delta_3 - \delta_1), \dots, (\delta_m - \delta_1)$ are the variables which have significance leading to only $(m - 1)$ independent rotor angles.

The process of matrix reduction removes the redundancy associated with the rotor angle. However the redundancy associated with the rotor speed (or slip) continues exist, which is indicated by 1-zero eigenvalue. This zero eigenvalue vanishes when

- (a) Mechanical damping is accounted on any machine.
- (b) Speed-governor model is considered.
- (c) Frequency-dependent load models are included.

Appendix C

Generator Modelling

C.1 Introduction:

A 3 phase synchronous machine is modelled in the rotor frame of reference as shown in Figure C.1. The figure shows 2 fictitious d and q stator windings representing three phase armature windings on the stator. The figure also depicts 2 rotor windings, including the field winding 'f' along d-axis and 2 rotor coils along q-axis. The short circuited coils, one along d-axis ('h') and two along q-axis ('g' and 'k') represent the effect of damper windings and eddy currents induced in the rotor mass. This representation of the rotor circuits is normally referred to as 2.2 model [1].

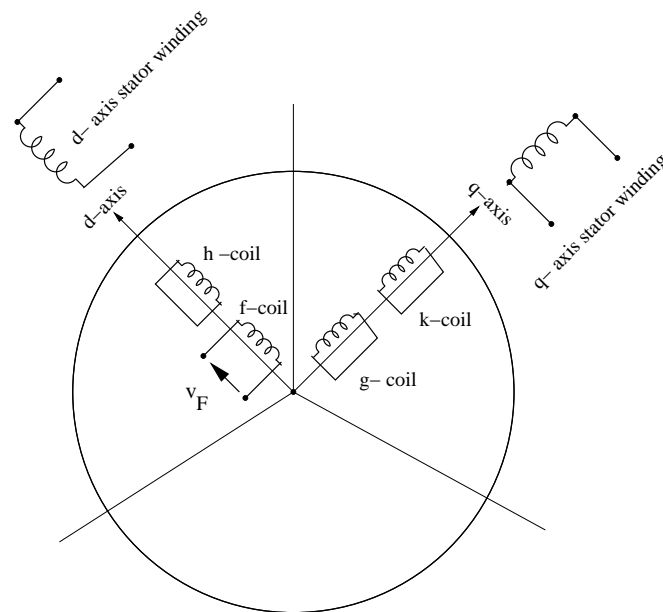


Figure C.1: 2.2 model of a Synchronous Machine.

C.2 Rotor Equations:

C.2.1 d-axis Equations:

For i^{th} generator the differential equations are written in the state-space form as follows:

$$\frac{d\psi_h}{dt} = \frac{1}{T_d''} [-\psi_h + \psi_d] \quad (C.1)$$

$$\frac{d\psi_f}{dt} = \frac{1}{T_d'} \left[-\psi_f + \psi_d + \frac{x_d' E_{fd}}{(x_d - x_d')} \right] \quad (C.2)$$

where

$$\psi_d = x_d'' i_d + E_q'' \quad (C.3)$$

$$E_q'' = \left[\frac{(x_d' - x_d'') \psi_h}{x_d'} + \frac{(x_d - x_d')}{x_d x_d'} x_d'' \psi_f \right] \quad (C.4)$$

C.2.2 q-axis Equations:

The differential equations are written in the state-space form as follows:

$$\frac{d\psi_g}{dt} = \frac{1}{T_q'} [-\psi_g + \psi_q] \quad (C.5)$$

$$\frac{d\psi_k}{dt} = \frac{1}{T_q''} [-\psi_k + \psi_q] \quad (C.6)$$

where

$$\psi_q = x_q'' i_q - E_d'' \quad (C.7)$$

$$E_d'' = - \left[\frac{(x_q' - x_q'') \psi_k}{x_q'} + \frac{(x_q - x_q')}{x_q x_q'} x_q'' \psi_g \right] \quad (C.8)$$

C.3 Stator Equations:

Neglecting stator transients and ignoring speed variations, the stator d- and q-axes voltage equations are given by

$$v_d = -i_d R_a - \psi_q \quad (C.9)$$

$$v_q = -i_q R_a + \psi_d \quad (C.10)$$

where v_d and v_q represent d- and q- axis generator terminal voltages respectively. Using (C.3) and (C.7) in (C.9) and (C.10), we have

$$v_d = -i_d R_a - x_q'' i_q + E_d'' \quad (\text{C.11})$$

$$v_q = -i_q R_a + x_d'' i_d + E_q'' \quad (\text{C.12})$$

C.4 Derivation of I_{Dg} and I_{Qg} :

Neglecting R_a , we have from (C.9) and (C.10),

$$v_q = \psi_d \quad (\text{C.13})$$

$$v_d = -\psi_q \quad (\text{C.14})$$

$$v_q + jv_d = V_g e^{j(\theta_g - \delta)} \quad (\text{C.15})$$

$$v_q = V_g \cos(\delta - \theta_g) \quad (\text{C.16})$$

$$v_d = -V_g \sin(\delta - \theta_g) \quad (\text{C.17})$$

$$\psi_d = V_g \cos(\delta - \theta_g) \quad (\text{C.18})$$

$$\psi_q = V_g \sin(\delta - \theta_g) \quad (\text{C.19})$$

Using (C.3), (C.7), (C.18) and (C.19) we have,

$$i_d = \frac{v_q - E_q''}{x_d''} = \frac{V_g \cos(\delta - \theta_g) - E_q''}{x_d''} \quad (\text{C.20})$$

$$i_q = \frac{E_d'' - v_d}{x_q''} = \frac{E_d'' + V_g \sin(\delta - \theta_g)}{x_q''} \quad (\text{C.21})$$

$$i_q + ji_d = \frac{E_d'' + V_g \sin(\delta - \theta_g)}{x_q''} + j \frac{V_g \cos(\delta - \theta_g) - E_q''}{x_d''} \quad (\text{C.22})$$

$$I_{Qg} + jI_{Dg} = (i_q + ji_d) e^{j\delta} \quad (\text{C.23})$$

$$I_{Dg} = \left[\frac{E_d'' + V_g \sin(\delta - \theta_g)}{x_q''} \right] \sin \delta + \left[\frac{V_g \cos(\delta - \theta_g) - E_q''}{x_d''} \right] \cos \delta \quad (\text{C.24})$$

$$I_{Qg} = \left[\frac{E_d'' + V_g \sin(\delta - \theta_g)}{x_q''} \right] \cos \delta - \left[\frac{V_g \cos(\delta - \theta_g) - E_q''}{x_d''} \right] \sin \delta \quad (\text{C.25})$$

From (C.4) and (C.8) we have,

$$E_q'' = C_1\psi_h + C_2\psi_f \quad (\text{C.26})$$

$$E_d'' = -C_3\psi_k - C_4\psi_g \quad (\text{C.27})$$

where

$$C_1 = \frac{(x_d' - x_d'')}{x_d'} \quad (\text{C.28})$$

$$C_2 = \frac{(x_d - x_d')x_d''}{x_dx_d'} \quad (\text{C.29})$$

$$C_3 = \frac{(x_q' - x_q'')}{x_q'} \quad (\text{C.30})$$

$$C_4 = \frac{(x_q - x_q')x_q''}{x_qx_q'} \quad (\text{C.31})$$

Therefore,

$$I_{Dg} = \frac{1}{x_q''} \left[-C_3\psi_k - C_4\psi_g + V_g \sin(\delta - \theta_g) \right] \sin \delta + \frac{1}{x_d''} \left[V_g \cos(\delta - \theta_g) - C_1\psi_h - C_2\psi_f \right] \cos \delta \quad (\text{C.32})$$

$$I_{Qg} = \frac{1}{x_q''} \left[-C_3\psi_k - C_4\psi_g + V_g \sin(\delta - \theta_g) \right] \cos \delta - \frac{1}{x_d''} \left[V_g \cos(\delta - \theta_g) - C_1\psi_h - C_2\psi_f \right] \sin \delta \quad (\text{C.33})$$

C.5 Swing Equations:

$$\frac{d\delta}{dt} = S_m \omega_B \quad (\text{C.34})$$

$$\frac{dS_m}{dt} = \frac{1}{2H} \left[-\overline{D}S_m + T_m - T_e \right] \quad (\text{C.35})$$

In terms of the flux-linkages and the generator winding currents, the electromagnetic torque is given by

$$T_e = (\psi_d i_q - \psi_q i_d) \quad (\text{C.36})$$

Using (C.18) - (C.21), (C.26) and (C.27), the above torque expression is modified as

$$\begin{aligned}
T_e = & \left[\frac{C_2}{x_d''} \left(V_g \psi_f \sin(\delta - \theta_g) \right) + \frac{C_1}{x_d''} \left(V_g \psi_h \sin(\delta - \theta_g) \right) - \frac{C_4}{x_q''} \left(V_g \psi_g \cos(\delta - \theta_g) \right) \right. \\
& \left. - \frac{C_3}{x_q''} \left(V_g \psi_k \cos(\delta - \theta_g) \right) + C_5 \left(\frac{V_g^2 \sin(2(\delta - \theta_g))}{2} \right) \right] \quad (C.37)
\end{aligned}$$

where

$$C_5 = \left(\frac{x_d'' - x_q''}{x_d'' x_q''} \right) \quad (C.38)$$

C.6 Modification of Differential Equations:

Using (C.18) and (C.19) in (C.1), (C.2), (C.5) and (C.6) we get

$$\frac{d\psi_f}{dt} = \frac{1}{T_d'} \left[-\psi_f + V_g \cos(\delta - \theta_g) + \left(\frac{x_d'}{x_d - x_d'} \right) E_{fd} \right] \quad (C.39)$$

$$\frac{d\psi_h}{dt} = \frac{1}{T_d''} \left[-\psi_h + V_g \cos(\delta - \theta_g) \right] \quad (C.40)$$

$$\frac{d\psi_g}{dt} = \frac{1}{T_q'} \left[-\psi_g + V_g \sin(\delta - \theta_g) \right] \quad (C.41)$$

$$\frac{d\psi_k}{dt} = \frac{1}{T_q''} \left[-\psi_k + V_g \sin(\delta - \theta_g) \right] \quad (C.42)$$

After linearizing the above equations, the non-zero elements of $[A_g]$, $[B_g^p]$, $[C_g]$ and $[D_g^p]$ matrices are given by

$$A_g(1, 2) = \omega_B \quad (C.43)$$

$$\begin{aligned}
A_g(2, 1) = & -\frac{1}{2H} \left[\frac{C_2 V_{g0} \psi_{f0} \cos(\delta_0 - \theta_{g0})}{x_d''} + \frac{C_1 V_{g0} \psi_{h0} \cos(\delta_0 - \theta_{g0})}{x_d''} + \frac{C_4 V_{g0} \psi_{g0} \sin(\delta_0 - \theta_{g0})}{x_q''} \right. \\
& \left. + \frac{C_3 V_{g0} \psi_{k0} \sin(\delta_0 - \theta_{g0})}{x_q''} + C_5 V_{g0}^2 \cos(2(\delta_0 - \theta_{g0})) \right] \quad (C.44)
\end{aligned}$$

$$A_g(2, 2) = -\frac{\overline{D}}{2H} \quad (\text{C.45})$$

$$A_g(2, 3) = -\frac{1}{2H} \left[\frac{C_2 V_{g0} \sin(\delta_0 - \theta_{g0})}{x_d''} \right] \quad (\text{C.46})$$

$$A_g(2, 4) = -\frac{1}{2H} \left[\frac{C_1 V_{g0} \sin(\delta_0 - \theta_{g0})}{x_d''} \right] \quad (\text{C.47})$$

$$A_g(2, 5) = \frac{1}{2H} \left[\frac{C_4 V_{g0} \cos(\delta_0 - \theta_{g0})}{x_q''} \right] \quad (\text{C.48})$$

$$A_g(2, 6) = \frac{1}{2H} \left[\frac{C_3 V_{g0} \cos(\delta_0 - \theta_{g0})}{x_q''} \right] \quad (\text{C.49})$$

$$A_g(3, 1) = -\frac{V_{g0} \sin(\delta_0 - \theta_{g0})}{T_d'} \quad (\text{C.50})$$

$$A_g(3, 3) = -\frac{1}{T_d'} \quad (\text{C.51})$$

$$A_g(3, 7) = \frac{1}{T_d'} \left[\frac{x_d'}{x_d - x_d'} \right] \quad (\text{C.52})$$

$$A_g(4, 1) = -\frac{V_{g0} \sin(\delta_0 - \theta_{g0})}{T_d''} \quad (\text{C.53})$$

$$A_g(4, 4) = -\frac{1}{T_d''} \quad (\text{C.54})$$

$$A_g(5, 1) = \frac{V_{g0} \cos(\delta_0 - \theta_{g0})}{T_q'} \quad (\text{C.55})$$

$$A_g(5, 5) = -\frac{1}{T_q'} \quad (\text{C.56})$$

$$A_g(6, 1) = \frac{V_{g0} \cos(\delta_0 - \theta_{g0})}{T_q''} \quad (\text{C.57})$$

$$A_g(6, 6) = -\frac{1}{T_q''} \quad (\text{C.58})$$

$$B_g^p(2, 1) = \frac{1}{2H} \left[\frac{C_2 \psi_{f0} \cos(\delta_0 - \theta_{g0})}{x_d''} + \frac{C_1 \psi_{h0} \cos(\delta_0 - \theta_{g0})}{x_d''} + \frac{C_4 \psi_{g0} \sin(\delta_0 - \theta_{g0})}{x_q''} \right. \\ \left. + \frac{C_3 \psi_{k0} \sin(\delta_0 - \theta_{g0})}{x_q''} + C_5 V_{g0} \cos(2(\delta_0 - \theta_{g0})) \right] \quad (C.59)$$

$$B_g^p(2, 2) = -\frac{1}{2H} \left[\frac{C_2 \psi_{f0} \sin(\delta_0 - \theta_{g0})}{x_d''} + \frac{C_1 \psi_{h0} \sin(\delta_0 - \theta_{g0})}{x_d''} - \frac{C_4 \psi_{g0} \cos(\delta_0 - \theta_{g0})}{x_q''} \right. \\ \left. - \frac{C_3 \psi_{k0} \cos(\delta_0 - \theta_{g0})}{x_q''} + C_5 V_{g0} \sin(2(\delta_0 - \theta_{g0})) \right] \quad (C.60)$$

$$B_g^p(3, 1) = \frac{\sin(\delta_0 - \theta_{g0})}{T_d'} \quad (C.61)$$

$$B_g^p(3, 2) = \frac{\cos(\delta_0 - \theta_{g0})}{T_d'} \quad (C.62)$$

$$B_g^p(4, 1) = \frac{\sin(\delta_0 - \theta_{g0})}{T_d''} \quad (C.63)$$

$$B_g^p(4, 2) = \frac{\cos(\delta_0 - \theta_{g0})}{T_d''} \quad (C.64)$$

$$B_g^p(5, 1) = -\frac{\cos(\delta_0 - \theta_{g0})}{T_q'} \quad (C.65)$$

$$B_g^p(5, 2) = \frac{\sin(\delta_0 - \theta_{g0})}{T_q'} \quad (C.66)$$

$$B_g^p(6, 1) = -\frac{\cos(\delta_0 - \theta_{g0})}{T_q''} \quad (C.67)$$

$$B_g^p(6, 2) = \frac{\sin(\delta_0 - \theta_{g0})}{T_q''} \quad (C.68)$$

$$C_g(1, 1) = \frac{V_{g0} \sin \delta_0 \cos(\delta_0 - \theta_{g0})}{x_q''} - \frac{V_{g0} \cos \delta_0 \sin(\delta_0 - \theta_{g0})}{x_d''} + I_{Qg0} \quad (\text{C.69})$$

$$C_g(1, 3) = -\frac{C_2 \cos \delta_0}{x_d''} \quad (\text{C.70})$$

$$C_g(1, 4) = -\frac{C_1 \cos \delta_0}{x_d''} \quad (\text{C.71})$$

$$C_g(1, 5) = -\frac{C_4 \sin \delta_0}{x_q''} \quad (\text{C.72})$$

$$C_g(1, 6) = -\frac{C_3 \sin \delta_0}{x_q''} \quad (\text{C.73})$$

$$C_g(2, 1) = \frac{V_{g0} \sin \delta_0 \sin(\delta_0 - \theta_{g0})}{x_d''} + \frac{V_{g0} \cos \delta_0 \cos(\delta_0 - \theta_{g0})}{x_q''} - I_{Dg0} \quad (\text{C.74})$$

$$C_g(2, 3) = \frac{C_2 \sin \delta_0}{x_d''} \quad (\text{C.75})$$

$$C_g(2, 4) = \frac{C_1 \sin \delta_0}{x_d''} \quad (\text{C.76})$$

$$C_g(2, 5) = -\frac{C_4 \cos \delta_0}{x_q''} \quad (\text{C.77})$$

$$C_g(2, 6) = -\frac{C_3 \cos \delta_0}{x_q''} \quad (\text{C.78})$$

$$D_g^p(1, 1) = \frac{\cos \delta_0 \sin(\delta_0 - \theta_{g0})}{x_d''} - \frac{\sin \delta_0 \cos(\delta_0 - \theta_{g0})}{x_q''} \quad (\text{C.79})$$

$$D_g^p(1, 2) = \frac{\cos \delta_0 \cos(\delta_0 - \theta_{g0})}{x_d''} + \frac{\sin \delta_0 \sin(\delta_0 - \theta_{g0})}{x_q''} \quad (\text{C.80})$$

$$D_g(2, 1) = -\frac{\sin \delta_0 \sin(\delta_0 - \theta_{g0})}{x_d''} - \frac{\cos \delta_0 \cos(\delta_0 - \theta_{g0})}{x_q''} \quad (\text{C.81})$$

$$D_g^p(2, 2) = -\frac{\sin \delta_0 \cos(\delta_0 - \theta_{g0})}{x_d''} + \frac{\cos \delta_0 \sin(\delta_0 - \theta_{g0})}{x_q''} \quad (\text{C.82})$$

C.7 Simplification of Machine Model:

Modifications to be made in 2.2 model to get various other simple models [1] are tabulated in Table C.1.

Model	Basic Modifications	Settings for No dynamic Saliency
2.2	-	$x_q'' = x_d''$
2.1	$x_q'' = x_q'$ and $T_{qo}'' \neq 0$	$x_q' = x_d''$
1.1	$x_d'' = x_d'$ and $T_{do}'' \neq 0$ $x_q'' = x_q'$ and $T_{qo}'' \neq 0$	$x_q' = x_d'$
1.0	$x_d'' = x_d'$ and $T_{do}'' \neq 0$ $x_q'' = x_q' = x_q$ and $T_{qo}'' \neq 0$ $T_{qo}' \neq 0$	$x_q = x_d'$
0.0 (classical)	$x_d'' = x_d'$ and $T_{do}'' \neq 0$ $T_{do}' = 10000$ (say) $x_q'' = x_q' = x_q = x_d'$ and $T_{qo}'' \neq 0, T_{qo}' \neq 0$	-

Table C.1: Simplifications in 2.2 model.

NOTE:

For classical model, the q-axis transient voltage, $E_q' = E_q''$ is assumed to be a constant. To achieve this in 2.2 model, one may require to disable exciter in addition to choosing an appropriate value for x_d relative to x_d' . For example, one may set $x_d = 6x_d'$.

Appendix D

Exciter Modelling

As per [2, 22], the following IEEE-type exciter models are considered.

D.1 Single Time Constant Static Exciter:

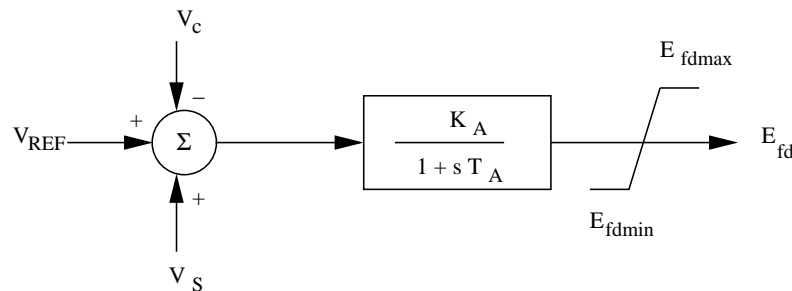


Figure D.1: Single time constant static excitation system.

The time delay associated with the bus voltage measuring transducer is neglected.

$$\frac{dE_{fd}}{dt} = \frac{1}{T_A} [-E_{fd} + K_A (V_{ref} + V_s - V_c)] \quad (D.1)$$

After linearizing (D.1), the non-zero elements of the matrices are given by,

$$A_g(7, 7) = -\frac{1}{T_A} \quad (D.2)$$

$$B_g^p(7, 2) = -\frac{K_A}{T_A} \quad (D.3)$$

$$E_g(7, 2) = \frac{K_A}{T_A} \quad (D.4)$$

D.2 IEEE-type DC1A Exciter:

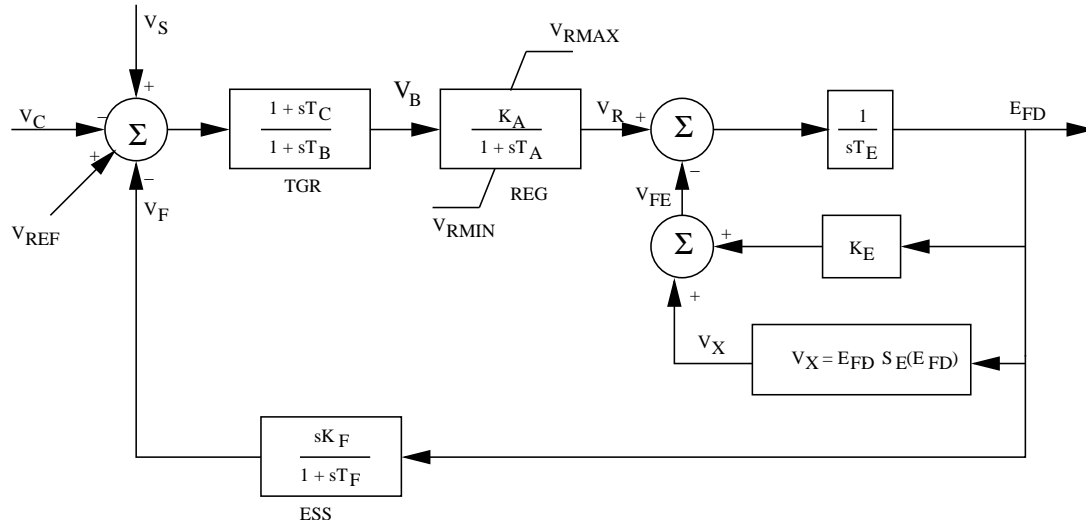


Figure D.2: IEEE-type DC1A excitation system.

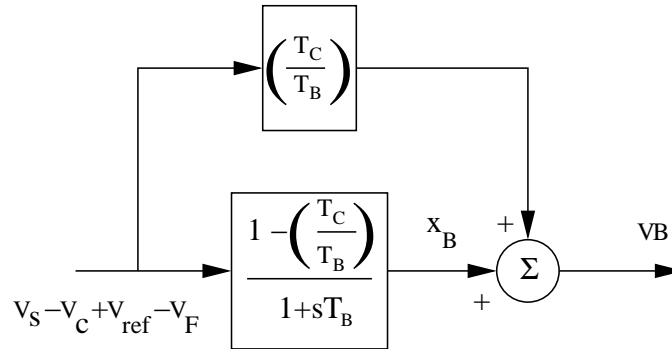


Figure D.3: TGR block.

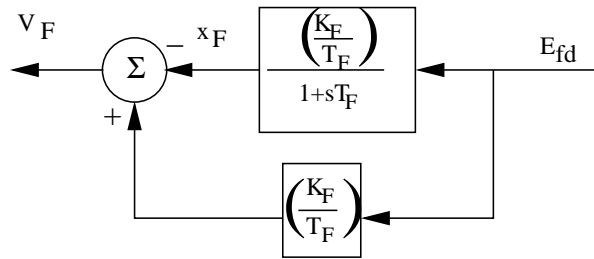


Figure D.4: ESS block.

NOTE:

1. The saturation function $S_E(E_{fd})$ is given by

$$S_E(E_{fd}) = A_s e^{B_s E_{fd}}$$

where A_s and B_s are to be determined from two sample points.

2. The time constant of the bus voltage measuring transducer is taken as 0.02 s and the corresponding differential equation is not considered for linearization.

The differential equations for the DC1A exciter are given by,

$$\frac{dx_F}{dt} = \frac{1}{T_F} \left[-x_F + \left(\frac{K_F}{T_F} \right) E_{fd} \right] \quad (D.5)$$

$$\frac{dx_B}{dt} = \frac{1}{T_B} \left[-x_B + \left(1 - \frac{T_C}{T_B} \right) \left(V_{ref} + V_s - V_c - \left(\frac{K_F}{T_F} \right) E_{fd} + x_F \right) \right] \quad (D.6)$$

$$\frac{dv_R}{dt} = \frac{1}{T_A} \left[-v_R + K_A \left(x_B + \frac{T_C}{T_B} \left[V_{ref} + V_s - V_c - \left(\frac{K_F}{T_F} \right) E_{fd} + x_F \right] \right) \right] \quad (D.7)$$

$$\frac{dE_{fd}}{dt} = \frac{1}{T_E} \left[- \left(K_E + A_s e^{B_s E_{fd}} \right) E_{fd} + v_R \right] \quad (D.8)$$

After linearizing the above equations, the non-zero elements of the matrices are given by,

$$A_g(7, 7) = -\frac{1}{T_E} \left[K_E + A_s (B_s E_{fd0} + 1) e^{(B_s E_{fd0})} \right] \quad (D.9)$$

$$A_g(7, 8) = \frac{1}{T_E} \quad (D.10)$$

$$A_g(8, 7) = -\frac{K_A T_C K_F}{T_A T_B T_F} \quad (D.11)$$

$$A_g(8, 8) = -\frac{1}{T_A} \quad (D.12)$$

$$A_g(8, 9) = \frac{K_A}{T_A} \quad (D.13)$$

$$A_g(8, 10) = \frac{K_A T_C}{T_A T_B} \quad (D.14)$$

$$A_g(9, 7) = -\frac{1}{T_B} \left[\left(1 - \frac{T_C}{T_B} \right) \frac{K_F}{T_F} \right] \quad (D.15)$$

$$A_g(9, 9) = -\frac{1}{T_B} \quad (D.16)$$

$$A_g(9, 10) = \frac{1}{T_B} \left[\left(1 - \frac{T_C}{T_B} \right) \right] \quad (D.17)$$

$$A_g(10, 7) = \frac{1}{T_F} \left[\frac{K_F}{T_F} \right] \quad (D.18)$$

$$A_g(10, 10) = -\frac{1}{T_F} \quad (D.19)$$

$$B_g^p(8, 2) = -\frac{K_A T_C}{T_A T_B} \quad (D.20)$$

$$B_g^p(9, 2) = -\frac{1}{T_B} \left[\left(1 - \frac{T_C}{T_B} \right) \right] \quad (D.21)$$

$$E_g(8, 2) = \frac{K_A T_C}{T_A T_B} \quad (D.22)$$

$$E_g(9, 2) = \frac{1}{T_B} \left[\left(1 - \frac{T_C}{T_B} \right) \right] \quad (D.23)$$

D.3 IEEE-type AC4A Exciter:

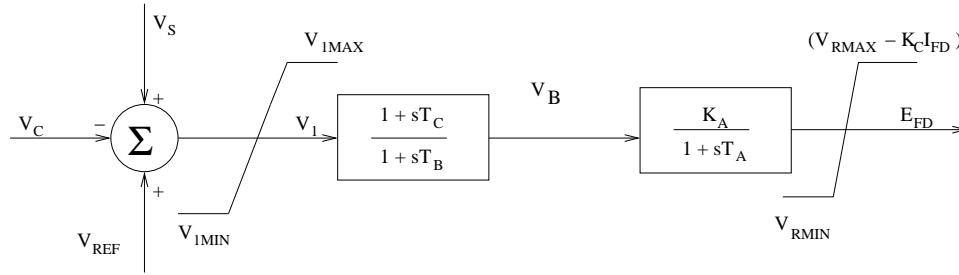


Figure D.5: IEEE-type AC4A excitation system.

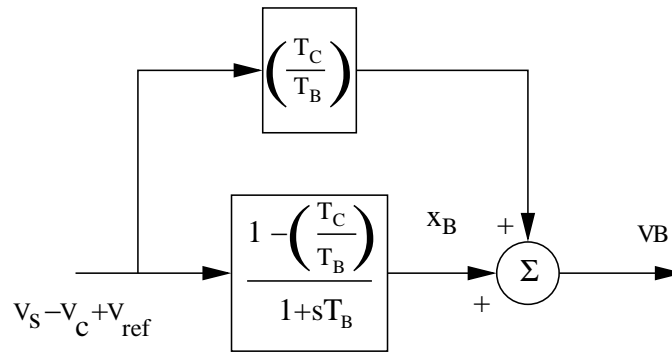


Figure D.6: TGR block.

The time constant of the bus voltage measuring transducer is taken as 0.02 s and the corresponding differential equation is not considered for linearization.

The differential equations for the IEEE-type AC4A excitation system are given by,

$$\frac{dx_B}{dt} = \frac{1}{T_B} \left[-x_B + \left(1 - \frac{T_C}{T_B} \right) (V_{ref} + V_s - V_c) \right] \quad (D.24)$$

$$\frac{dE_{fd}}{dt} = \frac{1}{T_A} \left[-E_{fd} + K_A \left(x_B + \frac{T_C}{T_B} [V_{ref} + V_s - V_c] \right) \right] \quad (D.25)$$

After linearizing the above equations, the non-zero elements of the matrices are given by,

$$A_g(7, 7) = -\frac{1}{T_A} \quad (\text{D.26})$$

$$A_g(7, 9) = \frac{K_A}{T_A} \quad (\text{D.27})$$

$$A_g(9, 9) = -\frac{1}{T_B} \quad (\text{D.28})$$

$$B_g^p(7, 2) = -\frac{K_A}{T_A} \frac{T_C}{T_B} \quad (\text{D.29})$$

$$B_g^p(9, 2) = -\frac{1}{T_B} \left[\left(1 - \frac{T_C}{T_B} \right) \right] \quad (\text{D.30})$$

$$E_g(7, 2) = \frac{K_A}{T_A} \frac{T_C}{T_B} \quad (\text{D.31})$$

$$E_g(9, 2) = \frac{1}{T_B} \left[\left(1 - \frac{T_C}{T_B} \right) \right] \quad (\text{D.32})$$

Appendix E

Turbine and Speed-governor Modelling

As per the IEEE committee report [23], the following are the typical types of turbine-governor are considered.

E.1 Hydro Turbine and its Speed Governor Model:

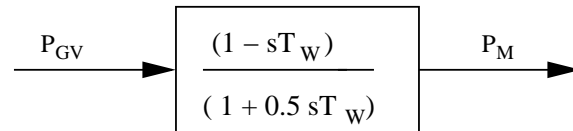


Figure E.1: Hydraulic turbine model.

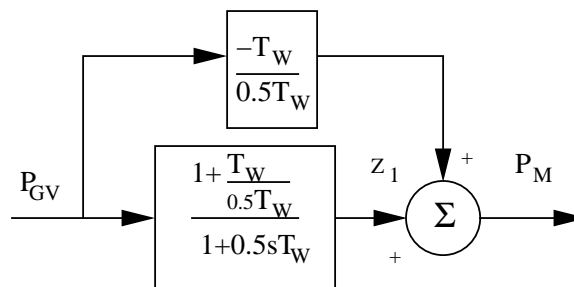


Figure E.2: Modified hydraulic turbine model.

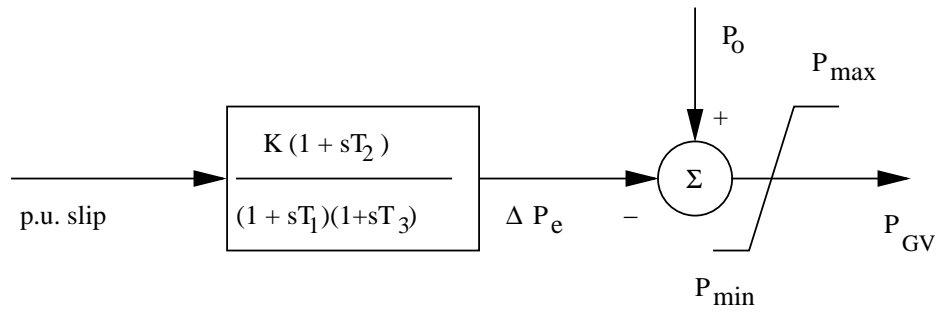


Figure E.3: Model of speed-governor for hydro turbines.

The above model is modified as shown below for the purpose of linearization.

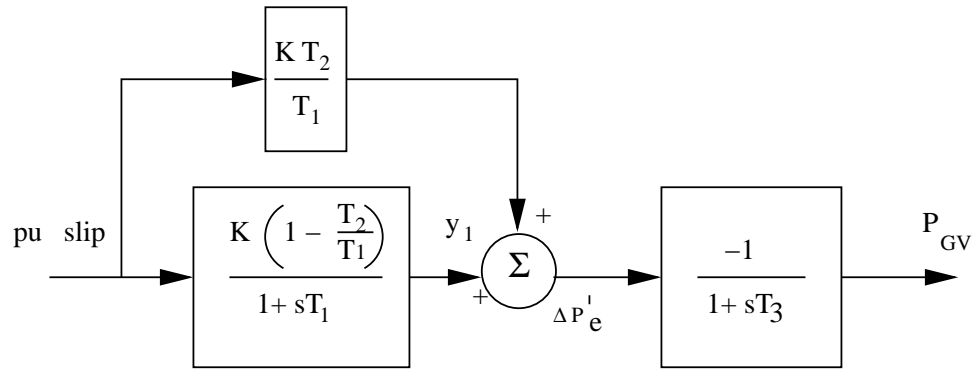


Figure E.4: Modified model of speed-governor for hydro turbine.

The differential equations for the hydro turbine and the speed-governor are given by,

$$\frac{dy_1}{dt} = \frac{1}{T_1} \left[K \left(1 - \frac{T_2}{T_1} \right) S_m - y_1 \right] \quad (\text{E.1})$$

$$\frac{dP_{GV}}{dt} = \frac{1}{T_3} \left[-K \frac{T_2}{T_1} S_m - y_1 - P_{GV} \right] \quad (\text{E.2})$$

$$\frac{dz_1}{dt} = \frac{2}{T_W} [3P_{GV} - z_1] \quad (\text{E.3})$$

$$P_M = z_1 - 2P_{GV} \quad (\text{E.4})$$

NOTE:

1. P_0 is a constant.
2. (E.4) is used in (C.35) in place of T_m .

After linearization of above equations the non-zero elements of the matrices are given by

$$A_g(2, 15) = -\frac{1}{H} \quad (\text{E.5})$$

$$A_g(2, 16) = \frac{1}{2H} \quad (\text{E.6})$$

$$A_g(14, 2) = \frac{K}{T_1} \left[\left(1 - \frac{T_2}{T_1} \right) \right] \quad (\text{E.7})$$

$$A_g(14, 14) = -\frac{1}{T_1} \quad (\text{E.8})$$

$$A_g(15, 2) = -\frac{K}{T_1} \frac{T_2}{T_3} \quad (\text{E.9})$$

$$A_g(15, 14) = -\frac{1}{T_3} \quad (\text{E.10})$$

$$A_g(15, 15) = -\frac{1}{T_3} \quad (\text{E.11})$$

$$A_g(16, 15) = \frac{6}{T_W} \quad (\text{E.12})$$

$$A_g(16, 16) = -\frac{2}{T_W} \quad (\text{E.13})$$

E.2 Reheat Type Steam Turbine and its Speed-governor Model:

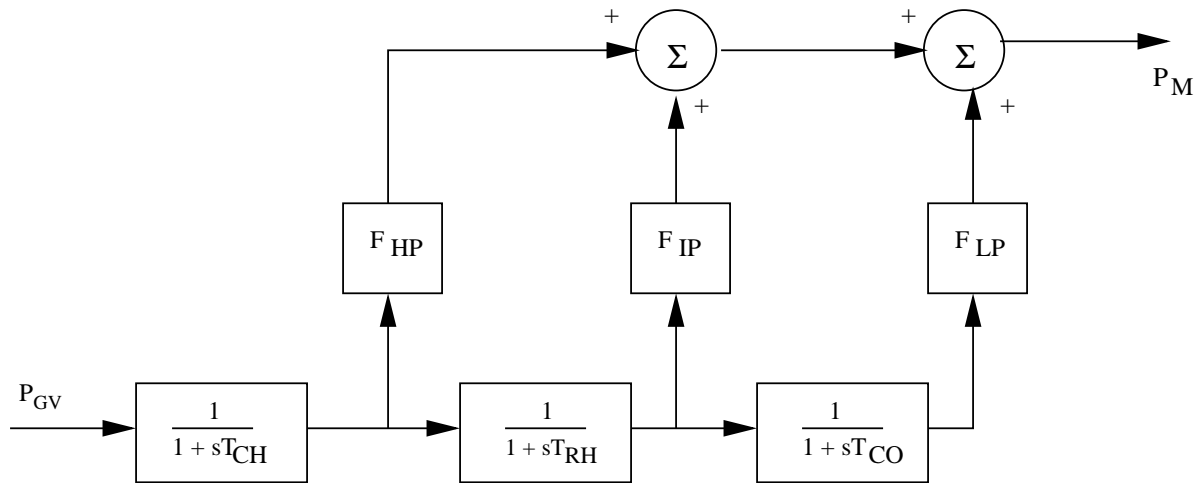


Figure E.5: Tandem compounded, single-reheat-type steam turbine model.

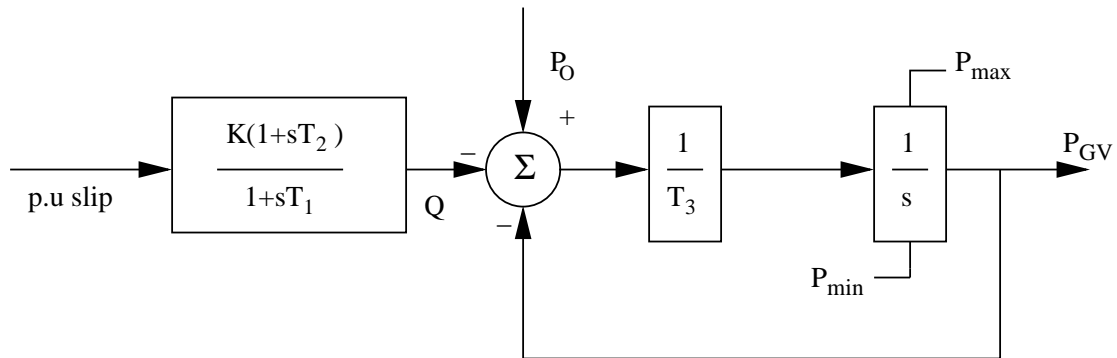


Figure E.6: Model for speed-governor for steam turbines.

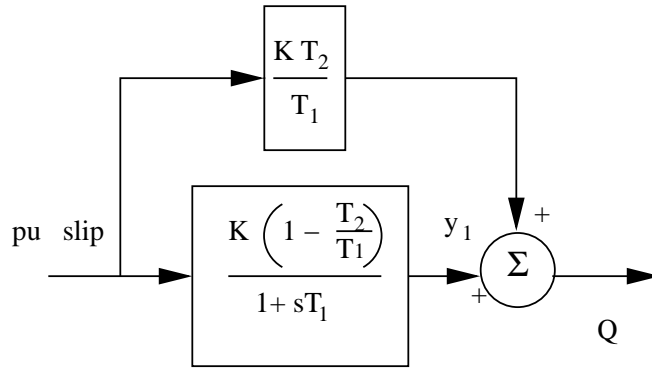


Figure E.7: Modified model for speed-governor for steam turbines.

The differential equations for the steam turbine and the associated speed-governor are given by,

$$\frac{dx_1}{dt} = \frac{1}{T_{CH}} (P_{GV} - x_1) \quad (\text{E.14})$$

$$\frac{dx_2}{dt} = \frac{1}{T_{RH}} (x_1 - x_2) \quad (\text{E.15})$$

$$\frac{dx_3}{dt} = \frac{1}{T_{CO}} (x_2 - x_3) \quad (\text{E.16})$$

$$\frac{dy_1}{dt} = \frac{1}{T_1} \left[K \left(1 - \frac{T_2}{T_1} \right) S_m - y_1 \right] \quad (\text{E.17})$$

$$\frac{dP_{GV}}{dt} = \frac{1}{T_3} \left[P_0 - K \frac{T_2}{T_1} S_m - y_1 - P_{GV} \right] \quad (\text{E.18})$$

$$P_M = F_{HP}x_1 + F_{IP}x_2 + F_{LP}x_3 \quad (\text{E.19})$$

NOTE:

1. P_0 is a constant.
2. (E.19) is used in (C.35) in place of T_m .

After linearization of above equations the non-zero elements of the matrices are given by,

$$A_g(2, 11) = \frac{F_{HP}}{2H} \quad (\text{E.20})$$

$$A_g(2, 12) = \frac{F_{IP}}{2H} \quad (\text{E.21})$$

$$A_g(2, 13) = \frac{F_{LP}}{2H} \quad (\text{E.22})$$

$$A_g(11, 11) = -\frac{1}{T_{CH}} \quad (\text{E.23})$$

$$A_g(11, 15) = \frac{1}{T_{CH}} \quad (\text{E.24})$$

$$A_g(12, 11) = \frac{1}{T_{RH}} \quad (\text{E.25})$$

$$A_g(12, 12) = -\frac{1}{T_{RH}} \quad (\text{E.26})$$

$$A_g(13, 12) = \frac{1}{T_{CO}} \quad (\text{E.27})$$

$$A_g(13, 13) = -\frac{1}{T_{C0}} \quad (\text{E.28})$$

$$A_g(14, 2) = \frac{K}{T_1} \left[\left(1 - \frac{T_2}{T_1} \right) \right] \quad (\text{E.29})$$

$$A_g(14, 14) = -\frac{1}{T_1} \quad (\text{E.30})$$

$$A_g(15, 2) = -\frac{K}{T_1} \frac{T_2}{T_3} \quad (\text{E.31})$$

$$A_g(15, 14) = -\frac{1}{T_3} \quad (\text{E.32})$$

$$A_g(15, 15) = -\frac{1}{T_3} \quad (\text{E.33})$$

Appendix F

Network Modelling

F.1 Introduction:

Transmission network mainly consists of transmission lines and transformers. Since the time constants of these elements are relatively small compared to the mechanical time constants, the network transients are neglected and the network is assumed to be in sinusoidal steady state. The modelling of these components are briefly discussed in the following sections:

F.2 Transmission Lines:

Transmission Lines are modelled as a nominal π circuit [9] as shown in Figure F.1.

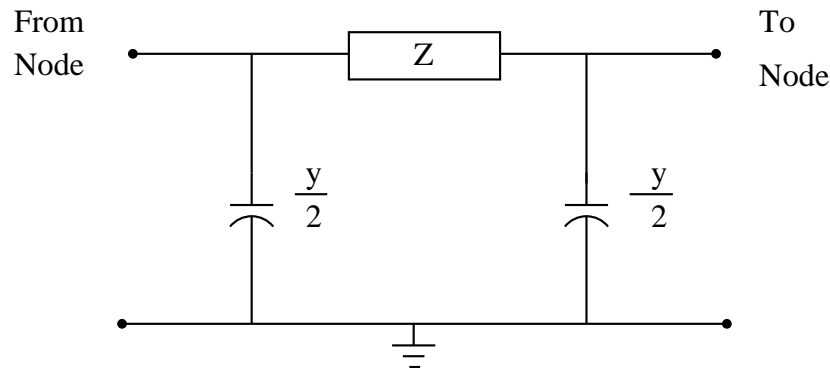


Figure F.1: Nominal π Model of transmission lines.

where,

Z : represents the series impedance of the line.

$\frac{y}{2}$: represents half of the total line charging y , at each node.

F.3 Transformers:

The transformers are generally used as inter-connecting (IC) transformers and generator transformers. These transformers are usually with off-nominal-turns-ratio and are modelled as equivalent π circuit [9] as shown in Figure F.2.

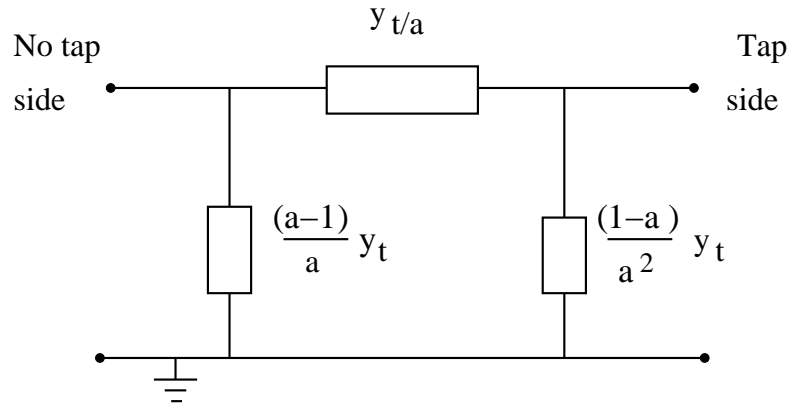


Figure F.2: Transformer Model

where,

$$y_t = \frac{1}{z_t}$$

z_t : represents the series impedance at nominal-turns-ratio.

a : represents per unit off-nominal tap position.

The transmission network is represented by an algebraic equation given by

$$Y_{BUS} \bar{V} = \bar{I} \quad (\text{F.1})$$

where

Y_{BUS} = Bus admittance matrix

\bar{V} = Vector of bus voltages

\bar{I} = Vector of injected bus currents

The above equation is obtained by writing the network equations in the node-frame of reference taking ground as the reference.

Appendix G

Static Loads

$$P_L = P_{L0} \left\{ \left(\frac{V}{V_0} \right)^{m_p} p_1 + \left(\frac{V}{V_0} \right)^{m_i} p_2 + \left(\frac{V}{V_0} \right)^{m_z} p_3 \right\} \quad (\text{G.1})$$

$$Q_L = Q_{L0} \left\{ \left(\frac{V}{V_0} \right)^{n_p} r_1 + \left(\frac{V}{V_0} \right)^{n_i} r_2 + \left(\frac{V}{V_0} \right)^{n_z} r_3 \right\} \quad (\text{G.2})$$

P_{L0} = initial value of the active component of load.

Q_{L0} = initial value of the reactive component of load.

V_0 = initial value of the bus voltage magnitude at load bus.

This model is also referred to as the ZIP model, since it consists of the sum of constant impedance (Z), constant current (I), and constant power (P) terms. The parameters of this model are the coefficients p_1 to p_3 and r_1 to r_3 , which define the proportion of each component. While selecting these fractions, it should be noted that

$$p_1 + p_2 + p_3 = 1$$

$$r_1 + r_2 + r_3 = 1$$

For real component of load power:

constant power $m_p = 0.0$

constant current $m_i = 1.0$

constant impedance $m_z = 2.0$

For reactive component of load power:

constant power $n_p = 0.0$

constant current $n_i = 1.0$

constant impedance $n_z = 2.0$

We know that

$$I_Q + jI_D = \left(\frac{P_L + jQ_L}{\bar{V}} \right)^* \quad (\text{G.3})$$

$$= \left(\frac{P_L - jQ_L}{\frac{V^2}{\bar{V}}} \right) \quad (\text{G.4})$$

$$= \left(\frac{P_L - jQ_L}{V^2} \right) \bar{V} \quad (\text{G.5})$$

$$= \left(\frac{P_L - jQ_L}{V^2} \right) (V_Q + jV_D) \quad (\text{G.6})$$

$$= \left(\frac{P_L}{V^2} V_Q + \frac{Q_L}{V^2} V_D \right) + j \left(\frac{P_L}{V^2} V_D - \frac{Q_L}{V^2} V_Q \right) \quad (\text{G.7})$$

Comparing the like terms, we get the Q and D components of the load current for j^{th} load bus as

$$I_Q = P_L \left(\frac{V_Q}{V^2} \right) + Q_L \left(\frac{V_D}{V^2} \right) \quad (\text{G.8})$$

$$I_D = P_L \left(\frac{V_D}{V^2} \right) - Q_L \left(\frac{V_Q}{V^2} \right) \quad (\text{G.9})$$

where the load bus voltage magnitude V is given by

$$V = \sqrt{V_Q^2 + V_D^2}$$

Linearizing (G.8) and (G.9), we get

$$\begin{aligned} \Delta I_Q = & \left[\frac{V_{Q0}}{V_0^2} \Delta P_L + \frac{V_{D0}}{V_0^2} \Delta Q_L + \frac{P_{L0}}{V_0^2} \Delta V_Q + \frac{Q_{L0}}{V_0^2} \Delta V_D \right. \\ & \left. + (P_{L0} V_{Q0} + Q_{L0} V_{D0}) \left(\frac{-2}{V_0^3} \right) \Delta V \right] \end{aligned} \quad (\text{G.10})$$

$$\begin{aligned} \Delta I_D = & \left[\frac{V_{D0}}{V_0^2} \Delta P_L - \frac{V_{Q0}}{V_0^2} \Delta Q_L + \frac{P_{L0}}{V_0^2} \Delta V_D - \frac{Q_{L0}}{V_0^2} \Delta V_Q \right. \\ & \left. + (P_{L0} V_{D0} - Q_{L0} V_{Q0}) \left(\frac{-2}{V_0^3} \right) \Delta V \right] \end{aligned} \quad (\text{G.11})$$

Considering only the first term in (G.1), one component of ΔP_L can be obtained as follows:

$$\begin{aligned} &= P_{L0} \left(\frac{1}{V_0} \right)^{m_p} p_1 m_p V_0^{(m_p-1)} \Delta V \\ &= p_1 m_p \left(\frac{P_{L0}}{V_0} \right) \Delta V \end{aligned}$$

Following the above procedure for the remaining two terms in (G.1), we have

$$\Delta P_L = m_k \left(\frac{P_{L0}}{V_0} \right) \Delta V \quad (\text{G.12})$$

where

$$m_k = m_p p_1 + m_i p_2 + m_z p_3$$

Similarly, ΔQ_L can be obtained as

$$\Delta Q_L = n_k \left(\frac{Q_{L0}}{V_0} \right) \Delta V \quad (\text{G.13})$$

where

$$n_k = n_p r_1 + n_i r_2 + n_z r_3$$

Using the result given in (B.5) we can write

$$\Delta V = \frac{V_{Q0}}{V_0} \Delta V_Q + \frac{V_{D0}}{V_0} \Delta V_D \quad (\text{G.14})$$

Substitution of (G.14), (G.12), and (G.13) in (G.10) and (G.11) yields

$$\Delta I_Q = G_{QQ} \Delta V_Q + B_{QD} \Delta V_D$$

$$\Delta I_D = -B_{DQ} \Delta V_Q + G_{DD} \Delta V_D$$

or

$$\begin{bmatrix} \Delta I_D \\ \Delta I_Q \end{bmatrix} = \begin{bmatrix} -B_{DQ} & G_{DD} \\ G_{QQ} & B_{QD} \end{bmatrix} \begin{bmatrix} \Delta V_Q \\ \Delta V_D \end{bmatrix}$$

where

$$B_{DQ} = \left[\frac{Q_{L0}}{V_0^2} \left((n_k - 2) \frac{V_{Q0}^2}{V_0^2} + 1 \right) - \frac{P_{L0}}{V_0^2} \left((m_k - 2) \frac{V_{Q0} V_{D0}}{V_0^2} \right) \right] \quad (\text{G.15})$$

$$B_{QD} = \left[\frac{Q_{L0}}{V_0^2} \left((n_k - 2) \frac{V_{D0}^2}{V_0^2} + 1 \right) + \frac{P_{L0}}{V_0^2} \left((m_k - 2) \frac{V_{Q0} V_{D0}}{V_0^2} \right) \right] \quad (\text{G.16})$$

$$G_{QQ} = \left[\frac{P_{L0}}{V_0^2} \left((m_k - 2) \frac{V_{Q0}^2}{V_0^2} + 1 \right) + \frac{Q_{L0}}{V_0^2} \left((n_k - 2) \frac{V_{Q0} V_{D0}}{V_0^2} \right) \right] \quad (\text{G.17})$$

$$G_{DD} = \left[\frac{P_{L0}}{V_0^2} \left((m_k - 2) \frac{V_{D0}^2}{V_0^2} + 1 \right) - \frac{Q_{L0}}{V_0^2} \left((n_k - 2) \frac{V_{Q0} V_{D0}}{V_0^2} \right) \right] \quad (\text{G.18})$$

Appendix H

Initial Condition Calculations

From the load-flow analysis, the following end results are noted:

1. Real power output of generator, P_{g0}
2. Reactive power output of generator, Q_{g0}
3. Terminal bus voltage, $V_{g0}\angle\theta_{g0}$

Using these values, the initial conditions of states variables are calculated as follows [1]:

1. Compute

$$\bar{V}_{g0} = V_{g0}(\cos \theta_{g0} + j \sin \theta_{g0}) \quad (\text{H.1})$$

$$\bar{I}_{g0} = \left(\frac{P_{g0} + jQ_{g0}}{\bar{V}_{g0}} \right)^* = I_{g0}\angle\phi_0 \quad (\text{H.2})$$

$$\bar{E}_{q0} = \bar{V}_{g0} + jx_q\bar{I}_{g0} \quad (\text{H.3})$$

$$\delta_0 = \angle\bar{E}_{q0} \quad (\text{H.4})$$

2. Compute

$$\begin{aligned} i_{q0} + ji_{d0} &= \bar{I}_{g0} e^{-j\delta_0} \\ &= I_{g0}\angle(\phi_0 - \delta_0) \end{aligned}$$

$$i_{q0} = I_{g0} \cos(\phi_0 - \delta_0) \quad (\text{H.5})$$

$$i_{d0} = I_{g0} \sin(\phi_0 - \delta_0) \quad (\text{H.6})$$

3. Compute

$$\begin{aligned} v_{q0} + jv_{d0} &= \bar{V}_{g0}e^{-j\delta_0} \\ &= V_{g0}\angle(\theta_{g0} - \delta_0) \end{aligned}$$

$$v_{q0} = V_{g0} \cos(\theta_{g0} - \delta_0) \quad (\text{H.7})$$

$$v_{d0} = V_{g0} \sin(\theta_{g0} - \delta_0) \quad (\text{H.8})$$

4. Compute

$$E_{fd0} = E_{q0} - (x_d - x_q)i_{d0} \quad (\text{H.9})$$

5. Compute

$$\psi_{d0} = v_{q0} \quad (\text{H.10})$$

$$\psi_{q0} = -v_{d0} \quad (\text{H.11})$$

6. Compute

$$\psi_{h0} = \psi_{d0} \quad (\text{H.12})$$

$$\psi_{f0} = \psi_{d0} + \frac{x_d'}{x_d - x_d'} E_{fd0} \quad (\text{H.13})$$

$$\psi_{k0} = \psi_{q0} \quad (\text{H.14})$$

$$\psi_{g0} = \psi_{q0} \quad (\text{H.15})$$

7. Compute

$$T_{m0} = P_{g0} \quad (\text{H.16})$$

8. Compute

The generator field current,

$$i_{f0} = \frac{(\psi_{f0} - \psi_{d0})}{x_{fl}} \quad (\text{H.17})$$

The exciter current,

$$I_{FD0} = x_d i_{f0} \quad (\text{H.18})$$

NOTE:

- In the above calculations, the armature resistance, R_a has been neglected.
- The initial condition of state variables are calculated for the operating point whose small-signal stability is to be determined.

Bibliography

- [1] K.R. Padiyar, *Power System Dynamics - Stability and Control*, BS Publications, Hyderabad, India, 2002.
- [2] P. Kundur, *Power System Stability and Control*, McGraw-Hill Inc., New York, 1994.
- [3] Graham Rogers, “Demystifying Power System Oscillations ”, *IEEE Computer Application in Power*, 1996.
- [4] Ogata K, *State Space Analysis of Control Systems*, Prentice-Hall, Englewood cliff, NJ, 1967.
- [5] Graham Rogers, *Power System Oscillations*, Kluwer Academic Publishers, London, 2000.
- [6] Nelson Martins, “Efficient Eigenvalue and Frequency Response Methods Applied to Power System Small-Signal Stability Studies,” *IEEE Transactions on Power Systems*, Vol. PWRs-1, No. 1, pp 217-224, February, 1986.
- [7] M. Klein, G.J. Rogers, S. Moorthy and P. Kundur, “Analytical Investigation of Factors Influencing Power System Stabilizers Performance,” *IEEE Trans.on Energy Conversion*, Vol.7, No.3, pp 382-390, September, 1992.
- [8] P.W. Sauer and M.A. Pai, *Power System Dynamics and Stability*, Prentice Hall, Upper Saddle River, New Jersey, 1998.
- [9] A.R. Bergen and V. Vittal, *Power System Analysis*, Pearson Education Asia, India, 2001.
- [10] P.G. Murthy and M.Pavella, *Transient Stability of Power Systems, Theory and Practice*, John Wiley & Sons Ltd., England, 1994.
- [11] Nelson Martins and L.T. G. Lima, “Determination of Suitable Locations for PSS and Static var Compensators for Damping Electromechanical Oscillations in Large Power systems,” *IEEE Transactions on Power Systems*, Vol. 5, No. 4, pp 1455-1469, November, 1990.

- [12] P.Kundur, G.R.Rogers, D.Y.Wong, L.Wang, M.G.Lauby, "A Comprehensive Computer Program Package for Small-Signal Stability Analysis of Power System," *IEEE Trans.on Power Systems*, Vol.5, No.4, November, 1990.
- [13] *Using MATLAB*, Version 5.3, Release 11, The Math Works Inc.
- [14] P. Kundur, D.C. Lee and H.M. Zein El-Din, "Power System Stabilizers for Thermal Units: Analytical Techniques and On-site Validation," *IEEE Trans.on Power Apparatus and Systems*, Vol. PAS-100, pp. 81-95, January, 1981.
- [15] H. Breulmann, E. Grebe, W. Winter, R. Witzmann, P. Dupuis, M.P. Houry, T. Margotin, J. Zerenyi, J. Dudzik, PSE S.A., J. Machowski, L. Martn, J. M. Rodriguez, E. Urretavizcaya, "Analysis and Damping of Inter-Area Oscillations in the UCTE/CENTREL Power System," CIGRE, Germany, 2000.
- [16] S.A.Soman, S.A.Khaparde and Shubha Pandit, "Computational Methods for Large Sparse power Systems Analysis, An Object Oriented Approach," Kluwer Academic Publishers, Netherlands, 2002.
- [17] Mariesa Crow, "Computational Methods for Electric Power System," CRC Press LLC, Landon, 2003.
- [18] J.G.Stoolweg, J.Person, A.M.van Voorden, G.C.Paap, W.L.Kling, "A Study of the Eigenvalue Analysis Capabilities of Power System Dynamics Simulation Software," 14th PSCC, Sevilla, 24-28 June, 2002.
- [19] *Using Simulink*, Version 3, Release 11, The Math Works Inc.
- [20] F.L.Pagola, I.J. Perez-Arriaga and G.C Verghese, "On Sensitivities, Residues and Participations: Applications to Oscillatory Stability Analysis and Control", *IEEE Trans. on power systems*, Vol.PWRS-4, No. 1, pp. 278-285, February., 1989.
- [21] G.C. Verghese, I.J. Perez-Arriaga, and F.C. Schweppe, " Selective Model Analysis with Application to Electric Power Systems, Part I: Heuristic Introduction, Part II: The Dynamic Stability Problem," *IEEE Trans. on power systems*, Vol.PAS-101, No. 9, pp. 3117-3134, September, 1982.
- [22] *IEEE Recommended Practice for Excitation Systems Model for Power System Stability Studies*, IEEE Standard 421.5-1992.
- [23] IEEE Committe Report, "Dynamic Models for Steam and Hydro Turbines in Power System Studies," *IEEE Trans. on Power Apparatus and Systems*, Vol.PAS-92, pp.1904-1915, November/December, 1973.

- [24] M. Klein, G.J. Rogers, P. Kundur, "A Fundamental Study of Inter-area Oscillations in Power System," *IEEE Transaction on Power Systems*, Vol.6, No. 3, pp. 914-921, August, 1991.
- [25] F.P.deMello and C.Concordia, "Concept of Synchronous Machine Stability as Affected by Excitation Control," *IEEE Trans.on Power Apparatus and Systems*, Vol.PAS-88, pp.316-329, April, 1969.
- [26] Hingorani N.G and Gyugyi.L, "Understanding FACTS," IEEE press, NewYork, 2000.
- [27] E.V. Larsen and D.A. Swann, "Applying Powers System Stabilizers, Part I; General Concepts, Part II; Performance Objectives and Tuning Concepts, Part III; Practical considerations ", *IEEE Trans on power Apparatus and Systems* Vol PAS-100, No.6, pp. 3017-3046, June, 1981.
- [28] P.Kundur, M.Klien, G.J. Rogers and M.S. Zwyno, "Application of Power System Stabilizers for Enhancement of Overall System Stability," *IEEE Trans.on Power Systems*, Vol 4, pp. 614-626, May, 1989.
- [29] K.E. Bollinger, A. Laha, R. Hamilton, T. Harras, "Power System Stabilizer Design Using Root Locus Methods," *IEEE Trans.on Power Apparatus and Systems*, Vol. PAS-94, pp.1484-1488, September/October, 1975.
- [30] Ogata K, " Modern Control Engineering," Prentice-Hall, N.J, July, 2001.
- [31] S.Lefebvre, "Tuning of Stabilizers in Multimachine Power System," *IEEE Trans.on Power Apparatus Systems*, Vol. PAS-102, No. 2, February, 1983.
- [32] D.C. Lee, R.E. Beaulieu and J.A.R. Service, "A Power System Stabilizer Using Speed and Electric Power Inputs-Design and Field Experience" *IEEE Trans.on Power Apparatus and Systems*, Vol. PAS-100, pp. 81-95, January, 1981.

Acknowledgments

The authors thank Prof. A.M.Kulkarni at IIT Bombay for his valuable suggestions and discussions regarding the programme implementation.

Please report bugs to: *knsa1234@yahoo.com*